

Feasibility of Spectrum Sharing Between Airborne Weather Radar and Wireless Local Area  
Networks

Ruffy Zarookian

Thesis submitted to the faculty of the Virginia Polytechnic Institute and State University in  
partial fulfillment of the requirements for the degree of

Master of Science  
In  
Electrical Engineering

Dr. Timothy Pratt

Dr. Mike Buehrer

Dr. Ira Jacobs

November 14, 2007

Blacksburg, Virginia

Keywords: Airborne Weather Radar, Interference, Radar, Spectrum Sharing, Wireless Local  
Area Networks, X Band, SHF Band, Wireless Communications

Feasibility of Spectrum Sharing Between Airborne Weather Radar and Wireless Local Area  
Networks  
Ruffy Zarookian

**ABSTRACT**

Emerging technologies such as wireless local area networks and cellular telephones have dramatically increased the use of wireless communications services within the last 10 years. The shortage of available spectrum exists due to increasing demand for wireless services and current spectrum allocation regulations. To alleviate this shortage, Research aims to improve spectral efficiency and to allow spectrum sharing between separately managed and non-coordinating communications systems.

This thesis explores the feasibility of spectrum sharing between airborne weather radar and wireless local area networks at 9.3 GHz – 9.5 GHz. Characteristics of flight paths of aircraft using airborne weather radar and the low duty cycle of radar transmissions offer unique opportunities for spectrum sharing. But it was found that the extremely sensitive receivers provide challenges for designing a communications system meant for widespread use. The probability of causing harmful interference to airborne weather radar is too great for most types of wireless local area networks, but a direct sequence spread spectrum scheme could share spectrum with airborne weather radar. Bit errors in wireless local area network links caused by airborne weather radar interference do not significantly decrease the performance of the wireless local area network system. The distribution of interference outside of the airborne weather radar receiver by using direct sequence spread spectrum combined with the acceptable bit error rates indicate that while spectrum sharing between airborne weather radar and wireless local area network at 9.3 GHz – 9.5 GHz is not feasible, direct sequence spread spectrum systems can share spectrum with airborne weather radars under more limited assumptions.

## **ACKNOWLEDGEMENTS**

First and foremost I would like to thank my committee chairman and graduate advisor, Dr. Timothy Pratt, for his tireless efforts. With his guidance, I was able to achieve greater levels of technical quality, and was able to present the research with equal skill. I also express my sincere gratitude to my committee members, Dr. Ira Jacobs and Dr. Michael Buehrer for their encouragement and expert advice in both academic and personal matters. I give my heartfelt appreciation to Dr. Kathleen Meehan, Dr. Chris Wyatt, and Dr. Claudio da Silva for their encouragement and aid that allowed me to continue my education and personal growth at Virginia Tech. Thank you to all my professors and Virginia Tech staff for providing me the best possible education in the best possible academic environment. I appreciate the support of all of my friends and colleagues especially Rick, Jen, and Tuan for their intelligent, diversionary discourses and my good friend Mike for his ever critical reviews. And finally to my mother, father, and brother for their unconditional support in all of its forms, thank you.

## TABLE OF CONTENTS

Abstract.....	ii
Acknowledgements.....	iii
Table of Contents.....	iv
Table of Contents.....	iv
List of Figures.....	vii
List of Tables.....	xii
Chapter 1 Introduction.....	1-1
1.1 Introduction.....	1-1
1.2 Analysis of Interference.....	1-2
1.3 Thesis Overview.....	1-5
Chapter 2 Spectrum Sharing.....	2-1
2.1 Radio Spectrum.....	2-2
2.2 Occupied Bandwidth of Radars and Communications Transmissions.....	2-5
2.2.1 Occupied Bandwidth of Radar Transmissions.....	2-5
2.2.2 Occupied Bandwidth of Communications Transmissions.....	2-11
2.3 Propagation, Noise, and Interference.....	2-13
2.3.1 Path Loss.....	2-13
2.3.2 Scattering.....	2-14
2.3.3 Noise and Interference.....	2-15
2.3.4 Absorption.....	2-16
2.4 Probability of Bit Error in Communications Systems.....	2-17
2.5 Radar Systems.....	2-25
2.5.1 Maximum Allowable Interference into Airborne Weather Radar.....	2-31
2.6 Regulation of Spectrum Allocations.....	2-33
Chapter 3 Calculation of Interference Levels Caused by Wireless Local Area Networks in Airborne Weather Radar.....	3-1
3.1 Assumptions for Interference Analysis.....	3-1
3.1.1 Flight Characteristics of Airborne Weather Radar Capable Aircraft.....	3-2

3.1.2 Typical Airborne Weather Radar .....	3-3
3.1.3 Link Densities for Wireless Local Area Networks.....	3-6
3.2 Coverage Area of Airborne Weather Radar .....	3-7
3.2.1 Radar Antenna Beam Pattern Model for Interference Analysis .....	3-8
3.2.2 Coverage Area Defined .....	3-10
3.3 Tools for Analysis of Interference .....	3-15
3.3.1 Total Effective Interference into AWR .....	3-15
3.3.2 Probability of Exceeding Maximum Allowable Received Interference Power into Airborne Weather Radars .....	3-18
3.4 Interference Scenarios .....	3-21
3.4.1 Scenario 1: Heavily Traveled Jetway .....	3-22
3.4.2 Scenario 2: Victor Airway .....	3-23
3.5 Interference into AWR from Narrowband Wireless Local Area Networks.....	3-25
3.6 Conclusion.....	3-31
Chapter 4 Effects of Airborne Weather Radar Interference on Wireless Local Area Networks .....	4-1
4.1 Determining the Number of Airborne Weather Radar Interferers .....	4-1
4.2 Probability of Bit Error of Wireless Local Area Networks in Shared Spectrum .....	4-6
4.3 Bit Error Rate of a Narrowband Wireless Local Area Network in Shared Spectrum	4-10
Chapter 5 Feasibility of Spectrum Sharing between Airborne Weather Radar and Wireless Local Area Networks .....	5-1
5.1 Review of Metrics, Scenarios, and Assumptions for Spectrum Sharing .....	5-1
5.2 Narrowband Wireless Local Area Network .....	5-5
5.2.1 Interference into Airborne Weather Radar from Narrowband Wireless Local Area Networks.....	5-7
5.2.2 Bit Error Rate of Narrowband Wireless Local Area Networks in Shared Spectrum with Airborne Weather Radar.....	5-12
5.2.3 Recommendation of Spectrum Sharing for Narrowband Wireless Local Area Networks.....	5-15

5.3 Direct Sequence Spread Spectrum Wireless Local Area Network .....	5-16
5.3.1 Interference into Airborne Weather Radar from Direct Sequence Spread Spectrum Wireless Local Area Networks.....	5-17
5.3.2 Bit Error Rate of Direct Sequence Spread Spectrum Wireless Local Area Networks in Shared Spectrum with Airborne Weather Radar .....	5-22
5.3.3 Recommendation of Spectrum Sharing for Direct Sequence Spread Spectrum Wireless Local Area Networks.....	5-24
5.4 Frequency Hopping Spread Spectrum Wireless Local Area Network.....	5-24
5.4.1 Interference into Airborne Weather Radar from Frequency hopping spread spectrum Wireless Local Area Networks .....	5-26
5.4.2 Bit Error Rate of Frequency hopping spread spectrum Wireless Local Area Networks in Shared Spectrum with Airborne Weather Radar .....	5-31
5.4.3 Recommendation of Spectrum Sharing for Frequency hopping spread spectrum Wireless Local Area Networks.....	5-33
5.5 Recommendations .....	5-34
Chapter 6 Conclusion.....	6-1
6.1 Metrics for Analysis of Interference in Shared Spectrum.....	6-1
6.2 Results of Spectrum Sharing Analysis .....	6-4
Appendix A Glossary of Terms and Acronyms.....	A-1
Appendix B Link Budgets for Wireless Local Area Networks .....	B-1
Appendix C Typical Airborne Weather Radars Characteristics .....	C-1
Appendix D United States Frequency Allocations at 9.3GHz-9.5GHz[12] .....	D-1
References.....	1

## LIST OF FIGURES

Figure 2-1. Electromagnetic spectrum from NTIA document [28]. .....	2-3
Figure 2-2. Energy spectral density of a signal with 60dB bandwidth of 20 MHz. The frequency content of a signal defined by the energy spectral density. The signal has a center frequency of $f_c$ and a 60 dB bandpass bandwidth of 20 MHz. ....	2-4
Figure 2-3. Spectrum mask with spectrum data from an aeronautical radionavigation radar. Measured data were collected from a live test. From NTIA document [25, 29]. .....	2-6
Figure 2-4. Radar pulse shape model for radar as defined by the NTIA in [25]. .....	2-7
Figure 2-5. Weather radar pulse operating on a single frequency, with a fixed pulse repetition rate and no modulation shown in NTIA document [25]. .....	2-8
Figure 2-6. Spectrum mask for weather radar with the pulse shape shown in Figure 2-5. This mask was calculated using NTIA supplied software [29]. .....	2-9
Figure 2-7. Spectrum mask for an airborne weather radar calculated. The specifications for the radar pulse was extracted from [16], and the mask was calculated using NTIA supplied software [29]. This radar is typical for an airborne weather radar and used as a baseline throughout this thesis. ....	2-10
Figure 2-8. Model of a communications system. Information flows from the source, is encoded for transmission, travels through the channel, then is recovered at the receiver for delivery to the destination. ....	2-18
Figure 2-9. Noise plus transmitted signal results in a noisy received signal. The transmit signal is shown in the top left with the symbol values shown as ‘*’. The noise is shown in the top right figure. The received signal ‘—’, sent signal ‘---’, and sampled symbol values ‘o’ are shown in the bottom plot. ....	2-19
Figure 2-10. Weather Radar Display. This display is a digital plan position indicator (PPI) showing azimuth and range of targets (weather phenomenon). Colors of targets indicate rain reflectivity, and the display is overlaid with geographic data shown as red lines. Image used with permission from Environment Canada [38]. ....	2-27

Figure 2-11. Antenna pattern. Sidelobes and the rear of the pattern are low compared to the main lobe. Image obtained from [24] used under term of the GNU Free Document License. .... 2-28

Figure 2-12. Lost targets due to low levels of interference shown by experiments by NTIA in [16]. .... 2-29

Figure 2-13. High levels of interference from a single direction cause an obscuring strobe on the radar display shown in experiments by NTIA in [16]. .... 2-30

Figure 2-14. Block diagram of test configuration used in [16]. Synthetic targets and interference signals are injected before the radio frequency filter. A spectrum analyzer placed directly after the intermediate frequency filter is viewed to calibrate the interference to noise ratio, and the display after the detector/signal processor is viewed to monitor the effects of the interference. .... 2-32

Figure 3-1. Antenna pattern model for interference analysis for an AWR with a 3 dB beamwidth of  $5^\circ$ . The constant gain pattern, shown as the solid red line, that results in equivalent received power has a beamwidth of  $5.2^\circ$  null to null and a constant gain of 32 dBi. The reference pattern, shown as the blue dashed line, varies by the cosine of the angle from peak gain. The mainlobe peak is at 32 dBi, the first sidelobe peaks at 9 dBi and the second sidelobe peaks at 1.3 dBi. .... 3-5

Figure 3-2. Coverage area for an aircraft at altitude  $h$  with a beamwidth,  $\theta$ , and tilt angle,  $\Psi$ . The angle from the horizon to the beam,  $\gamma$ , is one half the beamwidth plus the tilt angle. The size of the coverage area is  $A$  with a major axis of  $C$  and a minor axis of  $C_H$ . The maximum and minimum possible separation between the AWR and WLAN links is  $R_{\max}$  and  $R_c$ , respectively. .... 3-8

Figure 3-3 : Coverage area for vertical beamwidth less than tilt angle. The dashed lines represent the radar beam. The solid line is the coverage path,  $C$ . The dotted lines mark lines used to aid calculations. The altitude of the aircraft is  $h$  and the beamwidth of the AWR is  $\theta$ . The angle from the horizon to the beam is one half the beamwidth plus the tilt angle,  $\gamma$ . The maximum and minimum possible separation between the AWR and WLAN links is  $R_{\max}$  and  $R_c$ , respectively. .... 3-11

Figure 3-4 : Coverage area for beamwidth greater than tilt angle. The dashed lines represent the radar beam. Notice that only one leg of the triangle intersects with the ground plane, the other extends upward. The solid line is the coverage path,  $C$ . The dotted lines mark lines used aid calculations. The altitude of the aircraft is  $h$  and the beamwidth of the AWR is  $\theta$ . The angle from the horizon to the beam is one half the beamwidth plus the tilt angle,  $\gamma$ . The maximum and minimum possible separation between the AWR and WLAN links is  $R_{max}$  and  $R_c$ , respectively. .... 3-13

Figure 3-5. Probability that the total effective interference received by all WLAN links in a coverage area,  $I_{total}$ , exceeds the maximum allowable received interference,  $I_{max}$ . Harmful interference is 100% likely in both jetways and Victor airways. .... 3-28

Figure 3-6. Expected interference above the maximum allowable interference versus the probability that a single WLAN interferes with a present AWR. Interference into AWR receivers is expected to be at least 25 dB higher than the allowable level in both jetways and Victor airways, regardless of probability that a single WLAN link interferes with a present AWR. .... 3-29

Figure 3-7. Expected interference above the maximum allowable interference versus WLAN transmit power. Interference into AWR receivers is expected to be at least 10 dB higher than the allowable level in both jetways and Victor airways with a minimum transmit power of 0.1 mW..... 3-30

Figure 3-8. Expected interference above the maximum allowable interference versus link density. The expected interference approaches maximum allowable level as the link density is decreased to below 1 per square kilometer. .... 3-31

Figure 4-1. Antenna pattern model for airborne weather radar to wireless local area network interference. The main lobe at a constant gain of 32 dBi is from  $-2.5^\circ$  to  $2.5^\circ$ . The first sidelobe has a gain of 9 dBi from  $+6.9^\circ$  to  $+8.9^\circ$ . The second sidelobe has a gain of -1.3 dBi from  $+11.6^\circ$  to  $+12.8^\circ$ . Gain outside of these regions are considered insignificant. .... 4-4

Figure 4-2. Projection of antenna radiation pattern onto the ground. The main lobe has 32 dB of gain. The first sidelobe has 9 dB of gain and the second sidelobe has 1.3 dB of gain. There are four coverage regions,  $C_0$  to  $C_4$  each with a maximum possible separation between

the AWR and a WLAN link  $R_{max,i}$  and a minimum such separation,  $R_{c,i}$  and a horizontal coverage path  $C_{H,i}$ . Each coverage region is a rectangular region with length of the coverage region and width the size of the midpoint between  $R_{c,i}$  and  $R_{max,i}$ . The aircraft is at altitude,  $h$ , and the entire coverage area has a length of  $C$ ..... 4-5

Figure 5-1. Probability that the total effective interference received by all WLAN links in a coverage area,  $I_{total}$ , exceeds the maximum allowable received interference,  $I_{max}$ . Harmful interference is 100% likely in both jetways and Victor airways. .... 5-10

Figure 5-2. Expected interference above the maximum allowable interference versus the probability that a single WLAN interferes with a present AWR,  $\rho$ . Interference into AWR receivers is expected to be at least 25 dB higher than the allowable level in both jetways and Victor airways..... 5-11

Figure 5-3. Expected interference above the maximum allowable interference versus link density. The expected interference approaches maximum allowable level as the link density is decreased to below 1 per kilometer..... 5-12

Figure 5-4. Bit error rate of a WLAN link in shared spectrum with AWRs versus the number of aircraft present carrying AWRs. Duty cycles and beamwidth for AWRs are representative of AWR specifications shown in Appendix C..... 5-14

Figure 5-5. Bit error rate of a WLAN link in shared spectrum with AWRs versus the duty cycle of the AWRs. Data points show duty cycles of real AWRs. Duty cycles of real AWRs reach 0.13, but duty cycles above 0.01 have unreasonably high BERs. WLANs operating under a jetway can expect an average of 37 interferers. In Victor airways the number of aircraft carrying AWR is 17..... 5-15

Figure 5-6. Expected interference above the maximum allowable interference versus WLAN transmit power. Interference into AWR receivers is expected to be at least 10 dB higher than the allowable level in both jetways and Victor airways with a minimum transmit power of 0.1 mW with the probability that a single WLAN link interferes with an AWR is 100%. . 5-20

Figure 5-7. Expected interference above the maximum allowable interference versus link density. The expected interference approaches maximum allowable level as the link density is decreased to below 5 per kilometer..... 5-21

Figure 5-8. Expected interference above the maximum allowable interference versus WLAN transmit power. Interference into AWR receivers is below the maximum level in both jetways and Victor airways with a minimum transmit power of 0.1 mW and a probability that a single WLAN link interferes with an AWR of 5%..... 5-22

Figure 5-9. Probability that the total effective interference received by all WLAN links in a coverage area exceeds the maximum allowable received interference. Harmful interference is 100% likely in both jetways and Victor airways..... 5-30

Figure 5-10. Bit error rate of a WLAN link in shared spectrum with AWRs versus the number of aircraft present carrying AWR. Duty cycles,  $\tau$ , are representative of duty cycles for AWRs shown in Appendix C..... 5-32

Figure 5-11. Bit error rate of a WLAN link in shared spectrum with AWR versus the duty cycle of the AWRs. Data points show duty cycles of real AWRs. Duty cycles of real AWRs reach 0.13, but duty cycles above 0.01 have unreasonably high BERs. An average of 37 and 17 AWRs interferers are plotted. WLANs operating under a jetway can expect an average of 37 interferers. In Victor airways the number of aircraft carrying AWR is 17..... 5-33

## LIST OF TABLES

Table 2-1. Total occupied bandpass bandwidth, $W$ , of phase or amplitude modulated signals using rect, sinc, and raised cosine pulses. The roll-off factor of a raised cosine pulse is $\alpha$ and $R_s$ is the symbol rate in seconds. The first null-to-null bandwidth of a rect pulse in time is $2R_s$ .	2-13
Table 3-1. Typical airborne weather radar specifications collected from [16, 21, 42-44] ...	3-4
Table 3-2. Parameter and values defined by a heavily traveled jetway.	3-23
Table 3-3. Parameter and values defined by a Victor airway.	3-24
Table 3-4. Parameters for narrowband WLAN to AWR interference calculations. The maximum allowable links is 204 links in a jetway and 83 links in a Victor airway. There are more links expected than allowed in a coverage area for both jetways and Victor airways. ...	3-27
Table 4-1. Power budget for narrowband WLAN link.	4-11
Table 4-2. Noise Power budget for narrowband WLAN receiver.	4-12
Table 4-3. Average number of interfering aircraft and interference to desired signal ratio for the main lobe and first two sidelobes of an airborne weather radar antenna pattern.	4-12
Table 5-1. Average number of interfering aircraft and interference to desired signal ratio for the main lobe and first two sidelobes of an airborne weather radar antenna pattern for a jetway.	5-5
Table 5-2. Average number of interfering aircraft and interference to desired signal ratio for the main lobe and first two sidelobes of an airborne weather radar antenna pattern for a Victor airway.	5-5
Table 5-3. Parameters for narrowband WLAN to AWR interference calculations. The maximum allowable links is 204 links in a jetway and 83 links in a Victor airway. There are more links expected than allowed in a coverage area for both jetways and Victor airways.	5-8
Table 5-4. Parameters for direct sequence spread spectrum WLAN to AWR interference calculations. The maximum allowable links is 20,127 links in a jetway and 8255 links in a	

Victor airway. The number of allowed links exceeds the number of expected links in a jetway and Victor airway coverage areas. .... 5-18

Table 5-5. Power budget for frequency hopping spread spectrum WLAN link..... 5-26

Table 5-6. Noise Power budget for frequency hopping spread spectrum WLAN receiver.5-26

Table 5-7. Parameters for frequency hopping spread spectrum WLAN to AWR interference calculations. The maximum allowable links is 80 links in a jetway and 32 links in a Victor airway. There are more links expected than allowed in a coverage area for both jetways and Victor airways..... 5-28

Table B-1. Power budget for narrowband WLAN link. .... B-1

Table B-2. Noise Power budget for narrowband WLAN receiver. .... B-1

Table B-3. Power budget for direct sequence spread spectrum WLAN link..... B-2

Table B-4. Noise Power budget for direct sequence spread spectrum WLAN receiver..... B-2

Table B-5. Power budget for frequency hopping spread spectrum WLAN link. .... B-3

Table B-6. Noise Power budget for frequency hopping spread spectrum WLAN receiver. B-3



# Chapter 1

## Introduction

### 1.1 Introduction

Emerging technologies such as wireless local area networks and cellular telephones have dramatically increased the use of wireless communications services within the last 10 years [1]. The shortage of available spectrum exists due to increasing demand for wireless services and current spectrum allocation regulations.

Research aims to improve spectral efficiency and to allow spectrum sharing between separately managed and non-coordinating communications systems. Current research focuses on complex sharing schemes at frequencies used for communications below 5.5 GHz. The complex sharing schemes include dynamic frequency selection, interference mitigation, and the concept of cognitive radio. [2-10]

Spectrum sharing in frequencies occupied by services other than communications can provide possible solutions to spectrum shortage. Spectrum from 9.3 GHz – 9.5 GHz is one such set of frequencies that is not currently allocated to radio communications devices. This spectrum is allocated to airborne weather radar (AWR) as a primary service [11, 12] (FCC Subpart e, 87.173(b)). Airborne weather radars are geographically sparse [13] and transmit intermittently. These two characteristics, in conjunction with the transmit powers and altitude of the aircraft, may allow spectrum sharing with wireless local area networks (WLANs).

This thesis explores the feasibility of spectrum sharing between airborne weather radar and wireless local area networks at 9.3GHz – 9.5GHz. Analysis of flight paths of

aircraft using airborne weather radar and the radar transceivers is conducted to determine if airborne weather radars have characteristics that allow spectrum sharing. Calculation of levels of radio frequency (RF) interference inflicted by wireless local area networks on airborne weather radar determines if RF interference on airborne weather radar prevents spectrum sharing. The level of interference from airborne weather radar into wireless local area networks is also calculated. This level of interference determines the bit error rate of wireless local area networks in the presence of airborne weather radar. Bit error rates that are too high will prevent spectrum sharing.

## **1.2 Analysis of Interference**

Airborne weather radars are used on commercial aircraft to detect harmful weather phenomenon. Most commercial aircraft travel in jetways or Victor airways. Airborne weather radar (AWR) use in these two airways is analyzed in this thesis to determine if spectrum sharing is feasible between AWRs and wireless local area networks (WLANs). The first scenario considers WLANs operating under a jetway. Jetways are heavily traveled by aircraft carrying AWR. The second scenario considers WLANs operating under a Victor airway. A Victor airway is the lowest altitude airspace regularly traveled by passenger aircraft carrying AWR. These two scenarios represent the worst possible conditions for spectrum sharing between AWR and WLANs based on the characteristics of aircraft operating under air traffic control. Total effective interference and BER in shared spectrum is used to analyze the scenarios. Total effective interference is used to determine the amount of RF interference inflicted on an AWR. The BER in shared spectrum is used to determine the performance of a WLAN. Analysis of these scenarios requires consideration of the properties of jetways and Victor airways, flight characteristics of aircraft carrying AWR, characteristics of AWR, and characteristics of WLANs.

The first scenario considers WLANs operating under a jetway. Jetways are airspace routes established by the Federal Aviation Administration (FAA) to carry air traffic at altitudes from 5486 meters (18,000 feet) above mean sea level to 18,228 meters (60,000 feet) mean sea level. Mean sea level (MSL) is the height of an object referenced from sea level. The FAA defines jetways as Class A airspace which are governed by strict aircraft separation rules. Separation between aircraft is maintained with the aid of ground based radar and air traffic control. Jetway traffic constitutes most aircraft flying above 5486 meters (18,000 feet) MSL. A jetway is the heaviest traveled airspace by aircraft carrying AWR; therefore, a scenario considering WLANs operating under a jetway is an indicator of one possible worst case performance of WLANs and AWR in shared spectrum. [14, 15]

The second scenario considers WLANs operating beneath a Victor airway. Victor airways are also airspace which designates a route in air, but Victor airways are at altitudes from 366 meters (1,200 feet) above ground level (AGL) to 5486 meters (18,000 feet) MSL. The FAA defines Victor airways as Class E airspace. Class E airspace is governed by aircraft separation rules which are maintained visually, or by ground based radar and air traffic control. A Victor airway is the lowest altitude route in which aircraft carry AWR; therefore, this scenario is also an indicator of worst case performance for AWR and WLANs operating in shared spectrum. [14, 15]

There are scenarios where spectrum sharing would not be feasible such as on approach paths to airports. These scenarios are not considered in this thesis and regulation restricting use of WLANs would remain intact.

Analyses of the two scenarios require examination of the characteristics of typical AWRs, typical aircraft carrying AWR, and WLANs. The characteristics examined for aircraft are velocity, altitude, and time interval between aircraft. Tilt angle, beamwidth, pulse power, occupied bandwidth, receiver bandwidth and maximum tolerable interference are examined for AWR. The characteristics examined for WLANs are transmit power, link density, spectrum spreading techniques, and transmit radio frequency.

To aid analysis of the scenarios, the characteristics of AWRs and WLANs are combined into the concept of total effective interference. Total effective interference is directly related to a subset of AWR characteristics (tilt angle, beamwidth, and receiver bandwidth), aircraft characteristic (altitude and range of the aircraft), and WLAN characteristics (transmit power, link density, spectrum spreading techniques, and transmit frequency). By adjusting the parameters of total effective interference, as defined by the scenario, the level of interference in an AWR from a WLAN can be quickly calculated. The metric used to measure the amount of interference inflicted by a WLAN on an AWR is interference to noise ratio (I/N).<sup>1</sup>

Interference from an AWR to a WLAN and interference from a WLAN to an AWR each require unique metrics and framework for analysis. The likelihood of interference from WLAN links exceeding the acceptable I/N of an AWR receiver determines if spectrum sharing is feasible. This likelihood depends on the physical separation between WLANs and the AWR, the transmit power of WLAN devices, and the link density of WLANs. These parameters determine how many WLAN will interfere with the AWR receiver and the strength of the received interference. Performance of WLAN links is measured by the bit error rate. Bit errors occur as AWRs transmit into a coverage area where the WLAN links are located. The more often a present AWR transmits or the more AWRs that are present, the higher the bit error rate of affected WLAN links.

---

<sup>1</sup> Although range reduction has been proposed as a metric for interference effects on radar, research ([16]) shows that interference to noise ratio correlates better with degradation of performance in radar systems. Performance of radar systems is defined as decreasing probability of detection of desired targets and increase in the amount of interference displayed to the operator.

## **1.3 Thesis Overview**

Chapter 1 identifies the need for spectrum sharing, describes the methods of analysis used, and provides an overview of the thesis. Chapter 2 discusses relevant technical topics including prior research pertaining to RF interference into radar ([16-20]), communication systems, and principles of AWR ([21-26]). Also, Chapter 2 reviews regulatory issues ([11, 27]) for spectrum sharing. Chapter 3 provides a full discussion of the analysis framework for interference into an AWR and quantifies the scenarios considered in this thesis. Chapter 4 derives the BER of WLAN links in shared spectrum with an AWR. Chapter 5 analyzes the scenarios and presents results of the analysis. Chapter 6 provides key findings and direction for future work.



## Chapter 2

# Spectrum Sharing

The bandwidth of radar and communications systems, propagation of electromagnetic signals, and receiver design will determine the feasibility of spectrum sharing between airborne weather radar and wireless local area networks. This chapter introduces these topics and provides the basis for development of metrics and analysis of the effects of interference in shared spectrum.

The occupied bandwidth of AWRs and WLANs determines the possibility of sharing spectrum in the dimension of frequency. Transmitting AWRs occupy the entire 9.3 GHz – 9.5 GHz range; therefore, there is no allocated spectrum that is unused when an AWR is present. This large occupied bandwidth prevents frequency separation, and thus necessitates study of signal propagation and receivers of AWRs and WLANs.

Interfering AWR transmissions in shared spectrum are modeled as a pulsed jammer from the perspective of WLANs. The effect of this interference is measured as the bit error rate (BER) performance of communications systems afflicted by pulsed jamming. Maximum allowable interference is the metric used for performance of an AWR afflicted by interference from WLANs. This metric is the level of interference before any detrimental effects occur. Whereas high BER can often be overcome by means of error correction and detection, any level of interference above the maximum allowable interference in a radar receiver is considered unacceptable. The maximum allowable interference into a radar has been determined by the NTIA report “Effects of RF Interference on Radar Receivers” ([16]) through analytical and experimental research.

A discussion of regulatory issues is also required to determine the feasibility of spectrum sharing. Spectrum sharing is not possible without approval of the Federal

Communications Commission (FCC), National Telecommunications and Information Administration (NTIA) and the International Telecommunications Union (ITU). These regulatory bodies establish requirements pertaining to spectrum allocations, allowable emissions, and sharing of spectrum.

## 2.1 Radio Spectrum

Spectrum is the range of electromagnetic (EM) waves<sup>2</sup> with frequencies from 1 Hz –  $10^{24}$  Hz. These waves are equivalently described by either wavelength (in meters) or frequency (in hertz) because the product of frequency and wavelength equals the speed of light.

EM signals can be described by power spectral density of the signal (PSD), also called the signal's frequency content, and the frequencies that the signal occupies. Spectrum and frequency both refer to the occupied frequencies of a signal and are used interchangeably.

Radio frequency spectrum is a subset of electromagnetic spectrum ranging from 3 kHz – 300 GHz [28]. The RF spectrum from 1 MHz – 40 GHz contains frequencies most commonly used by services such as communications and radio detection and ranging (radar). Figure 2-1 shows the entire electromagnetic spectrum including the RF frequency range.

---

<sup>2</sup> Electromagnetic waves are called waves, emissions or signals depending on context.

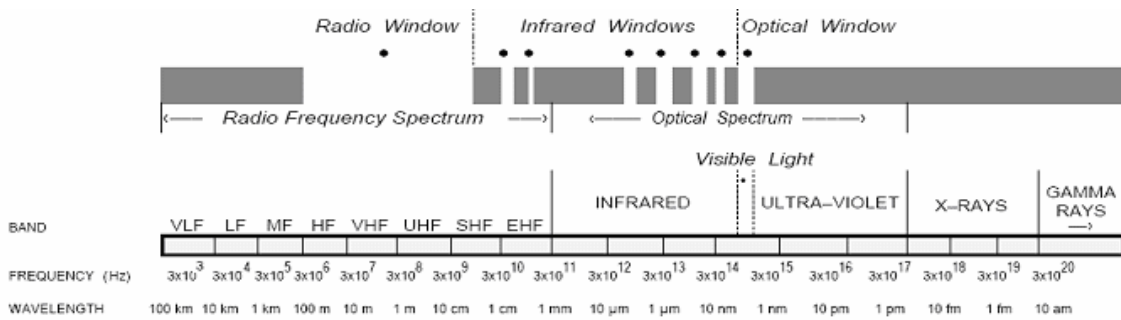


Figure 2-1. Electromagnetic spectrum from NTIA document [28].

Services are allocated to different parts of the RF spectrum to prevent interference between and within the allocated parts of the RF spectrum. Allocations for spectrum can be licensed or unlicensed. Regulations limit interference and allow sharing of the finite RF spectrum range for both licensed and unlicensed spectrum allocations.

Often a license is required to operate in allocated spectrum. Depending on regulations, the license can limit the geographic region of operation, times of allowed operation, and frequency content of emissions; thereby, providing spectrum sharing in the dimensions of space, time, and frequency. Licenses to operate in spectrum are often acquired from the FCC through allocation auctions that can reach billions of dollars. In turn, the FCC guarantees license holders protection from interference in their allocated spectrum.

Some spectrum, such as frequencies from 2.4 GHz – 2.4835 GHz and 5.15 GHz – 5.25 GHz, is called unlicensed spectrum. No license is required to operate in this spectrum allowing end users to purchase and deploy devices without restrictions on their operation. The FCC does impose limits on power and frequency content of emissions produced by devices operating in unlicensed spectrum but unlike licensed spectrum, protection from interference is not guaranteed.

The bandwidth of a signal is the spectrum that the signal occupies at power levels above a specified threshold; alternatively, the power of the signal can be specified relative to

the peak power. For example, the energy spectral density in Figure 2-2 shows the bandwidth of a signal. The signal is centered at frequency  $f_c$  with a bandpass bandwidth of 20 MHz measured at 60 dB below peak power.

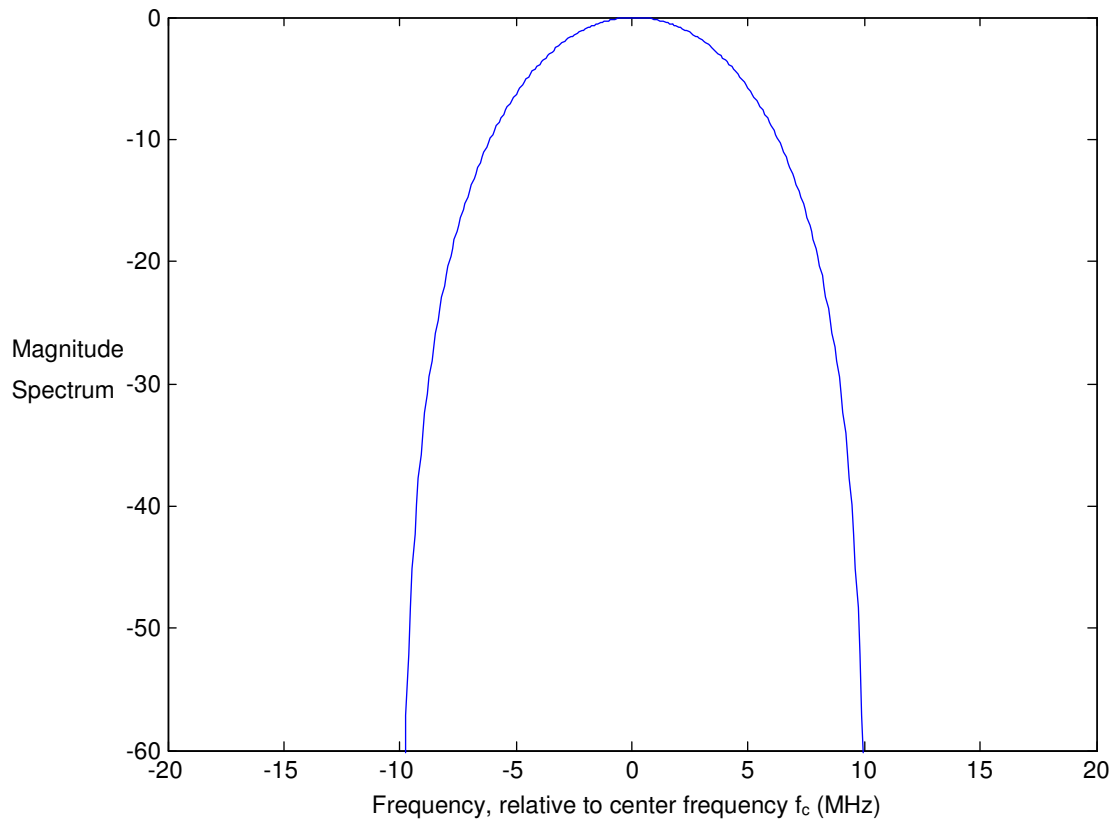


Figure 2-2. Energy spectral density of a signal with 60dB bandwidth of 20 MHz. The frequency content of a signal defined by the energy spectral density. The signal has a center frequency of  $f_c$  and a 60 dB bandpass bandwidth of 20 MHz.

## **2.2 Occupied Bandwidth of Radars and Communications Transmissions**

The occupied bandwidth of airborne weather radars (AWRs) and wireless local area networks (WLANs) determines the possibility of sharing spectrum in the dimension of frequency. Spectrum can be shared by assigning different frequencies or opportunistically using unused frequencies in an allocated band. This cannot be done in this case because transmitting AWRs can occupy the entire 9.3 GHz – 9.5 GHz range; therefore, there is no allocated spectrum that is unused when an AWR is present.

The bandwidth of an AWR is estimated by models provide by the National Telecommunications Information Administration (NTIA). These models show that AWR emissions are wideband, occupying the entire 9.3 GHz – 9.5 GHz range. Additionally, the bandpass bandwidth of communications systems is defined in terms of the modulation scheme of the system.

### **2.2.1 Occupied Bandwidth of Radar Transmissions**

Radars operate by transmitting pulses and receiving signals scattered back by targets to determine range, velocity, and type of target. Pulses used by radars are subject to regulations established by the FCC. Regulation for maximum bandwidth and power are defined mathematically by a plot called a spectrum mask. Spectrum masks are calculated from a radar pulse shape model developed by the NTIA [25, 29]. The pulse shape model is defined in the time domain but the spectrum mask fully describes the maximum allowable emissions in the frequency domain.

Figure 2-3 shows a typical spectrum mask of a radar pulse overlaid with the frequency response of the pulse measured from a live test. The mask is shown by a dashed line and the pulse spectrum is a solid line. The frequency response complies with regulation by not exceeding the spectrum mask.

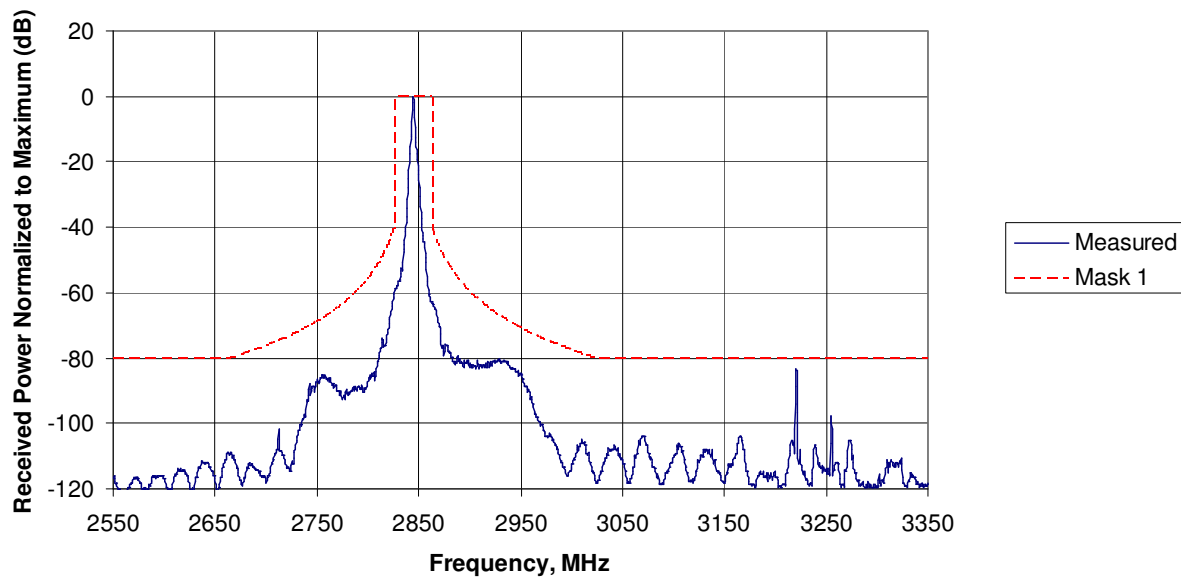


Figure 2-3. Spectrum mask with spectrum data from an aeronautical radionavigation radar. Measured data were collected from a live test. From NTIA document [25, 29].

The model pulse shape does not regulate the time pulses; in fact, the model is defined by parameters measured from radar time pulses. Spectrum masks which are calculated from the model regulate radar emissions. Figure 2-4 shows the NTIA defined pulse shape model [25]. Additionally, the NTIA supplies a software program, [29], to calculate the spectrum mask from the radar pulse shape’s time domain parameters. The following description provided by the NTIA clearly defines the model parameters [25]:

“Pulse width,  $t$ , is defined at the 6dB points (50% voltage points) of radar pulses. The rise time,  $t_r$ , or fall time,  $t_f$ , is measured between the 10%–90% voltage (-20dB to -0.9dB) points on a pulse’s leading or trailing edge, respectively, as shown in [Figure 2-4]. For coded pulses,  $t_r$  and  $t_f$  are the rise and fall times of the sub-pulses. If sub-pulses are not discernable, then  $t_r$  is defined to be 40% of the time required to switch from one phase or chip to the next.”

When using a linear scale the parameters are described as percent of peak voltage. On the logarithmic scale the measurements are relative to peak power. In general, shorter pulse

width, steeper rise times, and steeper fall times will require wider allowed bandwidth in the spectrum mask.

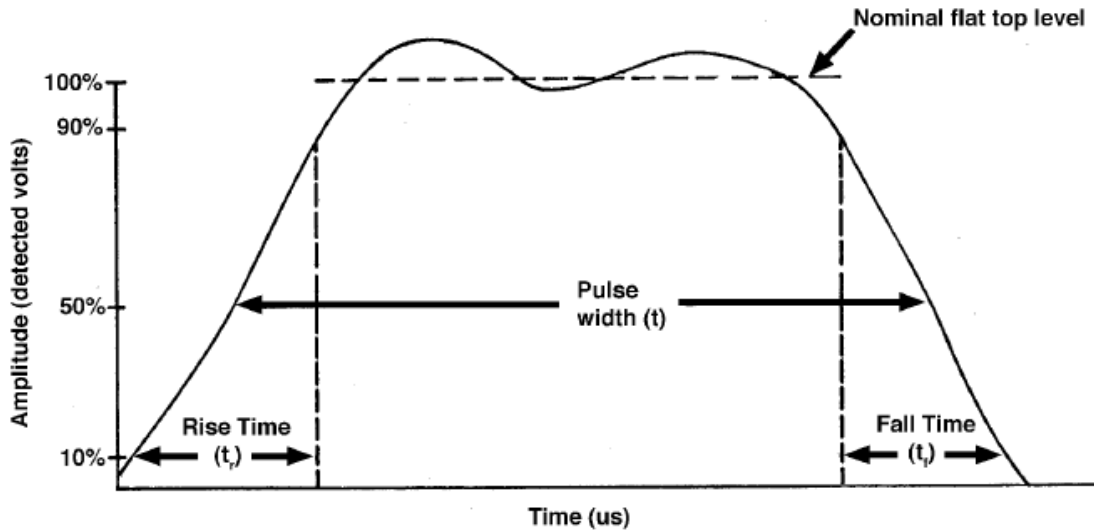


Figure 2-4. Radar pulse shape model for radar as defined by the NTIA in [25].

Figure 2-5 shows a pulse measured from a live test of a weather radar. These data were measured from a radar operating on a single frequency, with a fixed pulse repetition rate and no modulation [25]. Notice that the pulse shape in Figure 2-5 does not exactly adhere to the pulse shape model in Figure 2-4. Nevertheless, a spectrum mask is calculated, shown in Figure 2-6, by inputting the pulse width and rise time of the measured pulse into the NTIA provided software.

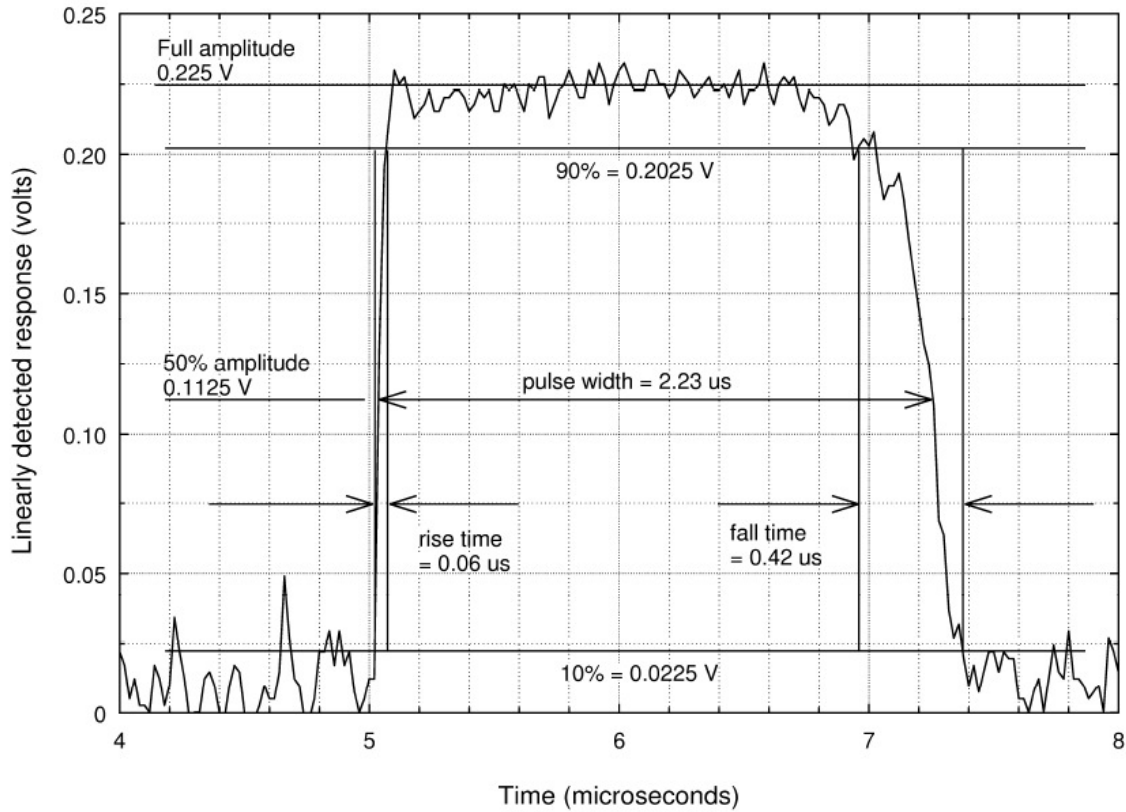


Figure 2-5. Weather radar pulse operating on a single frequency, with a fixed pulse repetition rate and no modulation shown in NTIA document [25].

The spectrum mask in Figure 2-6 calculated from a tested airborne weather radar is divided into three regions. The first region is the peak power region; emissions in these frequencies are allowed peak power. The peak power region would typically contain the main lobe of the pulse and any high power sidelobes. The second region is the 40 dB region. This region limits emissions to 40 dB below peak power and slowly dies off to 60 dB below peak power. The 60 dB region defines where the spectrum has almost completely died off and extends to all bands outside of the 40 dB region.

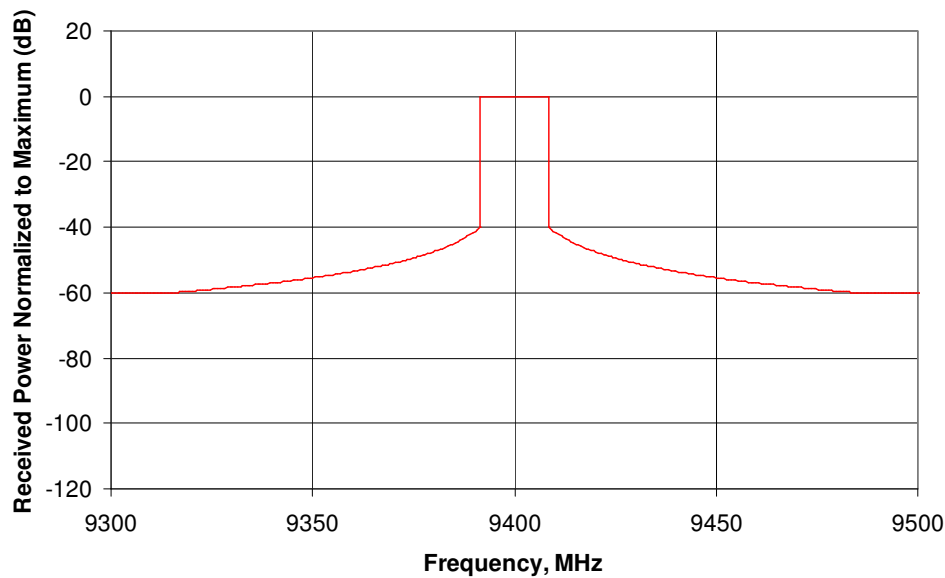


Figure 2-6. Spectrum mask for weather radar of the pulse shape shown in Figure 2-5. This mask was calculated using NTIA supplied software [29].

### 2.2.1.1 Occupied Bandwidth of Airborne Weather Radars

Airborne weather radar typically occupies a large amount of bandwidth. Figure 2-7 shows the spectrum mask of three different types of pulses from an airborne weather radar (AWR). The parameters of typical AWR pulses were extracted from [16]. The AWR on page 125 of [16] is used as an example throughout this thesis. The spectrum mask for an unmodulated pulse produced by the AWR is shown as a solid line in Figure 2-7. The dashed line shows Mask 2. Mask 2 is produced from the specifications for a pulse coded with a Barker sequence. Mask 3 is a frequency hopping pulse shown as a dotted line.

Mask 1 in Figure 2-7 was produced using the specifications for an unmodulated pulse typical of AWR. The pulse width is  $0.19 \mu\text{s}$ , the rise time is  $0.01 \mu\text{s}$ , and the pulse repetition frequency (prf) is 2000 pulses per second (pps). The spectrum of this pulse shape is allowed 142 MHz of bandwidth at peak power before it must be reduced to 40 dB below peak power. Mask 2 was produced using a coded pulse, modulated by a Barker sequence. Mask 2 has a

much smaller bandwidth than Mask 1: 1 MHz at peak power compared to 142 MHz. The smaller bandwidth of Mask 2 is due to its greater pulse width of 234  $\mu\text{s}$  and a longer rise/fall time of 1  $\mu\text{s}$ . Mask 3 is defined by a frequency hopping waveform. The pulse shape used is the same as for Mask 1, but the pulses are hopped to different center frequencies from 9310 MHz to 9410 MHz. Frequency hopping increases the bandwidth at peak power to 242 MHz.

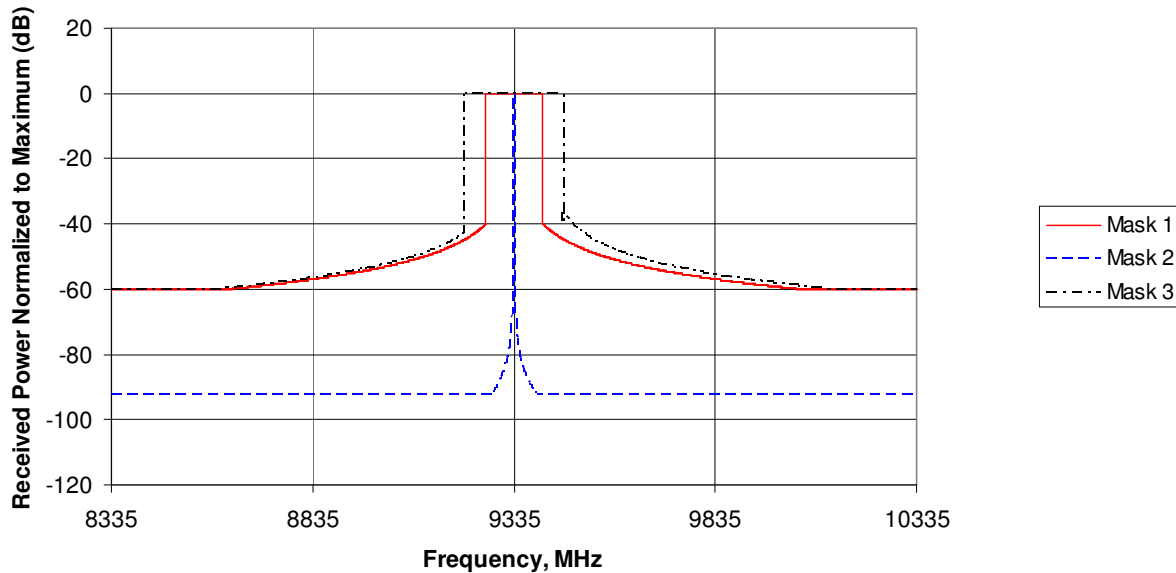


Figure 2-7. Spectrum mask for an airborne weather radar calculated. The specifications for the radar pulse was extracted from [16], and the mask was calculated using NTIA supplied software [29]. This radar is typical for an airborne weather radar and used as a baseline throughout this thesis.

Occupied bandwidth of airborne weather radar is estimated from the spectrum masks in Figure 2-7 . This estimation was necessary because data on typical airborne weather radar pulse spectra could not be found in the literature. Mask 1 and Mask 3 show that radar pulses from a typical airborne weather radar can occupy large portions of the allocated spectrum. Additionally, airborne weather radar operating in the frequency range from 9.3 GHz – 9.5 GHz are exempt from adhering to spectrum masks defined by [25, 29] as noted in Chapter 5, Section 5.5.1 of [12]. Due to the wide bandwidth estimates via spectrum masks

and lack of regulations, it must be assumed that the entire band of 9.3 GHz – 9.5 GHz is occupied when an airborne weather radar is transmitting.

## 2.2.2 Occupied Bandwidth of Communications Transmissions

Radar and communications systems have fundamentally different functions that require different pulse shapes. Radar systems use pulses for ranging and detection while digital communications systems use pulses to transmit information bearing symbols. The goal of digital communications systems is to transmit undistorted symbols at the fastest possible rate using the minimum possible bandwidth.

The maximum rate of undistorted symbol transfer is achieved by using pulses that satisfy the Nyquist zero intersymbol interference (ISI) criterion. The Nyquist zero ISI criterion states that an arbitrary pulse shape can be used regardless of its duration in time if every pulse in a pulse stream except for the current pulse equals a constant at integer multiples of the pulse period. We will concentrate our analysis on raised cosine pulses which are zero ISI pulses widely used to design and analyze communications systems.

The bandwidth of a pulse stream is measured by the power spectral density (PSD) of the pulse stream. The PSD is determined by the energy spectral density (ESD) of the pulse shapes used in the stream. Bandwidth of the ESD, which gives the bandwidth of the signal, is determined by the pulse shape in time and the symbol rate. The time pulse determines the general shape of the ESD while the symbol rate determines the bandwidth of the ESD.

How the bit rate and pulse shape determine the ESD which give the bandwidth of a signal as represented by the PSD is briefly justified below. The power spectral density (PSD), shown in (2.1), measures the bandwidth of a pulse stream [30].

$$P_x(f) = \frac{\sigma_a^2}{T_s} |G(f)|^2 + \frac{m_a}{T_s} \sum_{n=-\infty}^{\infty} \left| G\left(\frac{n}{T_s}\right) \right|^2 \delta\left(f - \frac{n}{T_s}\right) \quad (2.1)$$

The first term of (2.1),  $\frac{\sigma_a^2}{T_s} |G(f)|^2$ , depends on the ESD of the pulse shape,  $|G(f)|^2$ , and the variance of the data,  $\sigma_a^2$ . The ESD of the pulse shape is the only parameter of the first term that is a function of frequency and therefore is the only term that defines bandwidth. The second term,  $\frac{m_a}{T_s} \sum_{n=-\infty}^{\infty} \left| G\left(\frac{n}{T_s}\right) \right|^2 \delta\left(f - \frac{n}{T_s}\right)$ , depends on the mean of the data,  $m_a$ , and the ESD. The second term has one parameter that is a function of frequency. The delta function,  $\delta\left(f - \frac{n}{T_s}\right)$ , causes spectral lines within the bandwidth of the pulse ESD [31]. The symbol period is  $T_s$ , and  $n$  is all integer values from negative infinity to positive infinity. Notice that the only frequency dependent term is the ESD of the pulse shape assuming that the mean of the data is zero. This thesis assumes zero mean data by using bi-polar non-return to zero pulses and thus the bandwidth of the signal depends only on the ESD of the pulse shape.

The total bandwidth of the ESD is determined by the specific parameters of the pulse in time. The ESD is dependent on the symbol rate; as the symbol rate increases bandwidth increases. Pulse shapes which spread the signal beyond a symbol period, such as sinc or raised cosine pulses, typically have lower bandwidth than pulses which are entirely contained within a symbol duration, such as a rect pulse. Higher symbol rates typically increase occupied bandwidth by decreasing the pulse width. Table 2-1 shows the total occupied bandpass bandwidth of phase or amplitude modulated signals that are commonly studied. The roll-off factor of a raised cosine pulse is  $\alpha$ , and  $R_s$  is the symbol rate in seconds.

Pulse Shape	Total Occupied Bandpass Bandwidth, $W$ Hz
rect pulse	infinite, dies off slowly
sinc pulse	$W = R_s$
raised cosine pulse	$W = R_s (1 + \alpha)$

Table 2-1. Total occupied bandpass bandwidth,  $W$ , of phase or amplitude modulated signals using rect, sinc, and raised cosine pulses. The roll-off factor of a raised cosine pulse is  $\alpha$  and  $R_s$  is the symbol rate in seconds. The first null-to-null bandwidth of a rect pulse in time is  $2R_s$ .

## 2.3 Propagation, Noise, and Interference

Operating in different frequencies is one method to avoid interference between two systems. Section 2.2 showed that airborne weather radar cannot be assumed to be using any less than the entire 9.3 GHz – 9.5 GHz frequency range. But, the same frequencies can be shared by two systems if the power of received emissions is below a harmful level. The power of received emissions is reduced by physical separation between the transmitter and receiver.

### 2.3.1 Path Loss

Electromagnetic transmissions lose power as they traverse a distance due to spreading of the signal. The phenomenon of decreasing power due to distance is called path loss and is modeled by the free space path loss equation. The free space path loss equation, also called the Friis transmission formula, is [31].

$$P_r = P_t G_t G_r \left( \frac{\lambda}{4\pi R} \right)^2 \text{ watts} \quad (2.2)$$

Received power,  $P_r$ , calculated by (2.2) depends on the transmitter power,  $P_t$ , the transmitter antenna gain,  $G_t$ , the receiver antenna gain,  $G_r$ , and free space pass loss,  $\left(\frac{4\pi R}{\lambda}\right)^2$ .

The transmitter and received power are in units of watts and the antenna gains are unitless. The total received power decreases with the square of distance. An AWR in flight has a direct line of sight to WLANs while allowing the use of (2.2) to model the received power from or to an AWR. Holding antenna gains constant, the path loss depends on the wavelength of the transmission,  $\lambda$ , in meters, and the distance between transmitter and receiver,  $R$ , in meters. Distance between the transmitter and receiver has a large effect on the received power because  $P_r$  decreases with the square of distance,  $R$ . The free space model can be modified to include losses from imperfect system components or losses from environmental factors which are often grouped into a parameter called miscellaneous loss,  $L_{misc}$ .

### 2.3.2 Scattering

Radars operate by transmitting electromagnetic waves and receiving the scatter returned from targets. The radar equation, shown in (2.3), models scattered waves as retransmissions of the original wave. Modeling scattering as a retransmission means that received power is reduced by range,  $R$ , in meters, raised to the fourth power.

$$P_r = P_t G^2 \left(\frac{\lambda}{4\pi R}\right)^2 \cdot \frac{\sigma}{4\pi R^2} = \frac{P_t G^2 \lambda^2 \sigma}{(4\pi)^3 R^4} \text{ watts} \quad (2.3)$$

The first term of (2.3),  $P_t G^2 \left(\frac{\lambda}{4\pi R}\right)^2$ , represents the parameters of the radar antenna, transmitter, and path loss. The parameter  $P_t$  is the transmit power in watts and  $G$  is the gain of the antenna. The second term,  $\frac{\sigma}{4\pi R^2}$ , models back scatter from the target. The energy scattered back to the radar depends on the radar cross section of the target,  $\sigma$ , and an  $R^2$  term

modeling the path loss back to the radar. The radar cross section is measured in meters squared and is determined by the target's physical size, shape, and material. Radar cross sections are difficult to calculate and are determined experimentally.

### 2.3.3 Noise and Interference

The effects of path loss reduce the received signal power significantly from the original transmitted power. At long ranges, the low power received signal becomes difficult to detect due to noise and interference introduced into the system.

Noise is unwanted energy introduced into any receiver from internal components of the receiver, natural sources, and from manmade devices that are not intentional radio transmitters. Noise generated by the internal components of the receiver, called thermal noise, is the fundamental limiting factor in receiver performance. Natural sources of noise are thermal emissions from the atmosphere (clear air and during precipitation), cosmic radiators such as the sun, or other black body emitters in the environment. Unintentional manmade sources of noise include RF emissions from electric motors, above-ground power lines, and automotive ignition systems. [16]

“Randomly distributed radio energy from all sources, both natural and manmade, combines to generate overall environmental background noise against which the radar receiver must always perform” [16]. Noise sources are unavoidable and generally uncontrollable, but background noise can be predicted and modeled with high reliability [16]. Thermal noise is modeled as additive white Gaussian noise (AWGN). AWGN is present at all frequencies with equal power, and all samples of the noise in time are uncorrelated and have a Gaussian probability distribution function. This important assumption is the basis of bit error rate (BER) calculations in communications systems. The noise power at the receiver,  $N_s$ , in watts is.

$$N_s = kT_e B_N \text{ watts} \quad (2.4)$$

The equivalent noise temperature,  $T_e$ , in degrees kelvin is total noise introduced into the receiver with all sources of noise modeled as a single black body radiator with temperature  $T_e$  [31, 32]. The noise bandwidth,  $R_b$ , in hertz is the data rate assuming raise cosine pulses, and  $k$  is the Boltzmann constant. Often a noise figure,  $F$ , is quoted as a measurement of the total noise of a system. The noise figure is related to  $T_e$  by (2.5). The noise figure must be a linear ratio (not in decibels) when used in (2.5). The reference temperature,  $T_o$ , is typically 290° K [33].

$$T_e = T_o (F - 1) \text{ kelvin} \quad (2.5)$$

Interference is unwanted radio energy (or the effects of) introduced into receivers from manmade, intentional radio transmitter sources such as communications or radar devices. Interference spectra and statistical characteristics are different from noise. Like noise, interference degrades radar receiver performance; unlike noise, interference can be controlled or avoided through spectrum engineering and spectrum management. An extensive study into the effects of manmade interference on radar was conducted by the NTIA in [16].

### **2.3.4 Absorption**

Absorption occurs when an EM wave comes in contact with a medium and energy is lost into the medium. Atmospheric absorption, attenuation of EM waves due to clear air, is negligible for frequencies below 10 GHz adding only 0.1 dB at 100 km [34]. Distances much smaller than 100 km are considered in this thesis and we can safely excluded clear air absorption in calculations for this study. To conduct a worst case analysis, attenuation caused by precipitation, though potentially large at 10 GHz, will not be considered.

Absorption losses by materials that are commonly found in urban and suburban environments are summarized in [35]. From [35] it can be inferred that a reasonable loss due to absorption of a wave propagating through a building is 6 dB. We will assume that the

WLAN communications system is operated indoors and include this 6 dB in all link calculations.

## 2.4 Probability of Bit Error in Communications Systems

Section 2.2.2 showed that communications systems are band limited. This allows many different systems to operate at the same time and at the same place but at different frequencies. Section 2.3 showed that power levels of signals decrease over increasing distance. This allows for spectrum sharing of physically separated systems at the same frequencies. Smaller bandwidth and lower transmit power will allow for greater sharing of the spectrum, but smaller bandwidth limits achievable bit rate and insufficient power increases bit errors. The ability of a receiver to properly decode the desired signal is limited by the signal to noise ratio of the desired signal or interference caused by undesired signals (signal to interference plus noise ratio).

A communications system can be modeled as a system in which information flows from a transmitter, through a channel, and to a receiver. Figure 2-8 shows a block diagram of the model of a digital communications system. Information is inputted into the transmitter and converted into a waveform for transmission. The waveform is typically a high frequency carrier modulated by an information bearing pulse stream. This waveform will occupy some bandwidth depending on pulse shape and symbol rate. The center frequency of the signal spectrum will be at the carrier frequency. As the signal is transported through the channel, propagation effects, modeled by the free space equation (2.2), reduce the signal power by the square of the distance. The signal is captured at the receiver and decoded to retrieve the transmitted information.

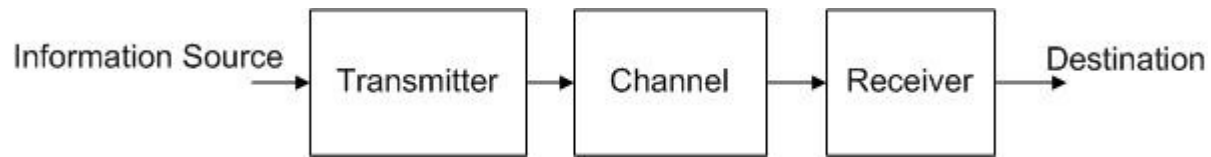


Figure 2-8. Model of a communications system. Information flows from the source, is encoded for transmission, travels through the channel, then is recovered at the receiver for delivery to the destination.

The bit error rate (BER) of a communications system in additive white Gaussian noise (AWGN) is measured by transmitting a pulse stream, adding white Gaussian noise, and decoding the symbol in the receiver. AWGN is present at all frequencies with equal power, and all samples of AWGN in time are uncorrelated. During simulations, received bits are compared to transmitted bits to determine the percent of bits that are different. This percentage of incorrectly decoded bits is the BER.

An example of bit error in a baseband digital communications link is shown in Figure 2-9. The transmit waveform is a sequence of rect pulses generated by modulating information bearing symbols with a rect pulse train. The symbols used in generating the waveform (shown as asterisks in Figure 2-9) can be two possible values: +1 or -1. The symbols were modulated onto a rect pulse stream resulting in a polar non-return to zero waveform. AWG noise was added to the signal resulting in the received signal power that is twice as strong as the noise power; or equivalently stated, the received signal has a SNR of 3dB. Ninety eight percent of the symbols were correctly decoded resulting in a bit error rate (BER) of 0.023 which agrees with the theoretical bit error rate at an SNR of 3 dB [32].

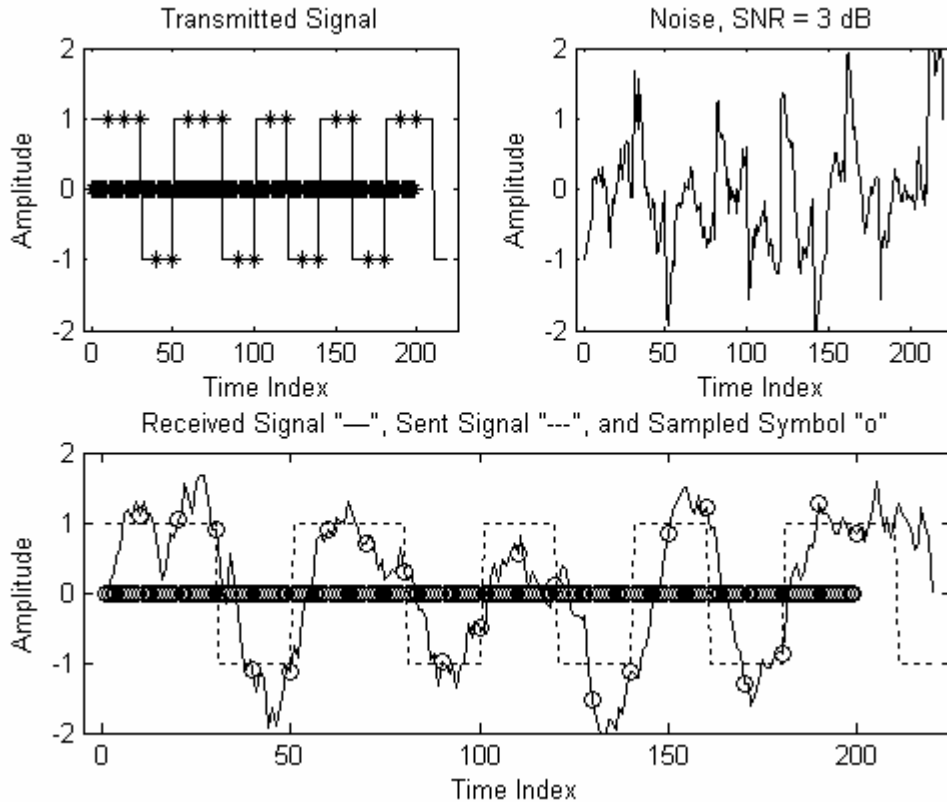


Figure 2-9. Noise plus transmitted signal results in a noisy received signal. The transmit signal is shown in the top left with the symbol values show as '\*'. The noise is shown in the top right figure. The received signal '—', sent signal '---', and sampled symbol values 'o' are shown in the bottom plot.

Symbols are decoded by sampling the signal at integer multiples of the pulse period and using a decision rule to determine whether the transmitted symbol was 1 or 0. A bit error occurs when the received bit is not decoded as the same value as the transmitted bit. Assuming perfect synchronization and undistorted zero ISI pulse shapes, integer multiples of the pulse period is the optimal sampling time to minimize BER. Though the time of sampling is optimal, the BER of a received signal in AWGN is further optimized by using a matched filter.

A decoder that performs better than a simple sampler for zero ISI pulse in AWGN is a matched filter. The matched filter provides the optimal SNR of the received signal corrupted by AWGN, regardless of pulse shape. Optimality is achieved by maximizing signal power and simultaneously minimizing noise power. The matched filter maximizes signal power by convolving a time reversed pulse shape generated in the receiver with the received signal for every pulse. The signal power is maximized because the convolution operation perfectly correlates (correlation of +1 or -1) the incoming pulse with a matching time pulse generated at the receiver. Because the noise is random and uncorrelated with the pulse shape the noise is minimized. Under the assumption of perfect synchronization between the incoming signal and the receiver and undistorted zero ISI pulse shapes the matched filter decoder provides the minimum possible BER in AWGN.

The probability of bit error<sup>3</sup> (BER),  $P_b$ , assuming binary modulation is shown in (2.6). Equation (2.6) says that the BER is the probability of choosing the symbol  $b_1$  when  $b_0$  is sent plus the probability of choosing  $b_0$  when  $b_1$  was sent, weighted by the probability of sending the respective symbol. The sent symbol is  $b$  while the received signal is the random variable  $\hat{b}$ . In the binary case, there are two possible values of  $b$ :  $b_1$  and  $b_0$ . The probability distribution of  $\hat{b}$  is Gaussian given the value of  $b$  due to the AWGN assumption. The probability of transmitting  $b_1$  or  $b_0$  is typically assumed equally likely and thus

$$P[b = b_1] = P[b = b_0] = \frac{1}{2}.$$

$$P_b[\hat{b} \neq b] = P[b = b_1]P[\hat{b} = b_0 | b = b_1] + P[b = b_0]P[\hat{b} = b_1 | b = b_0] \quad (2.6)$$

Equation (2.7) generalizes the BER for a signal modulation with  $M$  symbols. The probability of symbol error is the probability that any symbol is misinterpreted for any other

---

<sup>3</sup> Probability of bit error is often called the bit error rate (BER). Bit error rate is somewhat a misnomer as it is not a rate but rather a probability, thus we attempt to use probability of bit error or BER as opposed to bit error rate.

symbol. From this general equation, the BER error of an arbitrary system can be modeled assuming a known probability density function of the random variable  $\hat{b}$  and probability of transmitting a particular bit.

$$P_e[\hat{b} \neq b] = \sum_{i=0}^{M-1} \sum_{j=i+1}^M P[b = b_i] P[\hat{b} = b_j | b = b_i] \quad (2.7)$$

Returning to the binary case, the BER for binary phase shift keying (BPSK) AWGN is (2.8) [30]. The parameter  $E_b$  is the energy per bit and  $N_0/2$  is the two-sided noise power spectral density. The  $Q$  function is defined as  $Q(x) = \frac{1}{2} \operatorname{erfc}\left(\frac{x}{\sqrt{2}}\right)$  where  $\operatorname{erfc}(x) \equiv \frac{e^{-x^2}}{\sqrt{\pi}x}$ .

$$P_b = Q\left(\sqrt{\frac{2E_b}{N_0}}\right) \quad (2.8)$$

For phase modulated signals, the energy per bit to noise power spectral density ratio ( $E_b/N_0$ ) can be converted to the more intuitive measurement of signal to noise ratio (SNR) by using (2.10). Equation (2.10) is derived from (2.9) assuming an ideal receiver and phase modulation. The SNR (linear) is equal to the energy-per-symbol ratio,  $E_s$ , assuming an ideal receiver using raised cosine pulses. The relationship between  $E_s$  and  $E_b$  is shown in (2.11) where  $M$  is the number of possible symbols in an M-ary modulation scheme. [32]

$$\frac{S}{N} = \frac{ST_s B}{N} \quad (2.9)$$

$$\frac{S}{N} = \frac{E_s}{N_0} \quad (2.10)$$

$$E_s = E_b \log_2(M) \quad (2.11)$$

The BER of non-coherent non-phase continuous M-ary frequency shift keying (MFSK) assuming half of the bits are incorrect on a symbol error is given by (2.12) [36].

Using (2.9) and noting that the bandwidth of non-coherent non-phase continuous MFSK is  $\frac{(M+1)}{T_s}$ , the BER can be expressed in terms of SNR as shown in (2.13).

$$P_e = \frac{M}{2(M-1)} \sum_{n=1}^{M-1} \binom{M-1}{n} \frac{(-1)^{n+1}}{n+1} e^{\left( \frac{n \log_2(M) E_s}{n+1 N_0} \right)} \quad (2.12)$$

$$P_e = \frac{M}{2(M-1)} \sum_{n=1}^{M-1} \binom{M-1}{n} \frac{(-1)^{n+1}}{n+1} e^{\left( \frac{n \log_2(M) S}{n+1 N} (M+1) \right)} \quad (2.13)$$

The probability of bit error due to a channel where an AWR is present can be modeled as a pulsed jamming channel. The BER in a pulsed jamming channel is the probability of bit error with no jammer plus probability of bit error with a jammer. These probabilities are weighted by the probability that the jammer is present. Equation (2.14) describes the probability of bit error in a jamming environment.

$$P_b = P[\text{no jammer}] P[\text{error|no jammer}] + P[\text{jammer}] P[\text{error|jammer}]. \quad (2.14)$$

During jamming the BER is related to the  $E_b/N_0$  with jamming as shown in (2.15). The jammer power spectral density,  $N_j$ , is the average power of the jammer divided by the jammer bandwidth. Equation (2.15) assumes continuous jamming over the entire bandwidth of the desired signal.

$$P[\text{error|jammer}] = Q \left( \sqrt{\frac{2E_b}{N_0 + N_j}} \right) \quad (2.15)$$

In a spectrum sharing scenario, the emissions from a communications system's transmissions can cause interference to other systems in the shared spectrum. To minimize this interference the transmit power of the communications system can be spread across a larger bandwidth. Techniques to spread the transmitted signal over a bandwidth much larger than the bandwidth necessary to carry the data are called spread spectrum techniques. "Spread spectrum can be defined as any modulation technique which (a) occupies a

bandwidth which is well beyond what is necessary for the data rate being transmitted and (b) uses a pseudorandom signal to obtain the increased bandwidth.”[37] Use of spread spectrum techniques gives the transmitted signal a noise like appearance with a low probability of detection [37]. The noise-like and low probability of detection characteristics of the spread signal can reduce the perceived interference on an unintended receiver by hiding the signal below the noise floor of the receiver. In addition to offering less interference, spread spectrum modulated signals are themselves resistant to interferers.

Two types of spread spectrum techniques are discussed: (1) direct sequence spread spectrum (DSSS) and (2) frequency hopping spread spectrum (FHSS). DSSS “involves increasing the signal bandwidth by multiplying the information signal by a high rate spreading waveform. The symbols of the spreading waveform are typically pseudo-random and are generated using a pseudo-random noise (PN) sequence.” [37] The high rate spreading waveform spreads the bandwidth of the signal due to a Fourier relationship that states that short pulses in time have large bandwidth. The chip rate, the symbol rate of the spreading waveform, determines the occupied bandwidth of the signal dominating the spectral effects of the symbol rate of the original unspread waveform. The ratio of the chip rate to the bit rate is called the spreading gain and directly relates to the benefits provided by spread spectrum [37]. FHSS spreads the data waveform by moving the frequency of the carrier from one band to another in a pseudo-random fashion. A pseudorandom sequence is used to change the center frequency of the carrier to one of N different non-overlapping frequency channels. In FHSS the number of different hopping frequencies, N, is called the spreading gain [37].

Sharing spectrum with AWRs will constitute a wideband pulsed jamming environment for WLANs. Resistance to this type of jamming can be achieved using spread spectrum techniques. For a BPSK DSSS modulated link the probability of bit error is [37].

$$P_b = (1-\rho)Q\left(\sqrt{\frac{2E_b}{N_0}}\right) + \rho Q\left(\sqrt{\frac{2E_b}{N_0 + N_j / \rho}}\right) \quad (2.16)$$

The probability of bit error for DSSS in a pulse jamming environment is comprised of two terms. The parameter  $\rho$  is the duty cycle of the jammer and the first term,

$(1-\rho)Q\left(\sqrt{\frac{2E_b}{N_0}}\right)$ , is only in effect when the jammer is not transmitting. In this case the

BER of a BPSK DSSS modulated signal is identical to the AWGN case. The effects of the jammer are reduced by the bandwidth of the spread signal due to the filter process in the receiver to unspread the desired signal. The reduction of jammer power because of despreading is one of the benefits of the spreading gain. Because the power of the jammer is concentrated into a shorter time, the effective power of the jammer increases as the duty cycle increases. This effect is shown as the scaling of the signal to interference ratio (SIR) by the duty cycle in (2.17). Equation (2.17) simplifies (2.16) by assuming bit errors caused by the pulsed jammer happen much more often than bit errors from noise [37].

$$P_b = \rho Q\left(\sqrt{\frac{2E_b\rho}{N_j}}\right) \quad (2.17)$$

The BER of a FHSS link in a pulsed jamming environment can be analyzed with a similar method as a DSSS in a pulsed jamming environment. Assuming the jammer occupies the entire band of the spread waveform, we can again use equation (2.14) which describes the probability of bit error in a jamming environment.

The probability of a FHSS signal in AWGN is the same as an MFSK signal. The probability of bit error with no jammer is as shown in (2.18) [36]. In (2.18) there are  $M$  possible symbols and  $k$  bits per symbol. The BER is the sum of all possible probabilities of mistaking one symbol for another weighted by the probability of transmitting each symbol. Again,  $E_b$  is the energy per bit and  $N_0/2$  is the two sided noise power spectral density.

$$P_e = \frac{M}{2(M-1)} \sum_{n=1}^{M-1} \binom{M-1}{n} \frac{(-1)^{n+1}}{n+1} e^{\left(\frac{-n E_s}{n+1 N_0}\right)} \quad (2.18)$$

Under the worst case assumptions that the probability of bit error during jamming is 50% and assuming that the jammer has a duty cycle of  $\rho$ , the probability of bit error for a FH/SS signal afflicted by a pulsed jammer is

$$P_e = (1 - \rho) \frac{M}{2(M-1)} \sum_{n=1}^{M-1} \binom{M-1}{n} \frac{(-1)^{n+1}}{n+1} e^{\left(-\frac{n E_s}{n+1 N_0}\right)} + \rho \frac{1}{2}. \quad (2.19)$$

In shared spectrum the probability of bit error in a communications system is determined by the received signal power, the noise power, by the likelihood of interference, and the power of the interference. The bit error rate of a narrowband or spread spectrum communications link in the presence of an AWR can be calculated assuming AWGN, zero ISI received symbols, and no timing errors in the receiver. Received interference from an AWR will typically be much greater than the received power of the desired signal and much greater than the noise. This high power received interference allows the assumption that BER during jamming is equal to 50%. The concepts and methods to calculate the probability of bit errors for communications links in the presence of pulsed jammers, which parallel the calculations for probability of bit error of WLANs due to interference from an AWR, is used to develop the final metrics for BER of WLAN links in shared spectrum.

## 2.5 Radar Systems

Radar is a system that uses electromagnetic waveforms to detect, locate, and measure properties of objects at a distance. Any aircraft, ship, vehicle, terrain feature, and weather phenomenon that reflect a sufficient amount of transmitted electromagnetic energy back to the radar receiver can be detected and analyzed. Traditionally, objects of interest to radar are called targets and returned scatters not of interest are called clutter [22].

Target presence, range, and angular position of targets are the fundamental measurements for pulsed radar. The range of a target from the radar is determined by

measuring the elapsed time between transmission of the pulse and receiving returned scatter. The angular position is determined by the beamwidth of the antenna and the position of the radar antenna as it sweeps  $360^\circ$  around the target area. Along with detection, range, and location, sophisticated processing can be employed on the received signal to extract other information. For example, AWRs display rain intensity and turbulence [21].

Figure 2-10 shows the operator's view of the information collected by the radar system. The presence of weather phenomenon is shown as colored areas over an axis showing range and angular position. Range is shown on the display as circles marked by tens of kilometers. Angular position is shown as  $0^\circ$  of azimuth on the y-axis and  $90^\circ$  on the x-axis. The different colors show rain intensity of the targets. Geographic data is overlaid on the display as red lines.

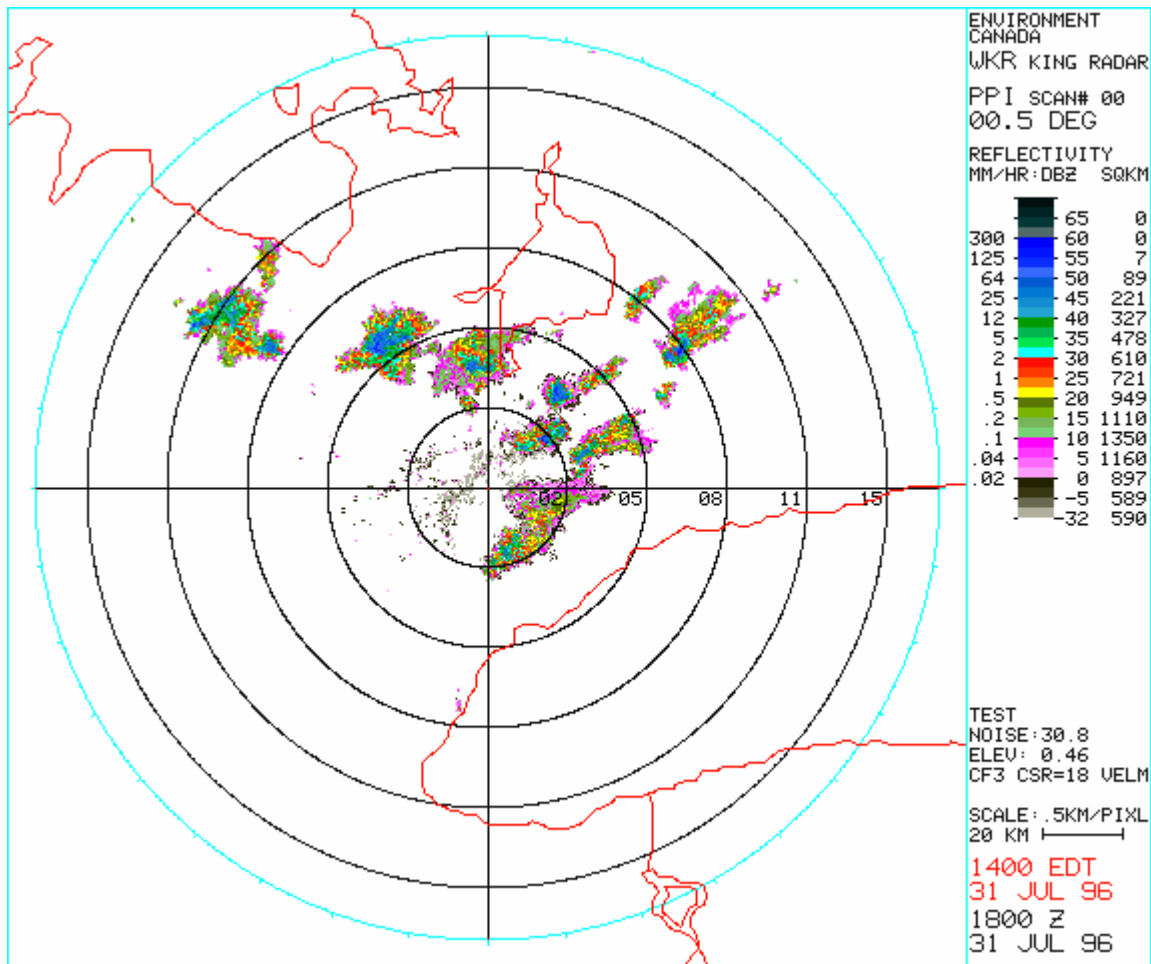


Figure 2-10. Weather Radar Display. This display is a digital plan position indicator (PPI) showing azimuth and range of targets (weather phenomenon). Colors of targets indicate rain reflectivity, and the display is overlaid with geographic data shown as red lines. Image used with permission from Environment Canada [38].

In the context of spectrum sharing between AWR and WLANs we are only interested in the coverage area of the radar. The coverage area is the area on the ground within the 3 dB beamwidth of a radar antenna pattern. We assume the coverage area is at the 0° azimuth position of the radar because this is the longest possible time of illumination as AWR fly directly over WLANs. Simple geometry using the beamwidth and distance from the radar to the ground along with the vertical tilt angle of the radar dish is used to calculate the coverage area. AWR beamwidths are typically from 2° - 5° degrees for both horizontal and vertical

directions (see Appendix C) [21, 22, 24]. Figure 2-11 shows a representative antenna pattern and identifies the beamwidth,  $\theta$ . The beamwidth, sidelobe ratios (relative gain between main lobe and sidelobe) and front-to-back ratio (relative gain between the main lobe and lobe directly opposite of the main lobe) is consistent with radars from [21, 22, 24, 25].

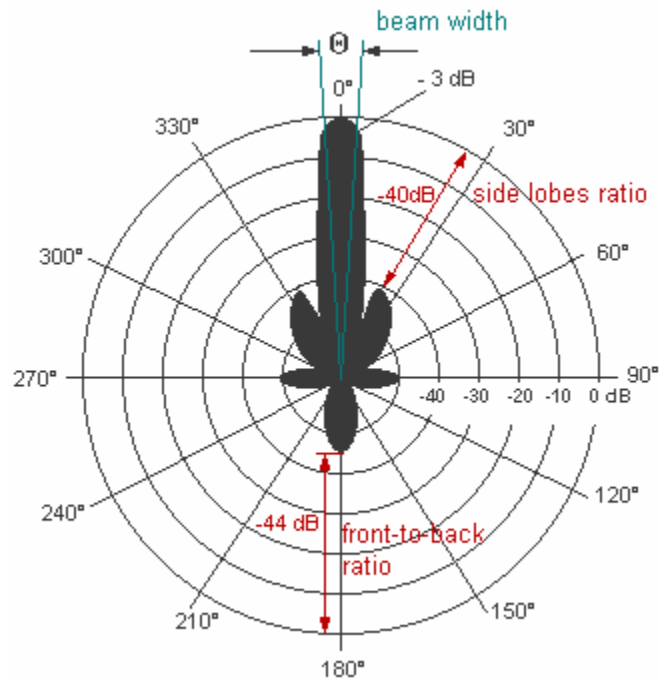


Figure 2-11. Antenna pattern. Sidelobes and the rear of the pattern are low compared to the main lobe. Image obtained from [24] used under term of the GNU Free Document License.

The method used to calculate coverage area and coverage areas used in the scenarios to analyze spectrum sharing is fully discussed in Chapter 3. The coverage area, (along with link density of WLANs, transmit power of WLANs links, radar receiver antenna gain) will determine the amount of interference received by the radar

The interference into a radar receiver results in a loss of desired targets. The loss of targets due to low levels of interference can be insidious in that they do not cause overt indications such as strobes on a radar display. A characteristic of radar detectors called the

constant false alarm rate (CFAR) detector explains the insidious nature of low level interference. Figure 2-12 shows the insidious effects of low level interference while Figure 2-13 shows that high levels of interference obscure targets, but interference is easily identified by the radar operator. [16]

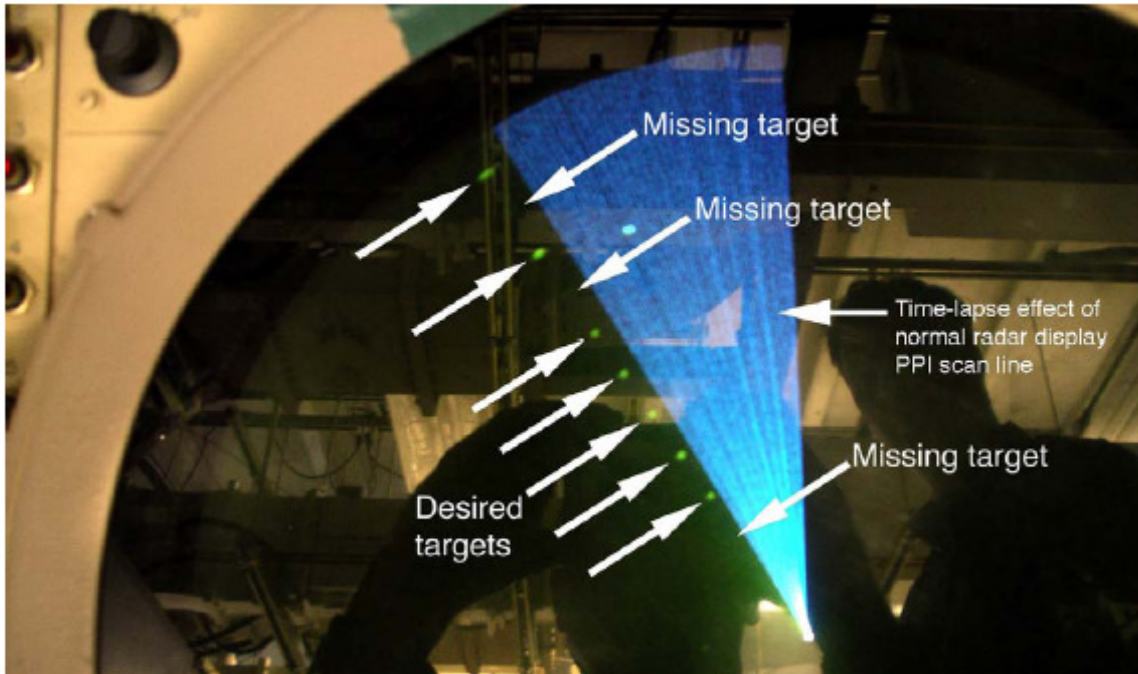


Figure 2-12. Lost targets due to low levels of interference shown by experiments by NTIA in [16].

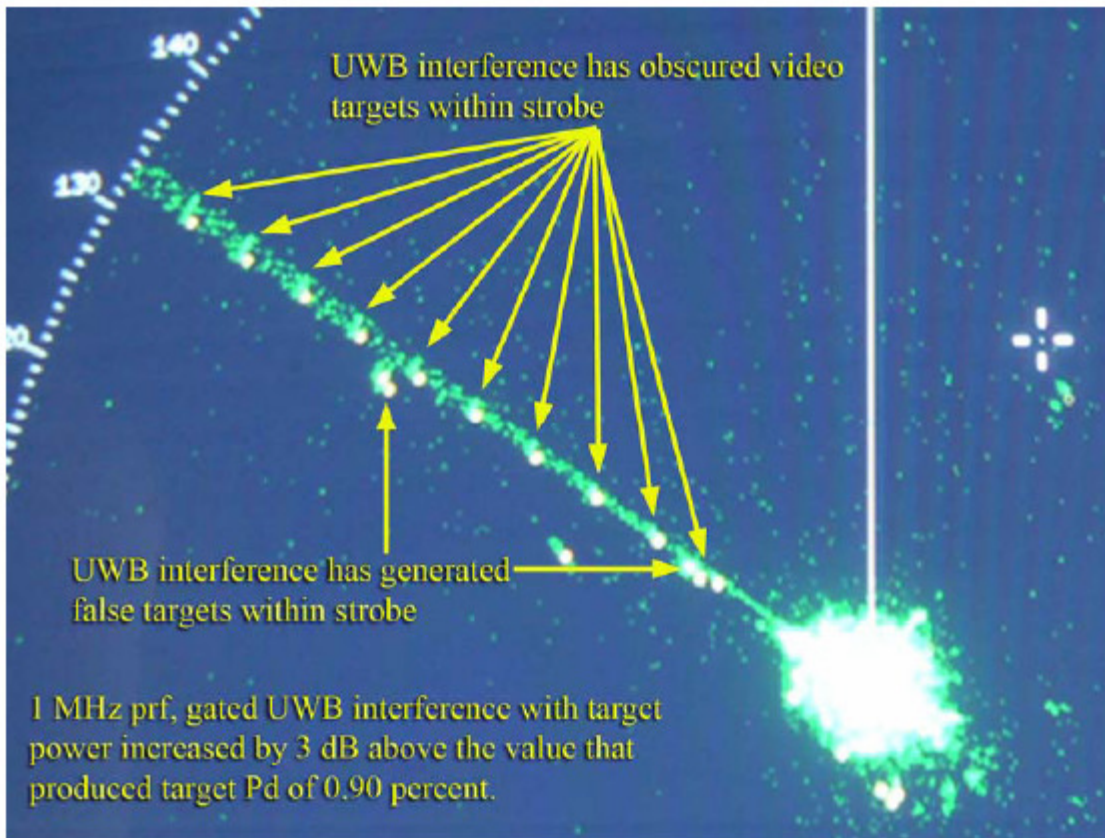


Figure 2-13. High levels of interference from a single direction cause an obscuring strobe on the radar display shown in experiments by NTIA in [16].

The likelihood that a target will be detected from reflected radar pulses, assuming that a target is present, is given by the probability of detection,  $P_d$ . The likelihood of the detector perceiving a target, when there is in fact no target, is called the probability of false alarm. These two probabilities cannot be simultaneously improved because they both increase with decreasing detector thresholds. If the output of the detector is greater than the threshold then a target is declared. If the output is less than the threshold, then no target is declared. High thresholds reject more false alarms but decrease the probability of detection. Low thresholds increase the probability of detection but also increase the probability of false alarm. Typical radars employ constant false alarm rate (CFAR) detectors. The detector holds the false alarm

rate constant by adjusting the detection threshold depending on signal power, level of noise, and level of clutter [16].

As the false alarm rate is held constant, the probability of detection decreases with additional noise, clutter, and interference. With less of these obscurities the threshold decreases, holding the false alarm rate constant but increasing the probability of detection. Interference causes the CFAR detector to automatically raise the detection threshold causing loss of targets without the operator's knowledge. Thus it is said that RF interference causes insidious degradation of performance. The maximum amount of interference tolerable by radar was determined analytically and experimentally in [16].

### **2.5.1 Maximum Allowable Interference into Airborne Weather Radar**

The NTIA report "Effects of RF Interference on Radar Receivers", [16], developed analytical results and presented experimental results showing the maximum allowable interference before degradations in AWR performance occur. Analytical results show that AWR are vulnerable to interference to noise ratios (I/N) greater than -14 dB. Experimental results show that I/N of -9 dB is the maximum allowable interference before detrimental effects are seen by the operator of AWRs. Interference to noise ratio is the ratio of interference power in watts relative to the noise power in watts. Thus the results of [16] state that the interference received by a radar must be held nearly an order of magnitude below the noise floor of the radar receiver. The noise floor of a typical AWR is -139 dBW ( $10^{-15}$  W) requiring extremely low levels of received interference on the order of  $10^{-16}$  W. From [16] it can be concluded that extremely low power transmissions from WLANs, or large physical separation, are required between AWR and WLANs to allow for spectrum sharing without harmful interference.

The block diagram in Figure 2-14 illustrates the test configuration used in [16]. Targets and interference were injected with a hardline coupling before the RF filter as opposed to radiated through the antenna. Hardline coupling allowed for precise

quantification of the levels of interference and its effect on radar performance, whereas, radiating targets and interference through the antenna could have caused undesired variations in the experimental data. A spectrum analyzer placed directly after the intermediate frequency (IF) filter was viewed to calibrate the I/N. The radar display after the detector and signal processing state was viewed to monitor the effects of the interference.

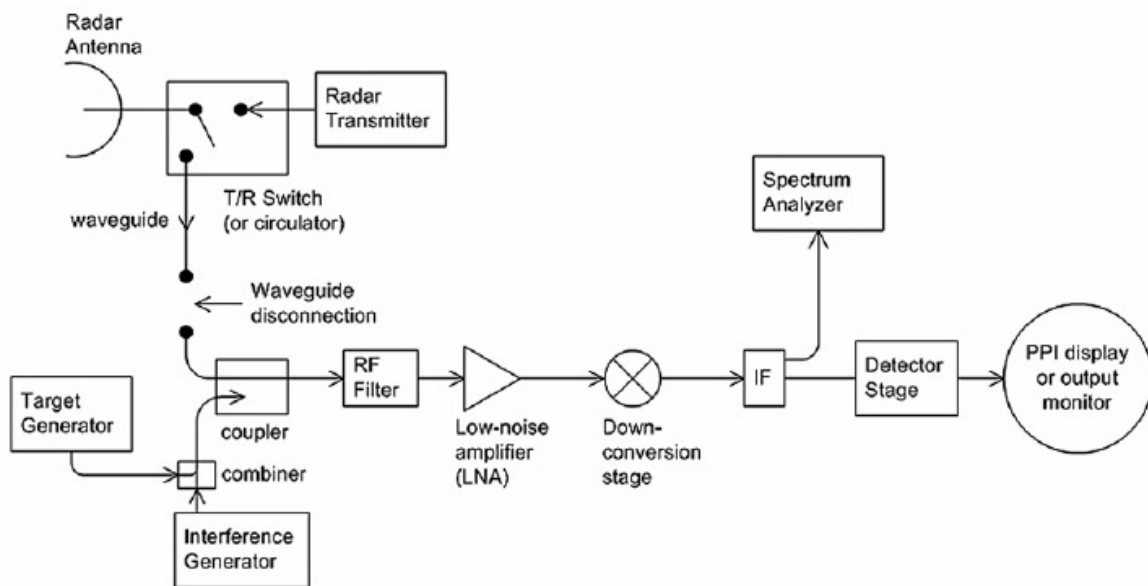


Figure 2-14. Block diagram of test configuration used in [16]. Synthetic targets and interference signals are injected before the radio frequency filter. A spectrum analyzer placed directly after the intermediate frequency filter is viewed to calibrate the interference to noise ratio, and the display after the detector/signal processor is viewed to monitor the effects of the interference.

Report [16] describes I/N measurements best by stating: “Whenever possible, the relative levels of interference,  $I$ , and receiver noise,  $N$ , were directly measured as I/N ratios within the IF section of each radar.... When no access was available to a radar’s IF section, then the radar receiver noise figure was measured and the I/N levels were computed.” When the I/N ratio could not be directly measured, noise power of the radar receiver was calculated using  $N = kT_e B_N$  as shown in (2.4). The equivalent noise temperature is

calculated from measured noise figure of the radar receiver using  $T_e = T_0 (F - 1)$  as defined in (2.5).

All emissions radiated by interferers will not necessarily contribute to interference power in the radar receiver. Any emissions outside of the IF bandwidth are rejected by the RF filter. To account for filtering of out of band interference [16] defines the on-tuned rejection factor (OTR). The OTR defines the lessened interference of emissions, in decibels, with bandwidths wider than the radar receiver IF section as shown in (2.20).

$$\left(\frac{I}{N}\right)_{IF} = \left(\frac{I}{N}\right)_T - OTR \text{ dB} \quad (2.20)$$

where:

$(I/N)_{IF}$  = interference to noise ratio in the bandwidth of the radar IF stage;

$(I/N)_T$  = interference to noise ratio that would occur if the radar IF bandwidth were equal to or wider than the bandwidth of the RF interference produced by the transmitter;

OTR = on-tuned rejection factor.

Report [16] defines the OTR, again in decibels, and all relevant parameters in (2.21)

$$\begin{aligned} OTR &= 0 && \text{for } B_{IF} \geq B_T \\ OTR &= 10 \log(B_T / B_{IF}) && \text{for } B_{IF} < B_T \end{aligned} \quad (2.21)$$

where:

$B_{IF}$  = radar receiver IF 3 dB bandwidth (Hz);

$B_T$  = transmitter 3 dB bandwidth of the interference signal (Hz).

## 2.6 Regulation of Spectrum Allocations

The National Telecommunications and Information Administration (NTIA), Federal Communications Commission (FCC), and the International Telecommunications Union (ITU) are regulatory bodies that coordinate standards and regulate spectrum. These

regulatory bodies allocate spectrum to services on a primary or secondary basis and set limits on maximum electromagnetic emissions in the occupied spectrum.

The NTIA “manages the Federal use of spectrum; performs cutting-edge telecommunications research and engineering, including resolving technical telecommunications issues for the Federal government and private sector; and administers infrastructure and public telecommunications facilities grants.”[39] The NTIA also aids the FCC in developing policy and engineering requirements. The NTIA line office, the Institute for Telecommunications Sciences (ITS), provides engineering support by reporting on research and experiments on the topic of spectrum sharing and interference into radar. Several references used in this thesis on engineering and research topics as well as policy and allocations topics were produced by the NTIA and its offices.

The primary means of information from the NTIA come from the NTIA Manual of Regulations and Procedures for Federal Radio Frequency Management (Red Book), [12]. The relevant parts of [12] for this thesis are:

- Chapter 4 provides a table of spectrum allocations and associated footnotes.
- Chapter 5 provides definitions of electromagnetic emissions measurements and requirements.
- Chapter 6 provides definitions of services for allocated spectrum.
- Chapter 10 provides policies and procedures for submission of electromagnetic compatibility reviews for telecommunications systems.

The FCC is responsible for “processing applications for licenses and other filings; analyzing complaints; conducting investigations; developing and implementing regulatory programs; and taking part in hearings.”[40]. The FCC is the regulatory body responsible for managing spectrum allocations and maintaining policy. The references from the FCC used in this thesis are primarily on the topic of policy and allocations which are codified in Title 47 of the Code of Federal Regulations, [41]. Relevant parts of [41] for this thesis are:

- Part 2.1 provides legal definitions of all terms used by the FCC and NTIA.
- Part 2.100 provides a statement of international regulations in force and a definition of how allocations are made.
- Part 2.105 provides definitions of secondary and primary services.
- Part 2.106 codifies the spectrum allocations made by the FCC or NTIA.
- Part 15 defines the operation of unlicensed devices.

Currently the 9.3GHz to 9.5GHz spectrum is allocated on a primary basis to Radionavigation page; 4-47 of section 4.1.3 of [12]. FCC footnote US66 page 4-130 of section 4.1.3 of [12] states, “The use of the band 9300-9500 MHz by the aeronautical radionavigation service is limited to airborne radars and associated airborne beacons”. Devices licensed to operate outside of USA and devices which are listed as secondary users are not considered in this thesis.



## **Chapter 3**

# **Calculation of Interference Levels Caused by Wireless Local Area Networks in Airborne Weather Radar**

Airborne weather radar (AWR) is designated as the primary service at 9.3 GHz – 9.5 GHz requiring any other system operating at these frequencies not to cause harmful interference. The interference collectively produced by a large number of wireless local area networks (WLANs) inside the coverage area of an AWR is measured by the total effective interference. Any interference above the maximum allowable interference level (an interference to noise ratio) is harmful to the AWR and must be avoided for spectrum sharing to be feasible. To find these values, the coverage area of AWR is defined and quantified using assumptions about aircraft flight patterns and AWR characteristics. The coverage area and number of links causing interference is calculated in two scenarios that represent the worst case for spectrum sharing: WLANs operating under a heavily traveled jetway and operating under a Victor airway. The scenarios and metrics developed in this chapter are used to determine the feasibility of spectrum sharing between AWR and WLANs.

### **3.1 Assumptions for Interference Analysis**

Several assumptions must be made to conduct analysis of spectrum sharing between airborne weather radar (AWR) and wireless local area networks (WLANs). The possible separations between AWR and WLANs, which determine the received interference, is limited by the flight characteristics of AWR capable aircraft. The area on the ground, called

the coverage area, that defines where interference can occur between an AWRs and WLANs is determined by the aircraft altitude, antenna beamwidth, and antenna tilt angles of the AWR. WLAN links which are assumed to be uniformly distributed within the coverage area cause interference to the AWR. The density of the uniformly distributed links is based on data collected by the US Census Bureau. These assumptions and metrics are applied to specific scenarios in Chapter 5, completing the feasibility analysis.

### **3.1.1 Flight Characteristics of Airborne Weather Radar Capable Aircraft**

The Federal Aviation Administration (FAA) regulates aircraft flight in the United States by establishing and regulating air routes. Air routes most commonly traveled by airborne weather radar capable aircraft are jetways and Victor airways. Interference analysis is conducted for these two types of air routes because that is where the majority of AWRs are expected. Radar instrumentation is required in jetways and many aircraft using Victor airways also carry AWR [14].

Arrival and departure of aircraft into airports is not considered in this thesis and the scope of analysis is limited to en route flight patterns. En route aircraft must stay within their designated flight path as determined by air traffic control (ATC). A minimum of 3700 meters (2 nautical miles) must be maintained in front of, behind, and to the sides of all aircraft. The minimum vertical separation between aircraft is 305 meters (1000 feet).

Jetways are airspace routes established by the FAA to carry air traffic at altitudes from 5486 meters (18,000 feet) mean sea level to 18,228 meters (60,000 feet) mean sea level. Mean sea level (MSL) is the height of an object referenced from sea level. The FAA defines jetways as Class A airspace, which are governed by strict aircraft separation rules. A jetway is the heaviest traveled airspace by aircraft carrying AWR; therefore, a scenario considering WLANs operating under a jetway is an indicator of worst case performance of WLANs and AWR in shared spectrum. Typical velocities of aircraft traveling in jetways are around 250 meters per second (about 485 knots). [14, 15]

Victor airways are another type of airspace route, but regulate air traffic at much lower altitudes when compared to jetways. Victor airways, defined as Class E airspace by the FAA, are at altitudes from 366 meters (1,200 feet) above ground level (AGL) to 5486 meters (18,000 feet) MSL. Class E airspace is governed by aircraft separation rules which are maintained visually, or by radar and air traffic control. A Victor airway is the lowest altitude route in which aircraft carry AWR; therefore, this scenario is also an indicator of worst case performance for AWR and WLANs operating in shared spectrum. Typical velocities of AWR capable aircraft traveling in Victor airways will be between 100 and 200 meters per second (about 200 - 390 knots). [14, 15]

The possible altitudes of AWR capable aircraft are bounded by the regulations for jetways and Victor airways, setting the bounds of possible coverage area size. The size and distance of coverage areas will determine the amount of received interference from WLANs into an AWR.

### **3.1.2 Typical Airborne Weather Radar**

AWR specifications vary, but some generalizations can be made to create a typical AWR to use in estimating performance. Specifications were collected from [16, 21, 42-44], among other sources, and combined to form typical AWR with the parameters shown in Table 3-1.

<b>Parameter</b>	<b>Value</b>
Peak Power	10,000 W
Pulse Repetition Frequency	1000 pps
Pulse Width	1 $\mu$ s
Duty Cycle	0.001 (0.1%)
Antenna Gain	32 dB
Vertical Beamwidth (3 dB)	5°
Horizontal Beamwidth (3 dB)	5°
Equivalent Power Vertical Beamwidth	5.2°
Equivalent Power Horizontal Beamwidth	5.2°
Tilt Angle	-15° to 15°
Scan Sector	90°
Receiver Bandwidth	2 MHz
Receiver System Noise Temperature	1580 K
Receiver Noise Floor	-133.6 dBW
Maximum Allowable Received Interference Power	-142.6 dBW
Maximum Allowable Interference ratio (interference to noise ratio, I/N )	-9 dB

Table 3-1. Typical airborne weather radar specifications collected from [16, 21, 42-44]

The level of interference received by the AWR from a WLAN is determined by the antenna gain in dB, beamwidth in degrees, and receiver bandwidth in MHz, transmit power of WLAN links in watts, and link density in links per square kilometer. The parameters peak power in watts, pulse repetition frequency in pulses per second, and pulse width in seconds determine the level of interference to WLANs. Interference into an AWR is received within an area covered by the radiation pattern of the AWR antenna.

The vertical and horizontal beamwidths determine the area from which interference is received by an AWR. AWR antennas typically use a pencil beam shape; accordingly, the gain of the antenna can be assumed to follow a pattern which diminishes by the cosine of the

angle away from peak gain [21, 22]. Typically, the 3 dB beamwidth is considered sufficient to determine the performance of a radar antenna, but for interference analysis, the entire antenna pattern must be considered to properly account for all received interference. Interference can be received into the AWR through regions in the main lobe beyond the 3 dB beamwidth or through side lobes of the antenna pattern. To conduct a tractable analysis, the antenna can be modeled by a single conical main lobe with constant gain. This conical main lobe is defined by the equivalent power beamwidth, the width of a constant gain region which provides the same effective received power as the main lobe of the reference antenna pattern. The constant gain pattern is compared to the reference pattern in Figure 3-1.

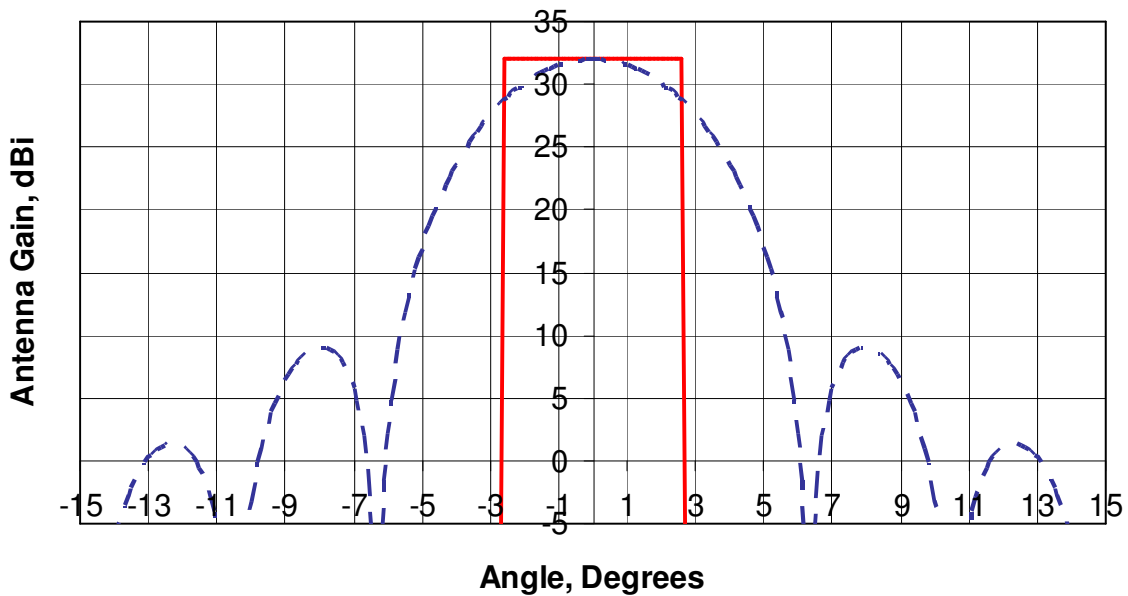


Figure 3-1. Antenna pattern model for interference analysis of an AWR with a 3 dB beamwidth of 5°. The constant gain pattern, shown as the solid red line, that results in equivalent received power has a beamwidth of 5.2° null to null and a constant gain of 32 dBi. The reference pattern, shown as the blue dashed line, varies by the cosine of the angle from peak gain. The mainlobe peak is at 32 dBi, the first sidelobe peaks at 9 dBi and the second sidelobe peaks at 1.3 dBi.

The radar beam is controlled in the direction perpendicular to the horizon by the tilt angle. The tilt angle is measured from the horizon level of the aircraft to the center of the beam. In this thesis, positive tilt angles point towards the Earth and negative tilt angles point

upwards. The recommended tilt angle for aircraft in Victor Airways is  $0^\circ$  to detect hazardous weather conditions. Aircraft in jetways are assumed to be using a tilt angle of  $1^\circ$  below horizontal to detect hazardous weather at the maximum possible distance [45, 46]. For spectrum sharing to be feasible, the total effective interference received from WLANs within the antenna radiation pattern must be less than the maximum allowable received interference power. The maximum allowable interference is an interference to noise level of -9 dB as discussed in [16].

### **3.1.3 Link Densities for Wireless Local Area Networks**

Link density is the number of WLAN links operating per unit area. This value is used to quantify the number of links inside a coverage area. Link density can be quantified by finding the average housing unit density and assuming a number of links per housing unit. Housing unit densities are 0 – 40 housing units per square kilometer for typical suburban areas and 40 – 1000 housing units per square kilometer in heavy suburban areas (e.g. suburbs of Los Angeles, New York, Washington D.C.). Heavily populated urban areas have 1000 – 2000 housing units per square kilometer consisting of mixed apartment and single family homes [47] [48]. WLAN transmissions are heavily attenuated in urban areas due to losses from line of sight obstructions and building penetration losses [35]. Because of the high attenuation in urban areas, the worst case of interference is in heavily populated suburban areas where there are a large number of links but line of sight is still maintained to an AWR. One thousand houses per square kilometer are assumed, with each house operating one WLAN device at a time. Links are assumed to be distributed uniformly in a given area to operate continuously.

The sizes of AWR coverage areas are commensurate with the area covered by large metropolitan areas; accordingly, the uniform distribution assumption is valid. The areas covered by large cities is on the order of one thousand square kilometers. For example, Los Angeles and its suburbs cover an area of about 50 miles (80 kilometers) by 25 miles

(40 kilometers) with a coverage area of 1,250 miles (3,200 square kilometers). The size of large cities on the East Coast is comparable to West Coast cities. New York and its suburbs cover an area of about 30 miles (48 kilometers) by 20 miles (32 kilometers) with a coverage area of 600 square miles (1,554 square kilometers). [49]

### **3.2 Coverage Area of Airborne Weather Radar**

The flight patterns and assumptions in Section 3.1 established the parameters necessary to begin analysis of airborne weather radar (AWR) and wireless local area network (WLAN) interference. The first step in this analysis is to determine the coverage area in which the interference between WLANs and an AWR will occur. The coverage area is defined by the vertical and horizontal antenna pattern of an AWR measured by the equivalent power beamwidth. The equivalent power beamwidth defines a rectangular antenna pattern that has the same gain and which produces the same received power as a reference antenna pattern. With this model, the radar antenna will emit and receive all emissions in a cone shaped volume. The cone is intersected by a plane representing the Earth, creating an elliptical coverage area on the ground. This area is shown in Figure 3-2. Any WLANs in this elliptical area will contribute to interference into an AWR according to the transmit power of each individual WLAN device, distance from the AWR, and radar receiver bandwidth in relation to interferer bandwidth (accounted for by the on-tune rejection factor [OTR]). The level of interference must be less than -142.6 dBW, which is 9 dB below the assumed radar receiver noise floor of -133.6 dBW.

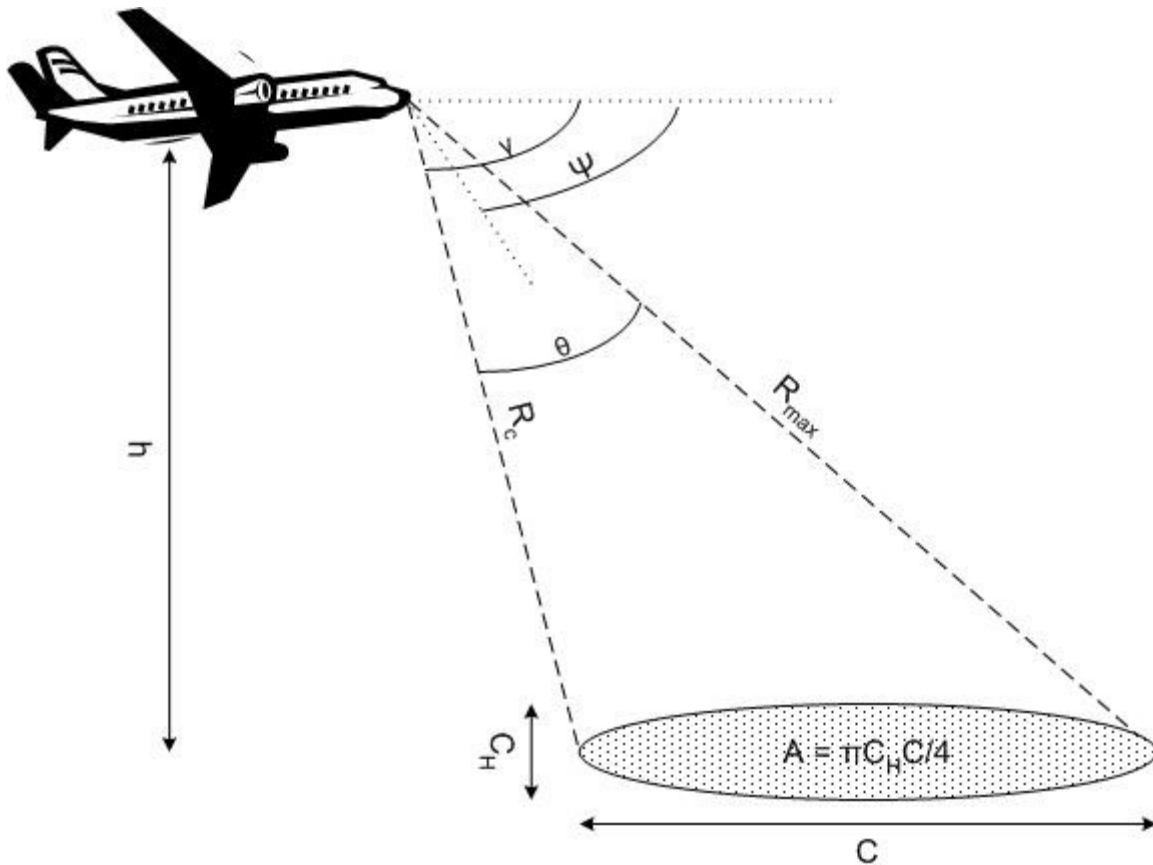


Figure 3-2. Coverage area for an aircraft at altitude  $h$  with a beamwidth,  $\theta$ , and tilt angle,  $\psi$ . The angle from the horizon to the beam,  $\gamma$ , is one half the beamwidth plus the tilt angle. The size of the coverage area is  $A$  with a major axis of  $C$  and a minor axis of  $C_H$ . The maximum and minimum possible separation between the AWR and WLAN links is  $R_{max}$  and  $R_c$ , respectively.

### 3.2.1 Radar Antenna Beam Pattern Model for Interference Analysis

Radar antennas are typically quoted as having beamwidths at the 3 dB points of the antenna main lobe. This 3 dB model of a radar antenna is not sufficient for interference calculation because sidelobes of the pattern can potentially collect significant amounts of interference. For the purpose of this analysis, the mainlobe of the radar antenna pattern is assumed to have a shape  $G(\theta)$  which varies by the cosine of the angle from peak gain over

the angular range of  $-90^\circ \leq \theta \leq 90^\circ$ . The peak gain is at  $0^\circ$  with the first sidelobe about 23 dB (or often lower in other models) below the peak [21, 22]. This antenna pattern, proposed for interference analysis by the National Telecommunications and Information Administration report “Mathematical Model for Radiation Patterns for Radar Antennas for Use in Interference Assessment”, is used as reference to develop the constant gain model [50]. The constant gain model is a variation of the reference pattern that provides a single rectangular lobe which produces the same effective received power as the entire front  $180^\circ$  of the reference pattern.

The process to determine the equivalent power beamwidth parallels the calculations for equivalent bandwidths. Let  $P_{eq}$  be the equivalent power that would be received by the reference model with peak gain normalized to 0 dB (linear ratio of 1), and the angle of peak gain equal to  $\theta_o$  in degrees. The equivalent received power is related to the equivalent beamwidth,  $BW_{eq}$  and peak received power  $|H(\theta_o)|^2$  in watts.

$$P_{eq} = BW_{eq} |H(\theta_o)|^2 \text{ watts} \quad (3.1)$$

The received energy from the cosine antenna pattern in terms of volts,  $H(\theta)$ , is [50]

$$H(\theta) = \frac{\cos\left(3.7353 \frac{\theta}{\theta_{3db}}\right)}{\left(1 - 5.6544 \left(\frac{\theta}{\theta_{3db}}\right)^2\right)} \text{ volts.} \quad (3.2)$$

The power received by the antenna,  $P$ , is

$$P = \int_{-\infty}^{\infty} |H(\theta)|^2 d\theta \text{ watts.} \quad (3.3)$$

Rearranging and setting  $P_{eq}$  equal to  $P$  results in the equivalent power beamwidth of

$$BW_{eq} = \frac{1}{|H(\theta_o)|^2} \int_{-\infty}^{\infty} |H(\theta)|^2 d\theta \text{ watts.} \quad (3.4)$$

The main lobe defined by the equivalent beamwidth is scaled by the peak gain of the antenna to produce the antenna pattern shown in Figure 3-1. The pattern is assumed to be identical in the horizontal and vertical direction resulting in a pencil beam shape in three dimensions.

A typical AWR has a gain of 32 dB in the main lobe and 3 dB vertical beamwidth of 5° (null to null beamwidth is approximately from -6° to 6°). Under the constant gain model, the main lobe extends from -2.6° to 2.6° with a gain of 32 dB over this entire range. This beam pattern model, shown in Figure 3-1, simplifies the coverage area calculation by simplifying the three dimensional reference antenna pattern into an area of constant gain which is then projected onto the Earth to create an elliptical coverage area.

### 3.2.2 Coverage Area Defined

The AWR is mounted on a moving aircraft, creating a conical spot beam which sweeps over WLANs in the path of the aircraft. The resulting coverage area, shown in Figure 3-2, is described by an ellipse created by the Earth's plane intersecting the conical radar beam. The Earth is assumed to be flat. Because the radar beam is projected well forward of the aircraft, the elliptical coverage area has a major axis determined by the antenna's vertical equivalent beamwidth and a minor axis determined by the horizontal equivalent beamwidth.

The horizontal coverage path (minor axis),  $C_H$ , and vertical coverage path (major axis),  $C$ , multiplied by  $\pi/4$  gives the coverage area,  $A$ . The minimum possible and maximum possible separations between the AWR and WLANs are  $R_c$  and  $R_{max}$ , respectively. These separations are determined by the aircraft altitude,  $h$ , and  $\gamma$  which is one half the equivalent power beamwidth,  $\theta$ , plus the tilt angle,  $\Psi$ . The minor axis of the coverage area,  $C_H$ , is determined by the angular resolution equation

$$C_H = 2 \left[ \frac{R_{max} + R_c}{2} \right] \sin \left( \frac{\theta}{2} \right), \quad (3.5)$$

where  $\theta$  is the equivalent beamwidth and  $\frac{R_{max} + R_c}{2}$  is the range to the center of the coverage region [22].

To find the vertical coverage,  $C$ , the coverage area can be described in two dimensions by a triangle. The first case, shown in Figure 3-3, is when the radar beam completely terminates both legs of the triangle onto the ground as the aircraft flies along the air route. In this case, the coverage area is an ellipse with a major axis of the coverage path which is determined by the equivalent vertical beamwidth. The second case, Figure 3-4, shows that the beam is projected past the horizon; in this case, the Earth plane terminates only one leg of the triangle representing the beam resulting in a truncated ellipse.

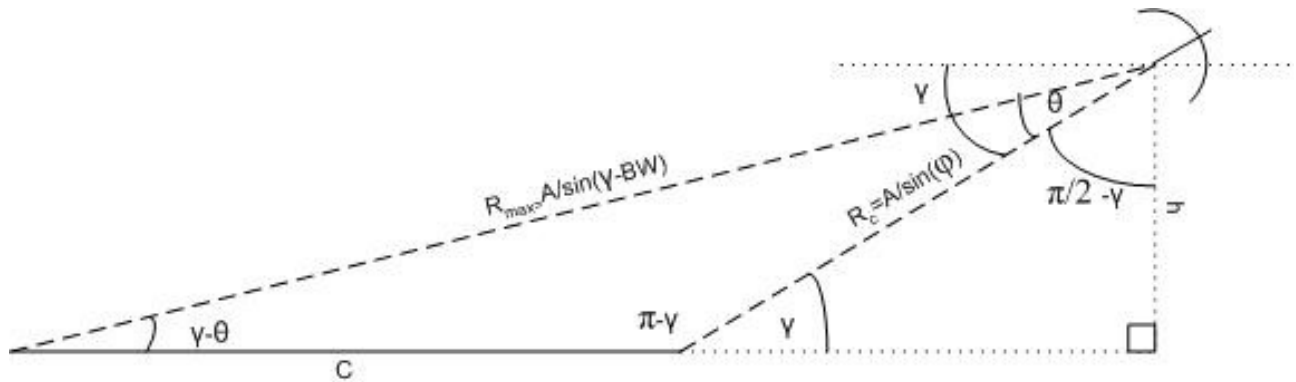


Figure 3-3 : Coverage area for vertical beamwidth less than tilt angle. The dashed lines represent the radar beam. The solid line is the coverage path,  $C$ . The dotted lines mark lines used to aid calculations. The altitude of the aircraft is  $h$  and the beamwidth of the AWR is  $\theta$ . The angle from the horizon to the beam is one half the beamwidth plus the tilt angle,  $\gamma$ . The maximum and minimum possible separation between the AWR and WLAN links is  $R_{max}$  and  $R_c$ , respectively.

From Figure 3-3 the coverage path,  $C$ , and coverage area can be determined. To determine  $C$ , the Law of Sine's as shown in (3.8) and (3.9) is used. Using the identities

$$\sin(\pi - \gamma) = \sin(\gamma) \quad (3.6)$$

and

$$R_{max} = h / \sin(\gamma - \theta), \quad (3.7)$$

the coverage path can be found in terms of known parameters: aircraft altitude, AWR tilt angle, and AWR vertical beamwidth. Assuming an elliptical coverage area, the coverage area,  $A$ , is found by multiplying the vertical coverage path by the horizontal coverage path and by  $\pi/4$ . The area of the ellipse that results from intersecting the beam cone with the Earth plane is shown in (3.10). Equation (3.11) shows the number of links,  $N_{WLAN}$ , given the coverage area and the link density,  $\eta$ .

$$\frac{C}{\sin(\theta)} = \frac{R_{max}}{\sin(\pi - \gamma)} \quad (3.8)$$

$$C = \frac{h \sin(\theta)}{\sin(\gamma - \theta) \sin(\gamma)} \text{ meters} \quad (3.9)$$

$$A = \frac{\pi C C_H}{4} \text{ square meters} \quad (3.10)$$

$$N_{WLAN} = A \eta \text{ links} \quad (3.11)$$

The previous case is valid when the AWR beam does not extend past the horizon, causing the long and short legs of the beam to intersect with the Earth plane. If the tilt angle is less than one half the beamwidth or if the beam projects past the horizon, then the long edge of the beam does not terminate on the ground and a different geometry shown in Figure 3-4 exists.

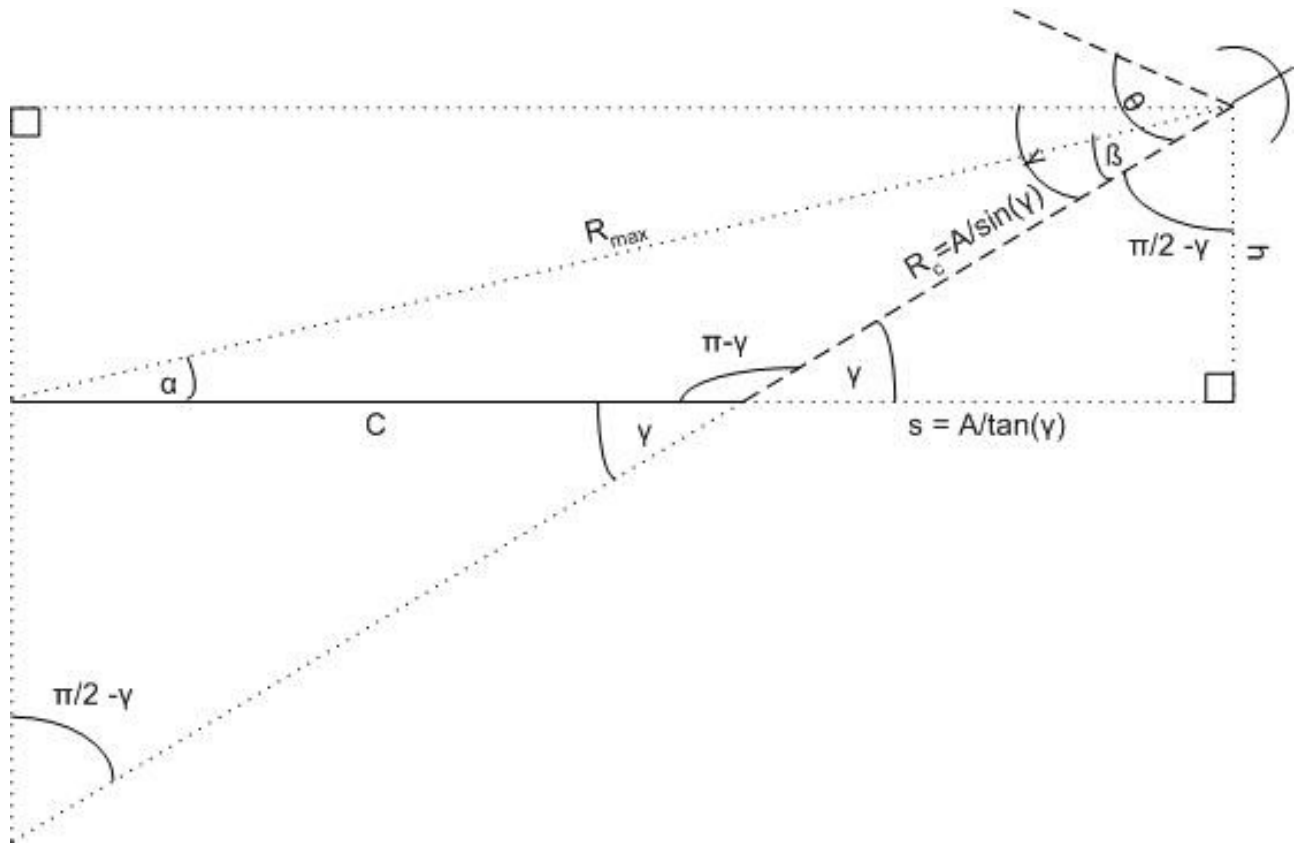


Figure 3-4 : Coverage area for beamwidth greater than tilt angle. The dashed lines represent the radar beam. Notice that only one leg of the triangle intersects with the ground plane, the other extends upward. The solid line is the coverage path,  $C$ . The dotted lines mark lines used aid calculations. The altitude of the aircraft is  $h$  and the beamwidth of the AWR is  $\theta$ . The angle from the horizon to the beam is one half the beamwidth plus the tilt angle,  $\gamma$ . The maximum and minimum possible separation between the AWR and WLAN links is  $R_{max}$  and  $R_c$ , respectively.

For the case in Figure 3-4, to determine the coverage path,  $C$ , the length  $C + s$  is found using the Law of Cosines as show in (3.12). This length is the base of the large dotted right triangle whose hypotenuse is  $R_{max}$ . Through algebraic manipulations and trigonometric identities shown in (3.13) and (3.14), the length of the coverage path, (3.15), can be found if  $R_{max}$  is known.

$$\cos(\alpha) = \frac{C + s}{R_{max}} \quad (3.12)$$

$$C = R_{\max} \cos(\alpha) - \frac{h}{\tan(\gamma)} \text{ meters} \quad (3.13)$$

$$C = R_{\max} \cos\left(\sin^{-1}\left(\frac{h}{R_{\max}}\right)\right) - s \quad (3.14)$$

$$C = R_{\max} \sqrt{1 - \left(\frac{h}{R_{\max}}\right)^2} - \frac{h}{\tan(\gamma)} \text{ meters} \quad (3.15)$$

In the second case,  $R_{\max}$  ranges from  $R_c$  to the horizon resulting in very large coverage areas. The maximum value of  $R_{\max}$  is at the horizon because the Earth is modeled as a flat plane and any interferers over the horizon do not produce harmful interference. The distance to the horizon is

$$D = \sqrt{2kR_e h} \text{ meters} , \quad (3.16)$$

where  $k = 4/3$ ,  $R_e =$  earth radius = 6,380 km,  $h =$  height of aircraft above ground in meters [22]. Using (3.16),  $R_{\max}$  is set to 432 kilometers away for aircraft in jetways and 288 kilometers away for aircraft in Victor airways.

The time when the communications system is in the coverage area is the service time,  $t_s$

$$t_s = \frac{1}{\mu} = \frac{C}{v} \text{ seconds} . \quad (3.17)$$

The coverage path length is  $C$ , and  $v$  is the velocity of the plane: 200 meters per second in Victor airways and 250 meters per second in jetways. The metric  $\frac{1}{\mu}$  is used as the service time in the queuing theory analysis of the number of interferers; its inverse is the departure rate.

Both cases of coverage regions are needed to find the coverage area. The specific case is chosen depending on the relationship between the tilt angle and the antenna

beamwidth. The tilt angle for each region is defined as the angle between horizontal and the center of the antenna main lobe. The coverage paths and coverage areas are found by varying the altitudes and tilt angles as required by the scenarios defined in Section 3.4. From the coverage area, the total number of WLAN transmitters is found by multiplying the link density with the coverage area.

### 3.3 Tools for Analysis of Interference

The coverage area and the number of wireless local area network (WLAN) links in the coverage area have been defined in Section 3.1 and 3.2; this section now uses the number of WLAN links, the coverage area, and the path loss equation to develop the metric of total effective interference. The total effective interference estimates the received interference level into an airborne weather radar (AWR). For spectrum sharing to be possible without causing degradations of performance to an AWR, the level of interference must be below the maximum allowable received interference level as established in Section 3.1.2, Table 3-1, given an interference to noise ratio of -9 dB in the radar receiver.

#### 3.3.1 Total Effective Interference into AWR

The interference received by an AWR from a single WLAN link, assuming a clear line of sight path between the AWR and WLAN is modeled by the free space path loss equation in (3.18). Clear line of sight causes the worst possible case interference, thus this analysis gives the maximum possible interference level.

$$P_r = \frac{P_t G_t G_r \lambda^2}{(4\pi)^2 R^2 L_{misc}} \text{ watts} \quad (3.18)$$

The transmitter power and antenna gain of the WLAN link are  $P_t$  and  $G_t$ . The AWR antenna gain is  $G_r$ . Wavelength,  $\lambda$ , at the center of the 9.3 GHz – 9.5 GHz band is assumed.

The separation between the AWR and WLAN transmitter is  $R$  and miscellaneous losses,  $L_{misc}$ , take into account any building/environment penetration losses or system component losses. Wavelength is 9.35 GHz and typical values:  $G_t = 32$  dB,  $G_r = 0$  dB and  $L_{misc} = -7$  dB are assumed. Miscellaneous losses of 6 dB are attributed to absorption losses as the signal penetrates the indoor environment and system losses provides the additional 1 dB [35]. Under these assumptions the received power into the AWR from a single link,  $P_r$ , becomes a function of the transmit power of the WLAN transmitter,  $P_t$ . The separation,  $R$ , is defined by the scenarios described in Section 3.4. The inference from all WLAN links in the coverage area is calculated to find the total effective interference in watts.

The total effective interference is calculated by finding the mean interference from the coverage area, and multiplying this mean by the total number of links in the coverage area. The mean interference received in the coverage area,  $I$ , is a random variable defined by a transformation of the uniformly distributed links. The number of links is assumed to be 1000 links per square kilometer to model links in a densely populated metropolitan area such as Los Angeles or New York. The random variable,  $R$ , models the separation of these uniformly distributed WLAN links from the AWR. The closest link in a region has a separation of  $R_c$  and the furthest of  $R_{max}$  as shown in Figure 3-3 and Figure 3-4. The mean interference,  $E[I]$  in watts, as a function of distance between the WLAN transmitter and AWR receiver,  $r$  in meters, is

$$E[I] = \int_{R_c}^{R_{max}} g(r) f_R(r) dr, \quad \begin{aligned} f_R(r) &= \frac{1}{R_{max} - R_c} \\ g(r) &= \frac{P_t G_t G_r \lambda^2}{(4\pi)^2 L_{misc} r^2} \end{aligned} \quad (3.19)$$

where the probability density function (pdf) of  $R$  is a uniform distribution  $f_R(r)$  [51]. The function,  $g(r)$ , is the received power of a signal as a function of distance which transforms

the random variable  $R$  to the random variable for the received interference,  $I$ . We assume the coverage area is densely loaded with links such that a continuous pdf can be assumed [51].

The derivation to represent  $I$  in terms of  $R_{max}$  and  $R_c$  is shown in (3.20), (3.21), (3.22), and (3.23). The result is that the mean of the received interference by an AWR is derived from the path loss equation where the value for separation is the product of the nearest and furthest possible WLAN transmitter.

$$E[I] = \int_{R_c}^{R_{max}} \frac{P_t G_t G_r \lambda^2}{(4\pi)^2 L_{misc} r^2} \left[ \frac{1}{R_{max} - R_c} \right] dr \quad (3.20)$$

$$E[I] = \frac{P_t G_t G_r \lambda^2}{(4\pi)^2 L_{misc}} \left[ \frac{1}{R_{max} - R_c} \right] \int_{R_c}^{R_{max}} \frac{1}{r^2} dr \quad (3.21)$$

$$E[I] = \frac{P_t G_t G_r \lambda^2}{(4\pi)^2 L_{misc}} \left[ \frac{1}{R_{max} - R_c} \right] \left( \frac{-1}{r} \right) \Big|_{R_c}^{R_{max}} \quad (3.22)$$

$$E[I] = \frac{P_t G_t G_r \lambda^2}{(4\pi)^2 L_{misc} (R_{max} R_c)} \text{ watts} \quad (3.23)$$

Interfering WLAN links are uniformly distributed across the coverage area. Consequently, the number of links can be multiplied by the mean received interference,  $E[I]$ , to obtain the total received interference power,  $I_{total}$ , as shown in (3.24),

$$I_{total} = E[I \cdot \eta A] = \eta A \cdot E[I] \text{ watts}, \quad (3.24)$$

where  $A$  is the coverage area in square meters and  $\eta$  is the link density in links per square kilometer.

The on-tune rejection factor (OTR) defined in [16] and fully discussed in Section 2.5.1 has thus far been excluded for clarity. The OTR is now reintroduced, in (3.25), to complete the derivation of total effective interference. The OTR reduces the total interference by accounting for interference filtered by the AWR receiver before the

intermediate frequency (IF) stage. The inclusion of the OTR factor is necessary because all interference calculations have been calibrated at the IF stage of radar receivers.

$$\begin{aligned} OTR &= 0 && \text{for } B_{IF} \geq B_T \\ OTR &= 10 \log(B_T / B_{IF}) && \text{for } B_{IF} < B_T \end{aligned} \quad (3.25)$$

In decibels, the total effective interference is

$$I_{effective} = 10 \log(I_{total}) - OTR \text{ dBW} . \quad (3.26)$$

Equation (3.24) or (3.26) can be extended to include other reductions or sources of interference depending on the scenarios defined in Section 3.4 and specific WLAN defined in Chapter 4.

### **3.3.2 Probability of Exceeding Maximum Allowable Received Interference Power into Airborne Weather Radars**

The likelihood that the total interference received by an AWR exceeds the maximum allowable received interference power determines the feasibility of spectrum sharing between wireless local area networks and airborne weather radar. This likelihood depends on the likelihood that a specified number of WLAN links are transmitting inside the coverage area of the AWR. The total interference was defined as a function of the number of WLAN links inside a coverage area in (3.24). In this section we introduce the possibility that not all WLAN links in the coverage area are interfering with the AWR. Non-interfering WLAN links could be operating on frequencies different than the radar receiver or transmitting intermittently. If necessary, gains or losses represented by the on-tune rejection factor or other conditions can be included as the scenario and WLAN type requires.

The probability of a single WLAN link inside the coverage area causing interference to a present AWR is the basic statistic from which the likelihood of harmful interference is derived. The event,  $X$ , of a single WLAN link inside the coverage area causing interference

to a present AWR has probability  $\rho$  as shown in (3.27): the probability of event  $X$  is a Bernoulli trial with a mean of  $\rho$ . A single WLAN device can either be causing interference, event  $X$ , or not causing interference, event not  $X$ .

$$P[X | \text{AWR is present}] = \rho \quad (3.27)$$

From the basic statistic,  $P[X]$ , the probability of at least one occurrence of event  $X$  is shown in (3.28) given a link density,  $\eta$ , a coverage area,  $A$ , and presence of a radar.

$$P[X | \text{AWR is present}, \eta, A] \quad (3.28)$$

Link density and coverage area are treated as constants, providing the result shown in (3.29). The expected number of interferers  $E[P[X | \text{AWR is present}, \eta, A]]$  is shown in (3.30). Again because  $\eta$  and  $A$  are constants, the expected number of interferers is the total number of WLAN links in a coverage area multiplied by the probability that they are transmitting into the AWR receiver.

$$P[X | \text{AWR is present}, \eta, A] = P[X | \text{AWR is present}] \cdot \eta A \quad (3.29)$$

$$E[P[X | \text{AWR is present}, \eta, A]] = \rho \cdot \eta A \quad (3.30)$$

The Bernoulli trial for each WLAN in the coverage area represented by (3.28) can be summed to create a binomial random variable,  $S_{\eta A}$ . The random variable  $S_{\eta A}$  is the total number of interfering links whose distribution represents the probability that  $m$  WLAN links in a coverage area are interfering with an AWR. The number of links,  $\eta A$ , is the number of trials in the binomial distribution. The probability that  $m$  WLAN links are interfering given a user density,  $\eta$ , a coverage area,  $A$ , and presence of a radar is shown in (3.31). Equation (3.32) shows the probability of  $m$  or fewer WLAN links are interfering with an AWR.

$$P[S_{\eta A} = m | \text{AWR is present}, \eta, A] = \binom{\eta A}{m} \rho^m (1 - \rho)^{\eta A - m} \quad (3.31)$$

$$P[S_{\eta A} \leq m | \text{AWR is present}, \eta, A] = \sum_{k=0}^m \binom{\eta A}{k} \rho^k (1-\rho)^{\eta A - k} \quad (3.32)$$

The maximum number of allowable links,  $m$ , can be found by manipulating (3.24),  $I_{total} = E[I \cdot \eta A] = \eta A \cdot E[I]$ . The resulting equation, (3.33), is found by replacing the number of WLAN users,  $\eta A$ , with  $m$ , and total effective interference,  $I_{total}$ , with the maximum allowable interference,  $I_{max}$ . Equation (3.34) results from solving for  $m$ . Equation (3.34) defines the number of links such that the received interference power at the AWR receiver is less than the maximum allowable received interference power,  $I_{max}$ . The number of allowable links is equal to the floor of  $I_{max}$  multiplied by the inverse of the expected value of interference generated within each coverage region. The expected value of interference is the received power from a WLAN transmitter defined by the free space path loss equation,

$$P_r = \frac{P_t G_t G_r \lambda^2}{(4\pi)^2 R^2 L_{misc}}. \quad \text{To account for the uniformly distributed links, the typical } 1/R^2$$

relationship is instead defined as the product  $R_{max} R_c$ , where  $R_{max}$  is the maximum possible separation between the interfering WLAN transmitters and an AWR, and  $R_c$  is the minimum separation.

$$I_{max} = m \cdot E[I] \quad (3.33)$$

$$m = \left\lfloor I_{max} \frac{(4\pi)^2 L_{misc} (R_{max} R_c)}{P_t G_t G_r \lambda^2} \right\rfloor \quad (3.34)$$

The probability of exceeding the maximum allowable interference, shown in (3.35), is derived by combining (3.32) and (3.34).

$$P[S_{\eta A} \leq m | \text{AWR is present}, \eta, A] = \sum_{k=0}^m \binom{\eta A}{k} \rho^k (1-\rho)^{\eta A - k} \quad (3.35)$$

Equation (3.35) can be rearranged to show the relationship between total interference of all active links,  $I_{total}$ , and the maximum tolerable interference,  $I_{max}$ , by multiplying the

random variables by the path loss. Additionally, we can find the probability that  $I_{total}$  exceeds  $I_{max}$  by taking the complement of (3.35). These manipulations result in (3.36), the probability that the total interference,  $I_{total}$ , exceeds the maximum allowable received interference power,  $I_{max}$ , given a link density, coverage area, and presence of a radar. If all links in the coverage area are active ( $\rho = 1$ ), then (3.24) can be used directly, restated here as (3.37). Equations (3.36) and (3.37) show the metric that is used to analyze the performance of AWR in shared spectrum.

$$P_I = P\left[I_{total} \geq I_{max} \mid \text{AWR is present}, \eta, A\right] = 1 - P\left[S_{\eta A} \leq \left[I_{max} \frac{(4\pi)^2 L_{misc} (R_{max} R_c)}{P_t G_t G_r \lambda^2}\right] \mid \text{AWR is present}, \eta, A\right] \quad (3.36)$$

$$P_I = P\left[I_{total} \geq I_{max} \mid \text{AWR is present}, \eta, A, \rho = 1\right] = \begin{cases} 1, & \eta A \cdot \frac{P_t G_t G_r \lambda^2}{(4\pi)^2 L_{misc} (R_{max} R_c)} > I_{max} \\ 0, & \eta A \cdot \frac{P_t G_t G_r \lambda^2}{(4\pi)^2 L_{misc} (R_{max} R_c)} \leq I_{max} \end{cases} \quad (3.37)$$

### 3.4 Interference Scenarios

This section further develops the probability of exceeding the maximum allowable interference power,  $P_I$ , of AWR. For each scenario, the coverage path and coverage area is calculated and the maximum and minimum possible separation between WLAN transmitters and AWR is determined. Using these parameters, along with the link density, the probability of exceeding the maximum allowable interference power can be calculated. The final probability depends on the transmit power and modulation of each type of WLAN described in Chapter 5.

Two scenarios are chosen to represent the most likely cases of interference. The first scenario, WLANs operating under a jetway, causes the most frequent interference to a WLAN due to the high rate of aircraft traffic in jetways. The second scenario, WLANs operating in a Victor airway, causes the highest level of interference to AWR due to the small separation between AWR and WLAN interferers.

### **3.4.1 Scenario 1: Heavily Traveled Jetway**

Data gathered from FlightAware, a flight tracking service [13], is used to specify the flight characteristics of an aircraft in a heavily traveled jetway. It was found that the jetway, J134, linking Washington Dulles International Airport (Washington, DC) [KIAD/IAD] and Los Angeles International Airport (Los Angeles, CA) [KLAX/LAX] is representative of heavily traveled jetways. This jetway provides typical values to use in the performance analysis of WLAN and AWR in shared spectrum. Aircraft in this jetway typically travel at velocities of 250 meters per second (485 knots) with an en route altitude of 11 kilometers (36,000 feet) mean seal level (msl) [13-15]. The AWR used in these flights typically set their tilt angle to  $1^\circ$  below the horizon to detect weather phenomenon [45, 46]. The equivalent power beamwidth is  $5.2^\circ$  as described in Table 3-1.

Using this altitude, beamwidth, and tilt angle, the maximum possible separation between AWR and WLANs,  $R_{max}$ , is 432 kilometers. The minimum possible separation,  $R_c$ , is 175 kilometers. The vertical coverage path,  $C$ , is 257 kilometers, and the horizontal coverage path,  $C_H$ , is 28 kilometers resulting in a coverage area,  $A$ , of 5,568 square kilometers. This coverage area would be completely filled by a major metropolitan area such as Los Angeles. Assuming link density of 1000 links per square kilometer, the total number of links in the coverage area,  $N_{WLAN} = A\eta$ , is  $5.6 \times 10^6$  links. These parameters, derived from assumptions and developed in this thesis, are summarized in Table 3-2.

Parameter	Symbol	Value	Derived From
Aircraft Altitude	$h$	11 kilometers	Flight pattern of aircraft [14, 15].
Aircraft Velocity	$v$	250 meters per second	Flight pattern of aircraft [14, 15].
Vertical Coverage Path	$C$	257 kilometers	$C = R_{\max} \sqrt{1 - \left(\frac{h}{R_{\max}}\right)^2} - \frac{h}{\tan(\gamma)}$ meters
Horizontal Coverage Path	$C_H$	28 kilometers	$C_H = 2 \left[ \frac{R_{\max} + R_c}{2} \right] \sin\left(\frac{\theta}{2}\right)$
Coverage Area	$A$	5,568 square kilometers	$A = \frac{\pi C_H C}{4}$
Maximum Possible Separation	$R_{\max}$	432 kilometers	$D = \sqrt{2kR_e h}$ meters
Minimum Possible Separation	$R_c$	175 kilometers	$R_c = \frac{h}{\sin(\gamma)}$
Number of WLAN links in coverage area	$N_{WLAN}$	$5.6 \times 10^6$ links	$N_{WLAN} = A\eta$

Table 3-2. Parameter and values defined by a heavily traveled jetway.

### 3.4.2 Scenario 2: Victor Airway

It was found that the airway, V143, linking Washington Dulles International Airport (Washington, DC) [KIAD/IAD] and Roanoke Regional Airport (Roanoke, VA) [KROA/ROA] is representative of Victor airways providing typical values to use in the performance analysis of WLAN and AWR in shared spectrum [13]. Aircraft in this airway typically travel at velocities of 200 meters per second (about 390 knots) with an en route altitude of 5 kilometers (16,000 feet) mean seal level (msl) [13-15]. Using the single

rectangular main lobe model, the AWR used in these flights have a tilt angle of  $0^\circ$  and a beamwidth of  $5.2^\circ$ .

Using these parameters,  $R_{max}$ , is 288 kilometers. The minimum possible separation,  $R_c$ , is 108 kilometers. The vertical coverage path,  $C$ , is 108 kilometers, and the horizontal coverage path,  $C_H$ , is 18 kilometers resulting in a coverage area,  $A$ , of 2,545 square kilometers. This coverage area would be completely filled by most metropolitan areas. Assuming link density of 1000 links per square kilometer, the total number of links in the coverage area,  $N_{WLAN} = A\eta$ , is  $2.5 \times 10^6$  links. These parameters, derived from assumptions and developed in this thesis, are summarized in Table 3-3.

Parameter	Symbol	Value	Derived From
Aircraft Altitude	$h$	5 kilometers	Flight pattern of aircraft [14, 15].
Aircraft Velocity	$v$	200 meters per second	Flight pattern of aircraft [14, 15].
Coverage Path	$C$	108 kilometers	$C = R_{max} \sqrt{1 - \left(\frac{h}{R_{max}}\right)^2} - \frac{h}{\tan(\gamma)} \text{ meters}$
Horizontal Coverage Path	$C_H$	18 kilometers	$C_H = 2 \left[ \frac{R_{max} + R_c}{2} \right] \sin\left(\frac{\theta}{2}\right)$
Coverage Area	$A$	2,545 square kilometers	$A = \frac{\pi C_H C}{4}$
Maximum Possible Separation	$R_{max}$	288 kilometers	$D = \sqrt{2kR_e h} \text{ meters}$
Minimum Possible Separation	$R_c$	108 kilometers	$R_c = \frac{h}{\sin(\gamma)}$
Number of WLAN links in coverage area	$N_{WLAN}$	$2.5 \times 10^6$ links	$N_{WLAN} = A\eta$

Table 3-3. Parameter and values defined by a Victor airway.

### 3.5 Interference into AWR from Narrowband Wireless Local Area Networks

Analysis of interference from narrowband digital WLAN links shows that significant interference is received by an AWR. For the WLAN links, a symbol rate,  $R_b$ , of 1 MHz is chosen to match the symbol rate of an 802.11b system and the bandwidth of Bluetooth [52, 53]. The bandpass bandwidth is 2 MHz resulting from raised root cosine pulses with a roll-off factor of 1. Occupied bandwidth,  $W$ , of a bandpass raised root cosine signal is related to the symbol rate times,  $R_s$ , and the roll-off factor  $\alpha$ .

$$W = R_s (1 + \alpha) \text{ Hz} \quad (3.38)$$

Binary phase shift keying (BPSK) modulation is used to reach the target BER of  $1 \times 10^{-4}$  with the required signal to noise ratio (SNR) of 8.4 dB. The required SNR for a BSPK signal in additive white Gaussian noise (AWGN) is calculated using (3.39). In (3.39), the probability of error,  $P_{eBPSK}$ , is related to the signal power,  $S$ , and the noise power,  $N$ . The BER calculation assumes an ideal coherent receiver with perfect synchronization and zero intersymbol interference.

$$P_{eBPSK} = Q\left(\sqrt{\frac{2S}{N}}\right) \quad (3.39)$$

To meet the target SNR at the WLAN receiver, a 1 mW transmitter is required. A 1 mW transmitter operating at 9.35 GHz separated from the receiver by 50 meters results in a SNR of 11.5 dB. The SNR of 11.5 dB provides a margin of 3.1 dB over the minimum required SNR; consequently, a reliable link exists. The link margin is required to overcome unexpected signal degradations and idealization in the analysis. This transmit power and distance is reasonable according to the assumptions and agrees with values of existing WLANs such as Bluetooth [53]. A link budget calculating the required transmit power for a narrowband wireless local area network link is included in Appendix B.

The coverage area for WLAN to AWR interference is determined by aircraft altitude, tilt angle, and beamwidth. From the coverage area and link density it was determined that there are  $5.6 \times 10^6$  links in coverage areas below jetways and  $2.5 \times 10^6$  links for Victor airways. The maximum and minimum possible separations between the AWR and WLAN links is  $R_{max}$  and  $R_c$ . These separations determine the expected amount of interference into the AWR receiver. These parameters along with the transmit power of the WLAN links are used to calculate the likelihood that the total effective interference from all WLAN links in a coverage area,  $I_{total}$ , exceeds the maximum allowable received interference power,  $I_{max}$ . This likelihood,  $P_I$ , shows that if the number of links in the coverage area,  $\eta A$ , is less than or equal to the maximum allowable links,  $m$ , then the probability of harmful interference is zero; otherwise, the interference will be harmful to AWR and spectrum sharing is not advisable. The maximum allowable links,  $m$ , is calculated using (5.10) with all parameters summarized in Table 3-4.

$$m = \left\lceil I_{max} \frac{(4\pi)^2 L_{misc} (R_{max} R_c)}{P_t G_t G_r \lambda^2} \right\rceil \text{ links} \quad (3.40)$$

Parameter		Value	Justification
$I_{max}$	= Maximum allowable received interference power	-142.6 dBW	Assumption [16]
$(4\pi)^2$		22.0 dB	Constant
$L_{misc}$	= losses due to building penetration and system losses	7.0 dB	Assumption [35]
$R_{max}R_c$	= Path loss distance is the product of the maximum and minimum possible separation between AWR and WLAN in a coverage area	108.8 dB meters squared for jetways	Derived from scenario
		104.9 dB meters squared for Victor airways	Derived from scenario
$P_t$	= WLAN transmitter power	-30.0 dBW	Derived from Link Budget
$G_t$	= WLAN transmitter antenna gain	0.0 dB	Assumption [52, 53]
$G_r$	= AWR receiver antenna gain	32.0 dB	Assumption see Table 3-1
$\lambda^2$	= wavelength at 9.35 GHz squared	-29.9 dB meters squared	Center frequency
$m$	= maximum allowable WLAN links	201 links for jetway scenario	Derived from (5.10)
		82 link for Victor airway scenario	

Table 3-4. Parameters for narrowband WLAN to AWR interference calculations. The maximum allowable links is 204 links in a jetway and 83 links in a Victor airway. There are more links expected than allowed in a coverage area for both jetways and Victor airways.

There are  $5.6 \times 10^6$  links in coverage areas below jetways and  $2.5 \times 10^6$  links for Victor airways, but the maximum allowable number of WLAN links is 201 for jetways and 82 for Victor airways. Assuming that all WLANs links interfere with AWR, a narrowband system can not be used in coverage area underneath jetways or Victor airways.

The assumption that all links interfere with AWR is overly pessimistic. A more sophisticated model is to assume that each WLAN link interferes with an AWR with a specified probability,  $\rho$ , which represents intermittent transmission of the WLAN link.

The parameter  $\rho$  is used in (5.3) to find  $P_I$ , the probability that the collective interference from all WLAN links in a coverage area causes harmful interference to an AWR. For all non-trivial values of  $\rho$ , interference is still 100% likely. Figure 3-5 shows that under the assumptions that each WLAN device transmits with 1mW of power, harmful interference is assured and spectrum sharing with AWR is not possible regardless of each individual link's probability of interfering. In fact, Figure 3-6 shows interference into AWR receivers is expected to be at least 25 dB higher than the allowable level.

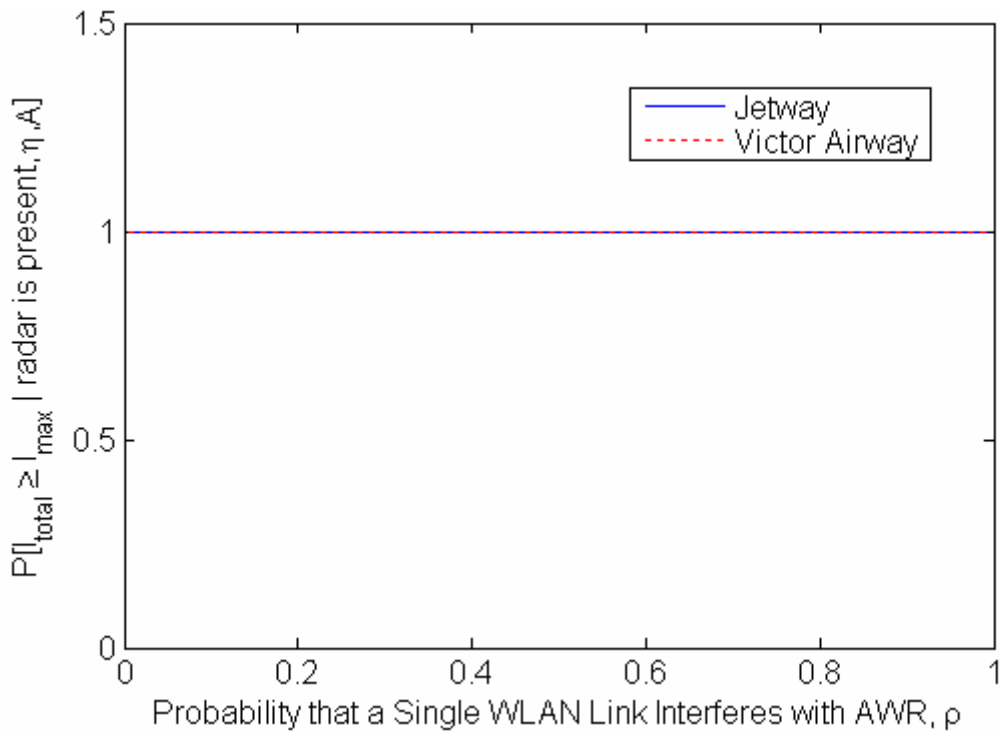


Figure 3-5. Probability that the total effective interference received by all WLAN links in a coverage area,  $I_{total}$ , exceeds the maximum allowable received interference,  $I_{max}$ . Harmful interference is 100% likely in both jetways and Victor airways.

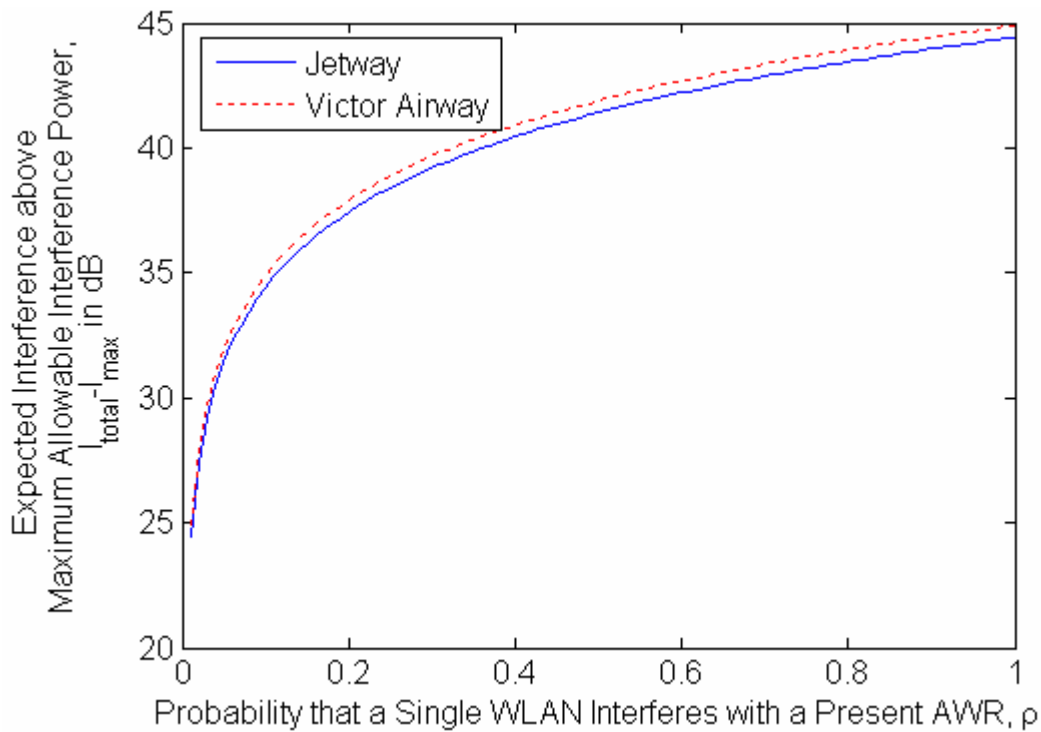


Figure 3-6. Expected interference above the maximum allowable interference versus the probability that a single WLAN interferes with a present AWR. Interference into AWR receivers is expected to be at least 25 dB higher than the allowable level in both jetways and Victor airways, regardless of probability that a single WLAN link interferes with a present AWR.

Holding the probability that a single WLAN link interferes with AWR constant at 1 and varying transmit power and link density also yields unfavorable results for spectrum sharing in most cases. Even with transmit power at 0.1 mW, the interference is expected to be at least 25 dB higher than the allowable level, as shown in Figure 3-7. Reducing the number of links per square kilometer, on the other hand, does reduce the expected interference to allowable levels. But Figure 3-8 shows that reductions below 1 link per square kilometer are required. A link density below 1 link per square kilometer is not acceptable for local area networks in urban areas, but other applications or scenarios for a communications system with extremely low link density may exist.

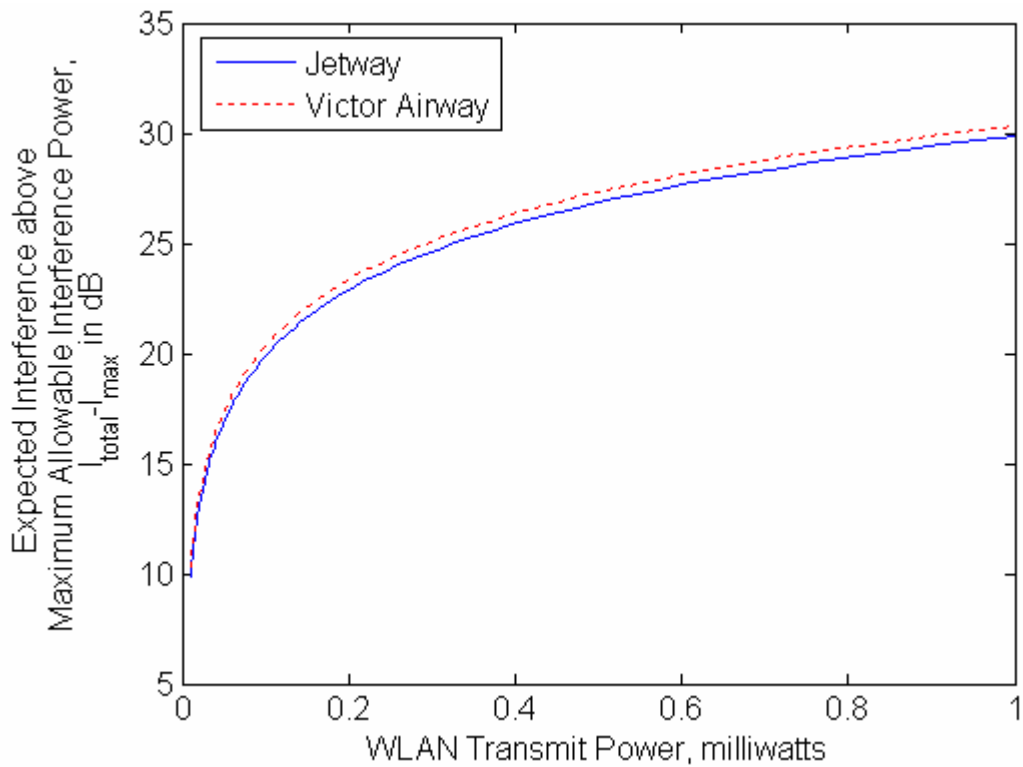


Figure 3-7. Expected interference above the maximum allowable interference versus WLAN transmit power. Interference into AWR receivers is expected to be at least 10 dB higher than the allowable level in both jetways and Victor airways with a minimum transmit power of 0.1 mW.

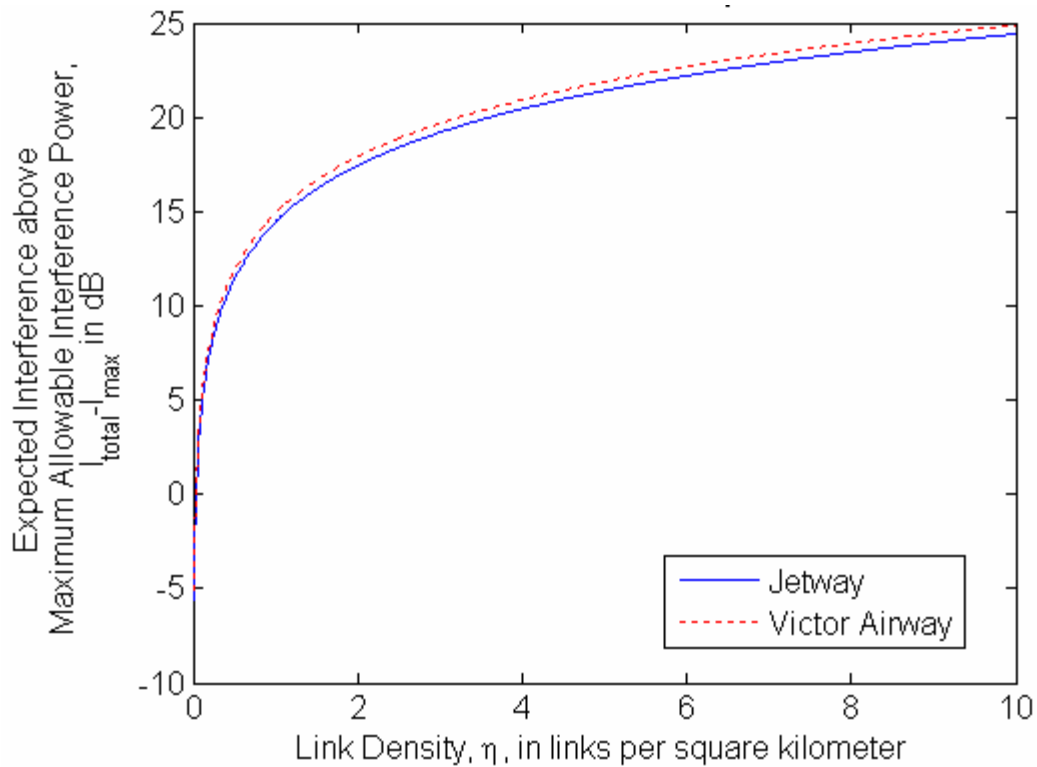


Figure 3-8. Expected interference above the maximum allowable interference versus link density. The expected interference approaches maximum allowable level as the link density is decreased to below 1 per square kilometer.

### 3.6 Conclusion

The definition of these scenarios completes the development of the performance metrics for interference into AWR from WLANs. If the likelihood that the total effective received interference power exceeds the allowable level, measured by metric developed in this chapter, then spectrum sharing is not feasible. It was shown that a simple narrowband digital communications link will cause interference above the allowable level for all realistic transmit powers and user densities. Chapter 4 develops metrics used to calculate the bit error rate of WLANs to measure the performance of WLANs in shared spectrum. Chapter 5 uses

transmit power and modulation of specific WLANs to quantify the probability of exceeding the maximum allowable interference power and to calculate the BER in shared spectrum, thus determining the feasibility of spectrum sharing between AWRs and WLANs.

## **Chapter 4**

# **Effects of Airborne Weather Radar Interference on Wireless Local Area Networks**

Airborne weather radar (AWR) is a primary service, so interference from wireless local area networks (WLANs) above harmful levels prevents the possibility of spectrum sharing. Harmful interference to an AWR prevents spectrum sharing, but bit errors caused by interference to WLANs can be tolerated. The likelihood of bit errors in a WLAN link caused by AWR interference is modeled as a communications link in a pulsed jammer environment. AWRs are modeled as jammers arriving with a Poisson distribution and departing with an exponential distribution as defined by a queuing system with infinite queues. Received AWR transmission into WLAN links are extremely powerful causing BERs of 50%; thus, the BER of WLANs in shared spectrum is determined by the expected number of interfering AWRs and the likelihood of receiving AWR transmissions.

### **4.1 Determining the Number of Airborne Weather Radar Interferers**

The Federal Aviation Administration (FAA) regulates aircraft flight in the United States by establishing and regulating air routes. Interference analysis is conducted assuming jetways and Victor airways because these are the air routes most commonly traveled by airborne weather radar (AWR) capable aircraft. Typical velocities of aircraft traveling in jetways are around 250 meters per second (about 485 knots), and aircraft in Victor airways travel at 200 meters per second (about 390 knots) [14, 15].

Specific data on the number of aircraft simultaneously interfering with a WLAN link could not be found in literature, but an estimate is developed in this thesis. The maximum

rate at which aircraft land at an airport is about 1 aircraft per 60 seconds [54]. Availability of runways at airports is the limiting factor for air traffic, implying that air routes (jetway and Victor airways) servicing airports have traffic rates equal to or less than 1 aircraft per 60 seconds on average per direction. This assumption is valid because if incoming traffic to airports is greater than the traffic handled by airports, delay for arrivals and departures would be infinite. In most cases, delay is finite; therefore, aircraft traffic in air routes is bounded by traffic at airports.

The previous estimate is verified by calculating the separation in time between aircraft. The minimum required separation between aircraft mandated by the FCC is 4 nautical miles (7400 meters) [12]. Dividing this distance by expected velocity of aircraft in jetways gives a time separation of about 2 aircraft per 60 seconds. Assuming aircraft fly in the same direction with the minimum allowable separation, the value of 2 aircraft per 60 seconds is used as the arrival rate of aircraft over WLANs in the jetway scenario. One aircraft per sixty seconds is assumed for Victor airways.

Queuing theory is used to model the arrival and departure of AWRs with the mean arrival rate determined by minimum aircraft separation and mean departure rate determined by coverage area and aircraft velocity. This probabilistic model of the number of AWRs is used to determine the BER of WLAN links in shared spectrum. Queuing theory models the presence of an AWR interferer because the event of an aircraft passing over a WLAN can be viewed as a user entering a queuing system. The aircraft is defined as the user and the path that the plane takes over a WLAN is defined as the server. Aircraft are assumed to arrive with a Poisson distribution which models events that occur “completely at random in time or space” [51]. Exponential service time, an assumption of queuing theory, is also applied to model the expected number of AWR interferers.

The  $M/M/\infty$  queuing system defined by Poisson distributed arrivals, exponential distributed departures, and infinite queues allows for tractable analysis of the number of

AWR interferers affecting a single WLAN link. The model, shown in (4.1), gives the probability that fewer than  $k$  AWRs are in the presence of a WLAN at any given time

$$P[N_{AWR} \leq k] = \sum_{j=0}^k \frac{a^j}{j!} e^{-a}, \quad a = \frac{\lambda}{\mu}, \quad (4.1)$$

where the random variable  $N_{AWR}$  is the number of radars,  $\lambda$  is the arrival rate of 2 aircraft per 60 seconds for jetways and 1 aircraft per 60 seconds for Victor airways. The service time,  $t_s$ , the inverse of the departure rate, is  $1/\mu$ .

The AWR will interfere with a WLAN with different severity according to the antenna pattern. Typical radar antenna gains are modeled as varying by the cosine of angle from peak gain. The gain as a linear ratio with its peak normalized to 1 is [50]

$$H(\theta) = \left( \frac{\cos\left(3.7353 \frac{\theta}{\theta_{3db}}\right)}{\left(1 - 5.6544 \left(\frac{\theta}{\theta_{3dB}}\right)^2\right)} \right)^2 \text{ watts.} \quad (4.2)$$

This reference antenna pattern, fully described in Chapter 3, is modified by creating a pattern with regions of constant gain over each lobe. The constant gain model is created by equating the peak gain for each lobe to the reference model and choosing a beamwidth for the constant gain model such that the power transmitted per lobe is equal to the transmitter power per lobe for the reference model. The antenna pattern used for interference analysis is shown in Figure 4-1. The main lobe, first sidelobe, and second sidelobe are projected onto coverage areas where the AWR gain is large enough to cause significant amounts of interference. Regions outside of these lobes are assumed not to cause interference and are difficult to model accurately [22].

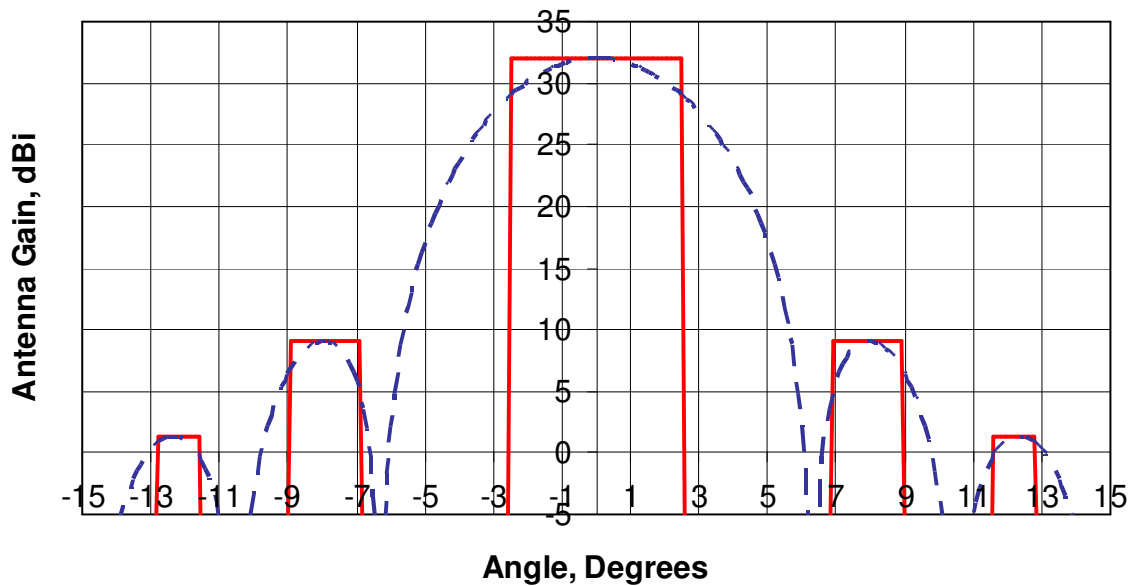


Figure 4-1. Antenna pattern model for airborne weather radar to wireless local area network interference. The main lobe at a constant gain of 32 dBi is from  $-2.5^{\circ}$  to  $2.5^{\circ}$ . The first sidelobe has a gain of 9 dBi from  $\pm 6.9^{\circ}$  to  $\pm 8.9^{\circ}$ . The second sidelobe has a gain of -1.3 dBi from  $\pm 11.6^{\circ}$  to  $\pm 12.8^{\circ}$ . Gain outside of these regions are considered insignificant.

Using the pattern in Figure 4-1, the coverage area of an AWR is comprised of regions of differing gains. Each of these coverage regions have their own tilt angles, beamwidths, and gains resulting in different transmitted powers, coverage areas, and service times illustrated in Figure 4-2.

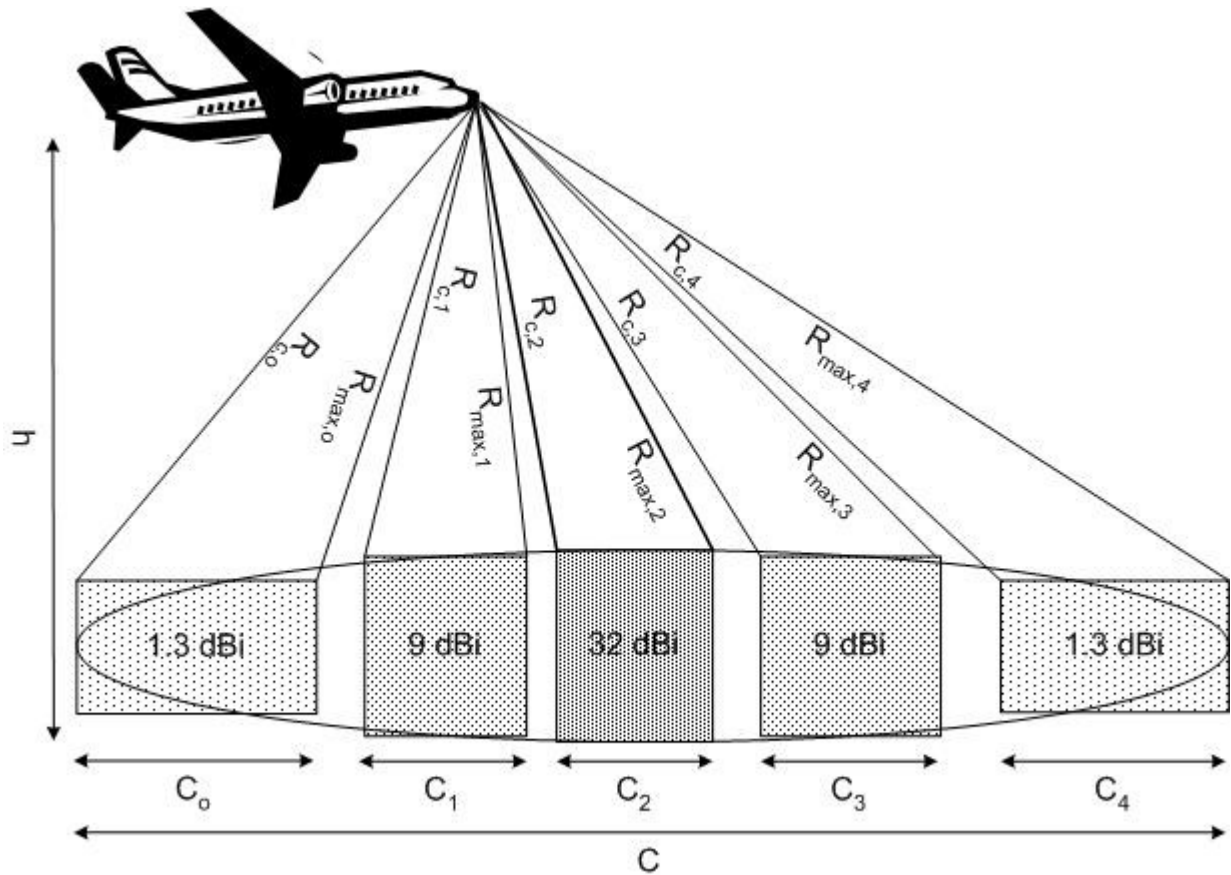


Figure 4-2. Projection of antenna radiation pattern onto the ground. The main lobe has 32 dB of gain. The first sidelobe has 9 dB of gain and the second sidelobe has 1.3 dB of gain. There are four coverage regions,  $C_0$  to  $C_4$  each with a maximum possible separation between the AWR and a WLAN link  $R_{max,i}$  and a minimum such separation,  $R_{c,i}$  and a horizontal coverage path  $C_{H,i}$ . Each coverage region is a rectangular region with length of the coverage region and width the size of the midpoint between  $R_{c,i}$  and  $R_{max,i}$ . The aircraft is at altitude,  $h$ , and the entire coverage area has a length of  $C$ .

Bit errors caused by AWR interference in each region are mutually exclusive allowing the total probability of error to be the sum of the probability of bit error in the main lobe, first sidelobe, second sidelobe, and regions with no interference. BER cause by AWR interference is found by weighting the probability that  $k$  AWRs are present in each region by the probability that the AWRs are actually transmitting into a WLAN receiver. The final

probability of bit error caused by spectrum sharing with AWRs depends on the duty cycle of the AWRs, the horizontal scanning of the AWRs, and the probability that  $k$  AWRs present.

## 4.2 Probability of Bit Error of Wireless Local Area Networks in Shared Spectrum

The BER of a WLAN link affected by an AWR is modeled as a pulsed jammer environment using

$$P_b = P[\text{no interference}]P[\text{error|no interference}] + P[\text{interference}]P[\text{error|interference}]. \quad (4.3)$$

The BER of a WLAN link in shared spectrum depends on the probability of receiving interference from an AWR,  $P[\text{interference}]$ , and the BER during this AWR interference,  $P[\text{error|interference}]$ . When interference is not present the BER depends on the WLAN modulation and signal to noise ratio which is easily calculated with established models [30, 31]. The probability of interference and bit errors given interference is actually defined by a sum of probabilities of bit error for each coverage region. Each coverage region will have its own probability of interference and BER in that region due to varying antenna gains and beamwidths over the considered sidelobes.

The probability density function (pdf) of the  $M/M/\infty$  queuing system used to model the arrival and departure of an AWR over a single WLAN link is described in (4.4). The mean number of AWRs,  $N_{AWR}$ , for this queuing system is shown in (4.5). The random variable  $N_{AWR}$  describes the number of users in the system, which is a random process of time. The departure rate, the inverse of service time is  $\mu$ , and the arrival rate is  $\lambda$ . [51]

$$p_j = \frac{a^j}{j!} e^{-a}, \quad j = 0, 1, 2, \dots \quad (4.4)$$

$$E[N_{AWR}] = a = \frac{\lambda}{\mu} \quad (4.5)$$

Service times, times when a WLAN is within a coverage area of traveling aircraft, vary from 700 to 900 seconds depending on the particular AWR, the velocity of the aircraft, and the altitude of the aircraft. Worst case arrival times are 2 aircraft per 60 seconds in jetways, and 1 aircraft per second in Victor airways.

The cumulative density function (cdf) of (4.4), shown in (4.6), is used to derive the probability that  $k$  or fewer AWRs are present. The required probabilities to calculate the second term of the overall BER, (4.3), are the probability that no AWRs are present,  $k = 0$ , and AWRs are present,  $k > 0$ . These two cases are shown in (4.7) and (4.8) for the no interference and interference case, respectively.

$$P[N_{AWR} \leq k] = \sum_{j=0}^k \frac{a^j}{j!} e^{-a} \quad (4.6)$$

$$P[\text{no interference}] = P[N_{AWR} = 0] = e^{-a} \quad (4.7)$$

$$P[\text{interference}] = P[N_{AWR} > 0] = 1 - e^{-a} \quad (4.8)$$

Equations (4.7) and (4.8) are combined with (4.3) to produce (4.9); equation (4.9) provides the BER for a WLAN link in shared spectrum assuming all AWRs are transmitting continuously.

$$P_b = e^{-a} P[\text{error|no interference}] + (1 - e^{-a}) P[\text{error|interference}] \quad (4.9)$$

Equation (4.9) incorporates the arrival and departure of an AWR into the BER calculation for a WLAN in shared spectrum, but does not model the intermittent nature of interference received from an AWR. AWRs transmit using a low duty cycle,  $D$ , and scan across  $90^\circ$  of azimuth direction. The horizontal scanning of the beam reduces the likelihood

of being affect by interference because the beam will not be over a WLAN link during the entire scan. The probability of being within the beamwidth given horizontal scanning over  $90^\circ$  is

$$P[\text{within beamwidth}|\text{horizontal scanning}] = \begin{cases} \frac{\theta}{90^\circ - \theta}, & \theta < 45^\circ \\ 1 & \theta \geq 45^\circ \end{cases} \quad (4.10)$$

The duty cycle and probability of being within the beamwidth is independent of the number of radars present; therefore, the probability of interference by  $k$  AWR is

$$P[k \text{ AWRs are interfering}] = \sum_{j=0}^k D \frac{\theta}{90^\circ - \theta} k P[N_{AWR} = k]. \quad (4.11)$$

Interference from multiple AWRs is assumed to be non-overlapping and each AWR will interfere simultaneously because of the low duty cycle. This simultaneous interference is expressed by multiplying the duty cycle and scanning factor by the number of present AWR, appropriately scaling the probability of interference. Thus the WLAN is affected by  $k$  AWRs a fraction of the time related to the likelihood that  $k$  AWR are present,  $P[N_{AWR} = k]$ , the

likelihood that a single AWR is interfering,  $D \frac{\theta}{90^\circ - \theta}$ , and the simultaneous effects of the  $k$  AWRs,  $\sum_{k=1}^{\infty} k P[N_{AWR} = k]$ .

The weighting of the probability of interference by the duty cycle and horizontal scanning is combined to form the parameter,  $\tau$ .

$$\tau = \begin{cases} D \frac{\theta}{90^\circ - \theta}, & \theta < 45^\circ \\ D & \theta \geq 45^\circ \end{cases} \quad (4.12)$$

To account for multiple transmitting AWRs, the analysis includes the duty cycle of the transmitters, and horizontal scanning of the antenna, and the probability that  $k = 1, 2, 3...$

AWR are present. With the duty cycle and scanning included in the analysis, the probability that  $k = 1, 2, 3, \dots$  AWRs are present must be summed to account for multiple transmitting AWRs as shown in (4.13). In (4.13),  $\tau$  represents the intermittent received interference from an AWR due to the low duty cycle and horizontal scanning.

$$P_b = e^{-a} P[\text{error|no interference}] + (1 - \tau) P[\text{error|no interference}] + \sum_{k=1}^{\infty} [\tau k P[N_{AWR} = k] P[\text{error|interference}]] \quad (4.13)$$

Noticing that  $\sum_{k=1}^{\infty} k P[N_{AWR} = k]$  is the expected value of  $N_{AWR}$ , (4.13) can be simplified to

$$P_b = (e^{-a} + (1 - \tau)) P[\text{error|no interference}] + \tau (a - e^{-a}) P[\text{error|interference}], \quad (4.14)$$

where the total probability of bit error,  $P_b$ , is equal to the bit error rates when 0 AWRs are present or any number of AWRs are present and not transmitting, plus the probability that  $k$  AWRs are present and transmitting.

Equation (4.14) provides the basis to calculate the BER of a WLAN in shared spectrum, but the segmentation of the coverage area into coverage regions must be considered. Equation (4.15) generalizes the total probability of bit error by including the five antenna coverage regions.

$$P_b = \sum_{i=0}^4 (e^{-a_i} + (1 - \tau_i)) P[\text{error|no interference}] + \sum_{i=0}^4 [\tau_i (a_i - e^{-a_i}) P[\text{error|interference in } i\text{th region}]] \quad (4.15)$$

Often the bit error rate caused by all lobes will be 50% and for simplicity  $\tau_i$  is chosen to equal the most likely probability,  $\tau_2$ , allowing the following simplification of the BER.

$$P_b \leq (e^{-a} + (1-\tau))P[\text{error|no interference}] + \tau(a - e^{-a})\frac{1}{2}, \quad (4.16)$$

where  $\tau = \max(\tau_0, \tau_1, \tau_2, \tau_3, \tau_4)$ , and  $a = \sum_{i=0}^4 a_i$

### 4.3 Bit Error Rate of a Narrowband Wireless Local Area Network in Shared Spectrum

A narrowband digital communications system provides a low complexity system to show the BER analysis of a WLAN link in shared spectrum. A symbol rate,  $R_b$ , of 1 MHz is chosen to match the symbol rate of an 802.11b system and the bandwidth of Bluetooth [52, 53]. The bandpass bandwidth is 2 MHz resulting from raised root cosine pulses with a chosen roll-off factor of 1. Occupied bandwidth,  $W$ , of a bandpass raised root cosine signal is related to the symbol rate times,  $R_s$ , and the roll-off factor  $\alpha$

$$W = R_s (1 + \alpha) \text{ Hz} \quad (4.17)$$

Noise bandwidth of the WLAN receiver is 1 MHz, numerically equal to the symbol rate  $R_s = R_b = 1 \text{ Mbps}$ . Binary phase shift keying (BPSK) modulation has the target BER of  $1 \times 10^{-4}$  with a signal to noise ratio (SNR) of 8.4 dB. The required SNR for a BPSK signal in additive white Gaussian noise (AWGN) is calculated using (4.18). In (4.18), the probability of error,  $P_{eBPSK}$ , is related to the signal power,  $S$ , and the noise power,  $N$ . The BER calculation assumes an ideal coherent receiver with perfect synchronization and zero intersymbol interference.

$$P_{eBPSK} = Q\left(\sqrt{\frac{2S}{N}}\right) \quad (4.18)$$

To meet the target SNR at the WLAN receiver, a link budget is used to determine the required transmit power. The transmit power is chosen to provide a SNR with sufficient link

margin to account for idealization in the analysis and unexpected signal degradations. The power budget in Table 4-1 calculates the required transmit power of a WLAN device. The transmit power is selected for a specified transmitter gain and receiver gain to overcome the effects of free space path loss and miscellaneous losses due to building penetration and system components. The noise power budget in Table 4-2 calculates the receiver noise power. For these calculations, a poor quality receiver with a noise figure of 10 dB is assumed.

A 1 mW transmitter operating at 9.35 GHz separated from the receiver by 50 meters results in a SNR of 11.5 dB when omni-directional antennas are employed in the links. The SNR of 11.5 dB provides a margin of 3.1 dB over the minimum required SNR; consequently, a reliable link exists. This transmit power and distance is reasonable according to the assumptions and agrees with values of existing WLANs such as Bluetooth [53].

<b>Parameter</b>	<b>Value</b>	<b>Justification</b>
$P_t$ = WLAN transmitter power	-30.0 dBW	Derived from Link Budget
$G_t$ = WLAN transmitter antenna gain	0.0 dB	Assumption [52, 53]
$G_r$ = WLAN receiver antenna gain	0.0 dB	Assumption [52, 53]
$L_p$ = Free space path loss at 9.35 GHz over 50 meter	-85.9 dB	Path Loss Equation
$L_{misc}$ = losses due to building penetration and system losses	-7.0 dB	Assumption [35]
$P_r$ = Received power at RF filter	-122.9 dBW	Derived from Link Budget

Table 4-1. Power budget for narrowband WLAN link.

Parameter		Value	Justification
k	= Boltzmann's constant	-228.6 dBW/K/Hz	Physical Value
T <sub>s</sub>	= 290(10 <sup>1</sup> - 1)	34.2 dBK	Assumption of inexpensive receiver
B <sub>N</sub>	= 1 MHz	60 dBHz	Assumption [52, 53]
N	= Receiver noise power	-134.4 dBW	Derived from Link Budget

Table 4-2. Noise Power budget for narrowband WLAN receiver.

The coverage regions and the total coverage area of the AWR depend on the angle of the beam depressed from the horizon and beamwidth of each pattern lobe. Table 4-3 shows that the average number of aircraft interfering with an AWR in the main lobe (region 2) is 15. WLAN in the first sidelobe has slightly less than 1 interfering AWR on average (region 3). The average number of AWRs illuminating WLAN links with the second sidelobe is near 0 but we have included on average 1 AWR interferer to allow for an extra margin of safety.

Region	Tilt	Beamwidth	R <sub>c</sub>	R <sub>max</sub>	Average Number of Aircraft	Interference to Desired Signal Ratio
0	12.2°	1.2°	N/A	N/A	0	N/A
1	7.9°	2.0°	N/A	N/A	0	N/A
2	0°	5.0°	112 km	288 km	15	20.9 dB
3	-7.9°	1.2°	32 km	41 km	1	34.9 dB
4	-12.2°	2.0°	22 km	24 km	1	38.7 dB

Table 4-3. Average number of interfering aircraft and interference to desired signal ratio for the main lobe and first two sidelobes of an airborne weather radar antenna pattern.

In all regions the received signal from an AWR is at least 20 dB higher than the desired WLAN signal, assuming a 1 mW WLAN transmitter power and a separation between

the WLAN receiver and transmitter of 50 meters. These values agree with standards for 802.11 b/g and Bluetooth [52, 53]. Interference power at least 200 times higher than desired signal level allows for the assumption that the BER of a WLAN link receiving AWR interference is 50%. Combining the BER during interference in each region and likelihood of receiving AWR caused interference yields (4.19). Equation (4.19) models the BER of a digital narrowband WLAN link in shared spectrum with AWR.

$$P_b = \sum_{i=0}^4 \left[ e^{-a_i} + (1 - \tau_i) \right] P[\text{error} | \text{no interference}] + \sum_{i=0}^4 \left[ \tau_i (a_i - e^{-a_i}) \right] P[\text{error} | \text{interference in } i\text{th region}] \quad (4.19)$$

Because the BER during interference regardless of the region is 50%, (4.19) is simplified to

$$P_b = \sum_{i=0}^4 \left[ e^{a_i} + (1 - \tau_i) \right] P[\text{error} | \text{no interference}] + 0.001(17 - e^{-17}) \frac{1}{2} \quad (4.20)$$

The remaining unknown in (4.20), the probability of bit error without interference, is calculated to be  $10^{-4}$  with a 3.1 dB margin using established models of BER of BPSK systems in AWGN. Thus, the final probability of bit error in a digital narrowband WLAN link in shared spectrum with AWR is

$$P_b = (e^{-17} + 1 - 10^{-5}) 10^{-4} + 10^{-5} (17 - e^{-17}) \frac{1}{2}, \quad (4.21)$$

where the beamwidth of each lobe is assumed to be  $5^\circ$  and assuming a duty cycle of 0.001 with the antenna pointed away from a single link 94% of the time. In a Victor airway, the total BER of a narrowband digital WLAN is simply  $3.5 * 10^{-4}$ . In a jetway, there are an average of 37 AWR that interfere either with the main lobe or sidelobes resulting in a BER of  $6.5 * 10^{-4}$ .

The effects of AWR interference on the BER of a digital narrowband WLAN in shared spectrum is on the order of  $10^{-4}$  with typical low duty cycle AWR scanning horizontally over  $90^\circ$ . To calculate this BER, the main lobe and first two sidelobes of the

AWR antenna pattern were considered to interfere with illuminated WLAN causing the worst case BER of 50%. This BER during interference is justified because the received power from AWR transmissions is at least 200 times greater than the desired information bearing signal. The BER of narrowband, frequency hopping spread spectrum, and direct sequence spread spectrum WLANs over a wider range of conditions are discussed in Chapter 5.

## Chapter 5

# Feasibility of Spectrum Sharing between Airborne Weather Radar and Wireless Local Area Networks

The feasibility of spectrum sharing between airborne weather radar (AWR) and wireless local area networks (WLANs) is determined by applying the metrics and assumptions developed in Chapter 2 and Chapter 3 to various types of WLANs. In this chapter, potential WLANs for spectrum sharing are defined and recommendations are made for each WLAN based on the results of the metric calculations. Calculations show that narrowband systems are not suitable for spectrum sharing, but direct sequence spread spectrum (DSSS) and frequency hopping spread spectrum (FHSS) systems warrant further study.

AWR is the primary service allocated to 9.3 GHz – 9.5 GHz requiring that any other systems operating on the same frequencies, such as WLANs, cause minimal interference. To measure interference received by AWR in shared spectrum, this thesis developed the metric of total effective interference,  $I_{total}$ . Any interference above the maximum allowable received interference power,  $I_{max}$ , is harmful to AWR and could violate exclusive use guarantees provided by the Federal Communications Commission (FCC) to AWR. For the FCC to allow spectrum sharing there must be a very low likelihood of exceeding  $I_{max}$ .

## 5.1 Review of Metrics, Scenarios, and Assumptions for Spectrum Sharing

Spectrum sharing between AWRs and WLANs occurs inside an area on the ground defined by the AWR antenna pattern. This coverage area is occupied by WLAN devices

transmitting and receiving within 9.3 GHz – 9.5 GHz. At any given moment, an AWR in shared spectrum receives interference from all WLAN links inside a coverage area that are transmitting within the receiver bandwidth of the AWR. Paralleling this received interference, AWRs cause interference to all WLANs in the coverage area by transmitting at the entire 9.3 GHz – 9.5 GHz range.

The received interference by an AWR from a coverage area, determined by the equivalent power beamwidth model, is measured by the likelihood that the number of WLANs in a coverage area,  $S_{\eta A}$ , is less than the number that causes harmful interference,  $m$ , shown in (5.1). Equation (5.1) assumes that an AWR is present, the user density is  $\eta$ , the coverage area is  $A$ , and that the probability of individual WLAN links interfering with AWR is  $\rho$ .

$$P[S_{\eta A} \leq m | \text{AWR is present}, \eta, A] = \sum_{k=0}^m \binom{\eta A}{k} \rho^k (1-\rho)^{\eta A - k} \quad (5.1)$$

Assuming WLAN links are distributed uniformly over the entire coverage area, the number of WLAN links required to exceed  $I_{max}$ , is

$$m = \left\lceil I_{max} \frac{(4\pi)^2 L_{misc} (R_{max} R_c)}{P_t G_t G_r \lambda^2} \right\rceil \text{ links}, \quad (5.2)$$

where the number of links,  $m$ , is  $I_{max}$  multiplied by the inverse of the path loss equation where the distance squared term in the path loss equation,  $R^2$ , is replaced by the product  $R_{max} R_c$ . The parameters of path loss are wavelength  $\lambda$ , WLAN transmit power,  $P_t$ , WLAN antenna gain,  $G_t$ , AWR antenna gain,  $G_r$ , distance squared  $R_{max} R_c$ , and miscellaneous losses  $L_{misc}$ .

Manipulating (5.1) produces (5.3), which shows the likelihood that the total effective interference,  $I_{total}$ , exceeds  $I_{max}$ . Equation (5.4) assumes all WLANs in a coverage area are interfering with a present AWR by setting  $\rho = 1$ . Equation (5.3) and (5.4) measures the effects of interference from the perspective of AWR. This likelihood, in conjunction with the

bit error rate of WLAN links in shared spectrum, determines the feasibility of spectrum sharing.

$$P_I = P[I_{total} \geq I_{max} | \text{AWR is present}, \eta, A] = 1 - P[S_{\eta A} \leq m | \text{AWR is present}, \eta, A] \quad (5.3)$$

$$P_I = P[I_{total} \geq I_{max} | \text{AWR is present}, \eta, A, \rho = 1] = \begin{cases} 1, & \eta A > m \\ 0, & \eta A \leq m \end{cases} \quad (5.4)$$

The reciprocal problem, interference from AWRs, cause bit errors which must be tolerated by WLAN links. The equivalent power beamwidth of the main lobe was sufficient to model the coverage area of WLAN to AWR interference; to accurately model the reciprocal problem, the coverage area is described by the main lobe and sidelobes of the antenna. The main lobe and first two sidelobes are considered resulting in (5.5) which measures the effects of AWR interference into WLANs as a bit error rate (BER).

$$P_b \leq (e^{-a} + (1 - \tau)) P[\text{error|no interference}] + \tau (a - e^{-a}) \frac{1}{2}, \quad (5.5)$$

where  $\tau = \max(\tau_0, \tau_1, \tau_2, \tau_3, \tau_4)$ , and  $a = \sum_{i=0}^4 a_i$

In (5.5),  $\tau$  weights the BER during interference,  $\tau (a - e^{-a}) \frac{1}{2}$ , and without interference  $(e^{-a} + 1 - \tau) P[\text{error|no interference}]$  to represent the intermittent transmission and horizontal scanning of the AWR. The parameter  $\tau$  is the probability that a present AWR is interfering with a specific WLAN,

$$\tau = \begin{cases} D \frac{\theta}{90^\circ - \theta}, & \theta < 45^\circ \\ D & \theta \geq 45^\circ \end{cases}, \quad (5.6)$$

where  $D$  is the duty cycle and  $\theta$  is the beamwidth of the main lobe of the antenna pattern. Equation (5.7) shows the mean number of AWR present,  $a$ , which is determined by the

arrival rate  $\lambda$  and the service time  $\frac{1}{\mu}$ . The mean number of AWR present is the sum of the mean number of AWR present in each of the  $i$ th coverage regions because these are mutually exclusive events.

$$E[N_{AWR}] = a = \sum_{i=0}^4 a_i = \sum_{i=0}^4 \frac{\lambda}{\mu_i} \text{ aircraft} \quad (5.7)$$

The BER rate during interference is assumed to be 50%. For WLANs in shared spectrum to operate reliably, a BER of  $10^{-2}$  must be attainable. The probability of error with no interference is calculated depending on the specific type of WLAN, and  $a$  is calculated depending on the sharing scenario.

Two scenarios are chosen to represent the worst cases of interference. The first scenario, WLANs operating under a jetway, causes the most frequent interference to a WLAN due to the jetway's high rate of traffic. The second scenario, WLANs operating in a Victor airway, causes the highest level of interference to AWR due to the small separation between AWR and WLAN interferers.

Aircraft in jetways typically travel at velocities of 250 meters per second (about 490 knots) with an en route altitude of 11 kilometers (36,000 feet) mean sea level (msl) [13-15]. Analysis from Chapter 3 determined the coverage area,  $A$ , is 5,568 square kilometers. The total number of links in the coverage area,  $N_{WLAN} = A\eta$ , is  $5.6 \times 10^6$  links, assuming a link density of 1000 links per square kilometer. Using the equivalent power beamwidth,  $R_{max}$  is 432 kilometers and  $R_c$  is 175 kilometers. The coverage area produced by aircraft in Victor airways is 2,545 square kilometers. These aircraft typically travel at velocities of 200 meters per second (about 390 knots) with an en route altitude of 5 kilometers (16,000 feet) msl [13-15]. Again, assuming link density of 1000 links per square kilometer the total number of links in the coverage area,  $N_{WLAN} = A\eta$ , is  $2.5 \times 10^6$  links. In Victor airways,  $R_{max}$  is 288 kilometers and  $R_c$  is 108 kilometers. The large number of links in coverage areas for both jetways and Victor airways will likely cause harmful interference to AWR.

For AWR to WLAN interference, the maximum and minimum possible separations for each coverage region,  $R_{max}$  and  $R_c$ , along with the average number of aircraft for jetways are shown in Table 5-1. Table 5-2 shows these values for Victor airways.

Region	Tilt	Beamwidth	$R_c$	$R_{max}$	Average Number of Aircraft
0	13.2°	1.2°	N/A	N/A	0
1	8.9°	2.0°	N/A	N/A	0
2	1°	5.0°	175 km	432 km	34
3	-6.9°	1.2°	64 km	80 km	2
4	-11.2°	2.0°	46 km	50 km	1

Table 5-1. Average number of interfering aircraft and interference to desired signal ratio for the main lobe and first two sidelobes of an airborne weather radar antenna pattern for a jetway.

Region	Tilt	Beamwidth	$R_c$	$R_{max}$	Average Number of Aircraft
0	12.2°	1.2°	N/A	N/A	0
1	7.9°	2.0°	N/A	N/A	0
2	0°	5.0°	112 km	288 km	15
3	-7.9°	1.2°	32 km	41 km	1
4	-12.2°	2.0°	22 km	24 km	1

Table 5-2. Average number of interfering aircraft and interference to desired signal ratio for the main lobe and first two sidelobes of an airborne weather radar antenna pattern for a Victor airway.

## 5.2 Narrowband Wireless Local Area Network

Initial analysis is performed on a narrowband digital communications system. A symbol rate,  $R_b$ , of 1 MHz is chosen to match the symbol rate of an 802.11b system and the

bandwidth of Bluetooth [52, 53]. The bandpass bandwidth is 2 MHz resulting from raised root cosine pulses with a chosen roll-off factor of 1. Occupied bandwidth,  $W$ , of a bandpass raised root cosine signal is related to the symbol rate,  $R_s$ , and the roll-off factor  $\alpha$

$$W = R_s (1 + \alpha) \text{ Hz} \quad (5.8)$$

Noise bandwidth of the WLAN receiver is 1 MHz, numerically equal to the symbol rate  $R_s = R_b = 1 \text{ Mbps}$  in this example. Binary phase shift keying (BPSK) modulation has the target BER of  $1 \times 10^{-4}$  with a signal to noise ratio (SNR) of 8.4 dB. The required SNR for a BPSK signal in additive white Gaussian noise (AWGN) is calculated using (5.9). In (5.9), the probability of error,  $P_{eBPSK}$ , is related to the signal power,  $S$ , and the noise power,  $N$ . The BER calculation assumes an ideal coherent receiver with perfect synchronization and zero intersymbol interference.

$$P_{eBPSK} = Q\left(\sqrt{\frac{2S}{N}}\right) \quad (5.9)$$

To meet the target SNR at the WLAN receiver, a 1 mW transmitter is required. A 1 mW transmitter operating at 9.35 GHz separated from the receiver by 50 meters results in a SNR of 11.5 dB when omni-directional antenna are employed in the links.. The SNR of 11.5 dB provides a margin of 3.1 dB over the minimum required SNR; consequently, a reliable link exists. The link margin is required to overcome unexpected signal degradations and idealization in the analysis. This transmit power and distance is reasonable according to the assumptions and agrees with values of existing WLANs such as Bluetooth [53]. A link budget calculating the required transmit power for a narrowband wireless local area network link is included in Appendix B.

### 5.2.1 Interference into Airborne Weather Radar from Narrowband Wireless Local Area Networks

The transmit power derived from the link budgets and verified against known systems is now used to calculate the likelihood that the total effective interference from all WLAN links in a coverage area,  $I_{total}$ , exceeds the maximum allowable received interference power,  $I_{max}$ . This likelihood,  $P_I$ , shows that if the number of links in the coverage area,  $\eta A$ , is less than or equal to the maximum allowable links,  $m$ , then the probability of harmful interference is zero; otherwise, the interference will be harmful to AWR and spectrum sharing is not advisable. The maximum allowable links,  $m$ , is calculated using (5.10) with all parameters summarized in Table 5-3.

$$m = \left\lfloor \frac{I_{max} (4\pi)^2 L_{misc} (R_{max} R_c)}{P_t G_t G_r \lambda^2} \right\rfloor \text{ links} \quad (5.10)$$

Parameter		Value	Justification
$I_{max}$	= Maximum allowable received interference power	-142.6 dBW	Assumption [16]
$(4\pi)^2$		22.0 dB	Constant
$L_{misc}$	= losses due to building penetration and system losses	7.0 dB	Assumption [35]
$R_{max}R_c$	= Path loss distance is the product of the maximum and minimum possible separation between AWR and WLAN in a coverage area	108.8 dB meters squared for jetways	Derived from scenario
		104.9 dB meters squared for Victor airways	Derived from scenario
$P_t$	= WLAN transmitter power	-30.0 dBW	Derived from Link Budget
$G_t$	= WLAN transmitter antenna gain	0.0 dB	Assumption [52, 53]
$G_r$	= AWR receiver antenna gain	32.0 dB	Assumption see Table 3-1
$\lambda^2$	= wavelength at 9.35 GHz squared	-29.9 dB meters squared	Center frequency
$m$	= maximum allowable WLAN links	201 links for jetway scenario	Derived from (5.10)
		82 link for Victor airway scenario	

Table 5-3. Parameters for narrowband WLAN to AWR interference calculations. The maximum allowable links is 204 links in a jetway and 83 links in a Victor airway. There are more links expected than allowed in a coverage area for both jetways and Victor airways.

There are  $5.6 \times 10^6$  links in coverage areas below jetways and  $2.5 \times 10^6$  links for Victor airways, but the maximum allowable number of WLAN links is 201 for jetways and 82 for Victor airways. Assuming that all WLANs links interfere with AWR, a narrowband system can not be used in coverage area underneath jetways or Victor airways.

The assumption that all links interfere with AWR is overly pessimistic. A more sophisticated model is to assume that each WLAN link interferes with AWR with a specified probability,  $\rho$ , that represents intermittent transmission of the WLAN link.

The parameter  $\rho$  is used in (5.3) to find  $P_I$ , the probability that the collective interference from all WLAN links in a coverage area causes harmful interference to a present AWR. For all non-trivial values of  $\rho$ , interference is still 100% likely. Figure 5-1 shows that under the assumptions that each WLAN device transmits with 1mW of power, harmful interference is assured, and spectrum sharing with AWR is not possible regardless of each individual link's probability of transmitting. In fact, the interference into AWR receivers is expected to be at least 25 dB higher than the allowable level, as shown in Figure 5-2.

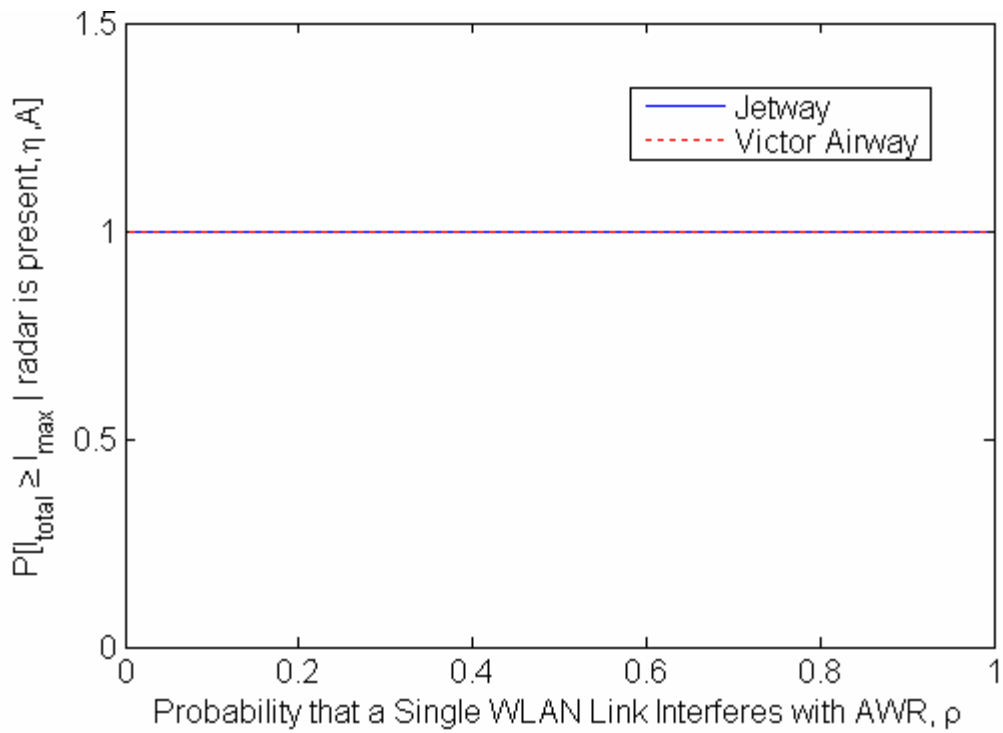


Figure 5-1. Probability that the total effective interference received by all WLAN links in a coverage area,  $I_{total}$ , exceeds the maximum allowable received interference,  $I_{max}$ . Harmful interference is 100% likely in both jetways and Victor airways.

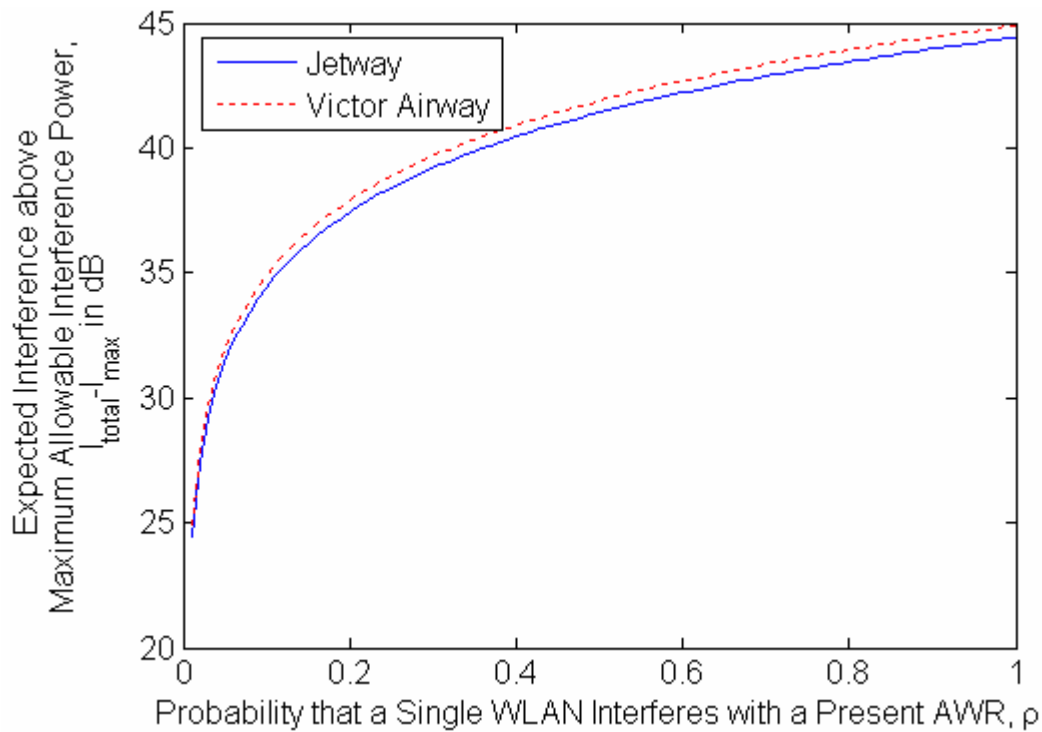


Figure 5-2. Expected interference above the maximum allowable interference versus the probability that a single WLAN interferes with a present AWR,  $\rho$ . Interference into AWR receivers is expected to be at least 25 dB higher than the allowable level in both jetways and Victor airways.

In most cases, holding the probability that a single WLAN link interferes constant (at 100%) and varying transmit power (from 0.1 mW to 1 mW) and link density (0 to 10 links per km) also yields unfavorable results for spectrum sharing. Even with transmit power at 0.1 mW, the interference is expected to be at least 25 dB higher than the allowable level. Reducing the number of links per square kilometer, on the other hand, does reduce the expected interference to allowable levels. But Figure 5-3 shows that reductions below 1 link per square kilometer are required. A link density below 1 link per kilometer is not acceptable for local area networks in urban areas, but other applications or scenarios for a communications system with extremely low link density may exist.

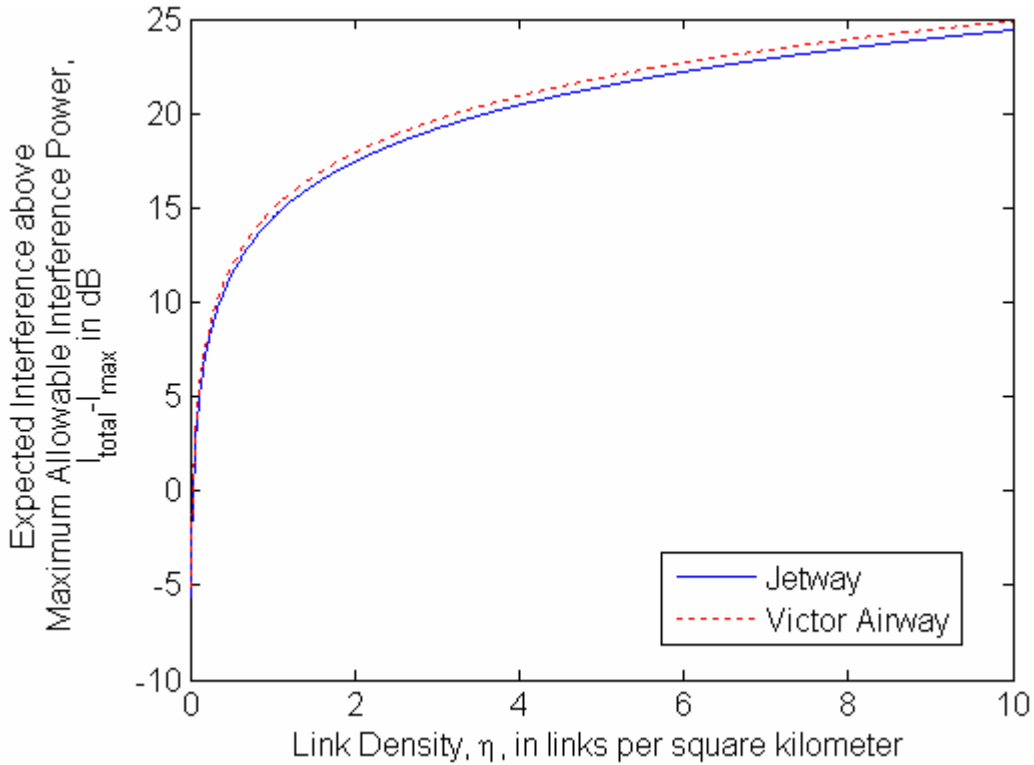


Figure 5-3. Expected interference above the maximum allowable interference versus link density. The expected interference approaches maximum allowable level as the link density is decreased to below 1 per kilometer.

### 5.2.2 Bit Error Rate of Narrowband Wireless Local Area Networks in Shared Spectrum with Airborne Weather Radar

The feasibility of spectrum sharing also depends on the performance of the WLAN links. Despite the in high levels of interference inflicted on AWRs, the interference into WLAN links is quite tolerable. The total BER, calculated with (5.5), in a jetway is  $6.5 \times 10^{-4}$  and in a Victor airway is  $3.5 \times 10^{-4}$ . Equation (5.5) is restated below where the average number of interferers,  $a$ , is 37 for the jetway scenario, and 17 for Victor airways.

$$P_b = (e^{-a} + (1-\tau))Q\left(\sqrt{\frac{2S}{N}}\right) + \tau(a - e^{-a})\frac{1}{2} \quad (5.5)$$

The BER with no interference is  $10^{-4}$  and the typical AWR duty cycle of 0.001 is chosen. The AWR scans side to side in the azimuth direction covering  $90^\circ$  with the beam reducing the time of interference by the scan factor,

$$\frac{\theta}{90^\circ - \theta}, \quad (5.11)$$

where  $\theta$  is the equivalent power beamwidth of the main lobe. The resulting weighting factor for the probability of interference,  $\tau$ , is  $6 \times 10^{-5}$ .

The BER of WLAN links in a coverage area with 37 AWR is only slightly worse than with 17 AWR. In fact, Figure 5-4 shows that bit errors are highly resistant to multiple aircraft carrying AWR. Even in the event that a WLAN link is within the coverage areas of 50 separate aircraft, the starred red curve shows the BER rate remains below  $10^{-3}$  for the typical duty cycle of 0.001 (0.1%) and scan factor of 0.06.

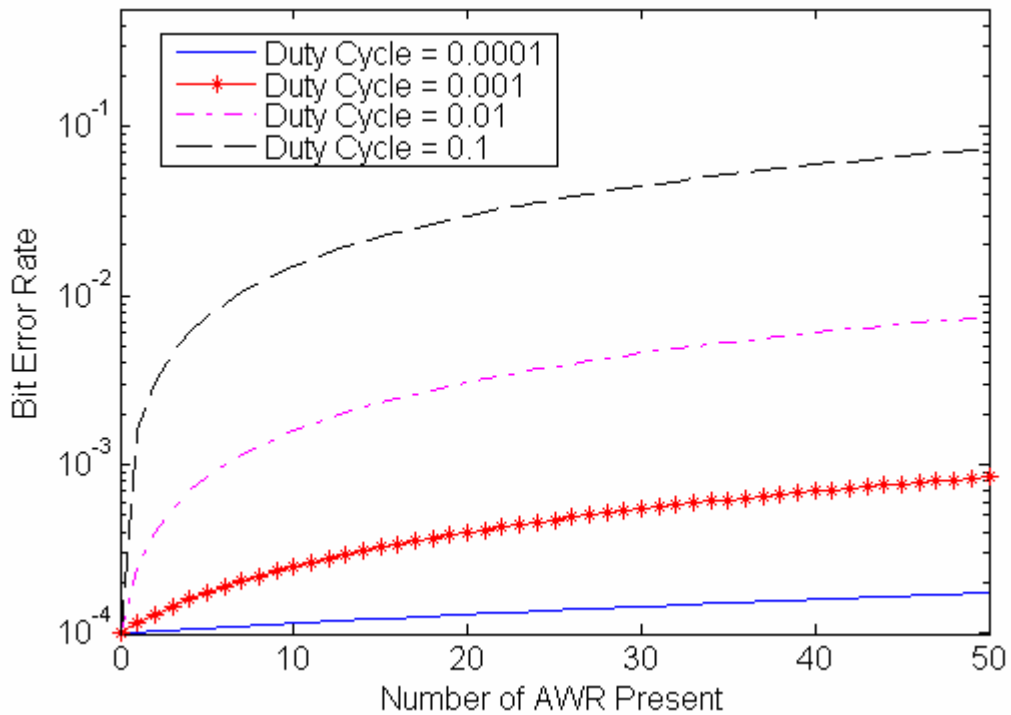


Figure 5-4. Bit error rate of a WLAN link in shared spectrum with AWRs versus the number of aircraft present carrying AWRs. Duty cycles and beamwidth for AWRs are representative of AWR specifications shown in Appendix C.

Although the BER is not sensitive to the number of AWR interferers, the duty cycle of the interferers greatly affects the BER. In Figure 5-5, a sharp rise in BER is seen as the duty cycle reaches 0.001 ( $\tau = 6 \times 10^{-5}$ ). Above an AWR's typical duty cycle of 0.001, BERs continue to increase to  $10^{-2}$  for both Victor airways and jetways.

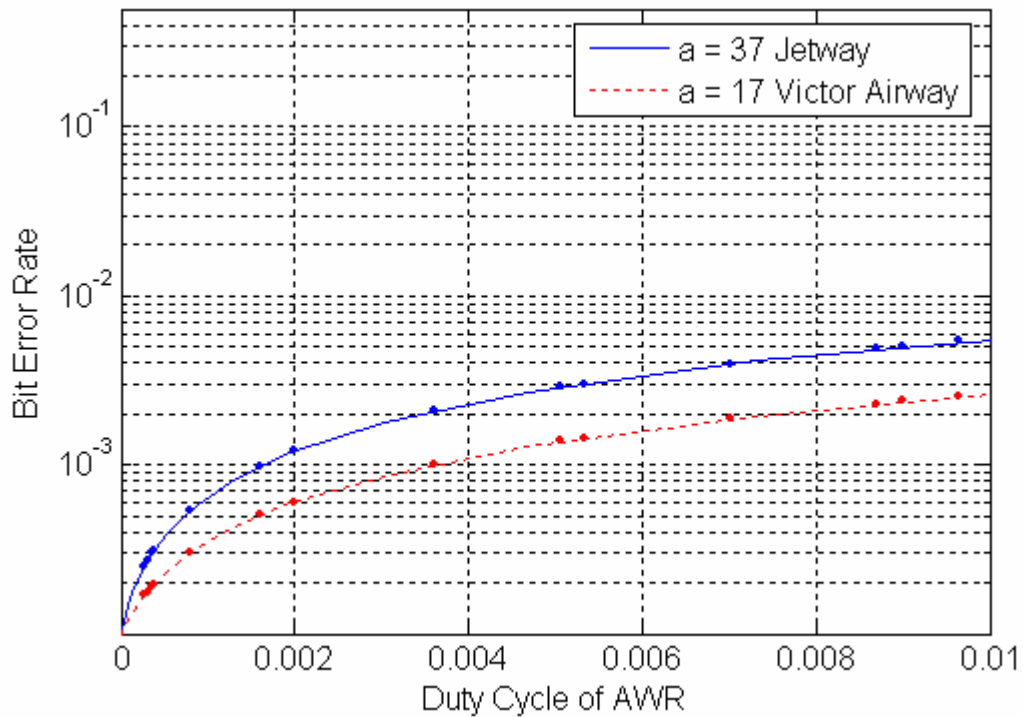


Figure 5-5. Bit error rate of a WLAN link in shared spectrum with AWRs versus the duty cycle of the AWRs. Data points show duty cycles of real AWRs. Duty cycles of real AWRs reach 0.13, but duty cycles above 0.01 have unreasonably high BERs. WLANs operating under a jetway can expect an average of 37 interferers. In Victor airways the number of aircraft carrying AWR is 17.

### 5.2.3 Recommendation of Spectrum Sharing for Narrowband Wireless Local Area Networks

Spectrum sharing between AWRs and narrowband digital WLAN systems is not advisable. The high probability of the WLAN links causing harmful interference to AWR does not allow spectrum sharing. Though AWR cannot tolerate the interference, the bit error rates in the WLAN links are sufficiently low to operate in shared spectrum.

### 5.3 Direct Sequence Spread Spectrum Wireless Local Area Network

The emissions from wireless local area network (WLAN) transmissions can cause interference to airborne weather radars (AWRs) in shared spectrum. To minimize this interference the transmit power of the WLAN links can be spread across a bandwidth larger than the AWR receiver bandwidth using direct sequence spread spectrum (DSSS) modulation. Power outside the receiver bandwidth does not cause interference and is modeled as a reduction of the total effective interference by the on-tune rejection factor (OTR) defined in decibels. The OTR is

$$\begin{aligned} OTR &= 0 && \text{for } B_{IF} \geq B_T \\ OTR &= 10 \log(B_T / B_{IF}) && \text{for } B_{IF} < B_T \end{aligned} \quad (5.12)$$

where  $B_{IF}$  is the 3 dB bandwidth of the AWR receiver and  $B_T$  is the transmitter 3 dB bandwidth in Hz [16]. The 3 dB bandwidth of a typical AWR receiver is 2 MHz as discussed in Section 3.1.2. The reduced interference is modeled by modifying of the maximum allowable users,  $m$ , to include the OTR.

$$m = \left\lfloor I_{max} \frac{(4\pi)^2 L_{misc} (R_{max} R_c)}{P_t G_t G_r \lambda^2} OTR \right\rfloor \text{ links.} \quad (5.13)$$

Using a data symbol rate,  $R_s$ , of 1 MHz to match the narrowband WLAN, a spreading gain of 200 is chosen in order to occupy the entire 9.3 GHz – 9.5 GHz range. The spreading gain,  $G$ , is the ratio of the total bandwidth of the signal to the data rate,

$$G = \frac{W}{R_s} = \frac{R_c}{R_s}, \quad (5.14)$$

where  $W$  is the total occupied bandwidth,  $R_b$  is the data symbol rate, and  $R_c$  is the rate of the spreading sequence called the chipping rate. The performance of a DSSS system in AWGN is identical to a narrowband system with the same assumptions requiring a 1 mW transmitter.

The data signal uses BPSK modulation to reach the target BER of  $1 \times 10^{-4}$  with the required signal to noise ratio (SNR) of 8.4 dB. The required SNR for a BSPK modulated DSSS signal in additive white Gaussian noise (AWGN) is identical to the required SNR for the narrowband case. A 1 mW transmitter provides a margin of 3.1 dB over the minimum required SNR. This transmit power and distance is verified against existing WLANs such as Bluetooth [53]. Appendix B presents a link budget calculating the required transmit power for this direct sequence spread spectrum link assuming no co-channel interference.

### 5.3.1 Interference into Airborne Weather Radar from Direct Sequence Spread Spectrum Wireless Local Area Networks

The transmit power is now used to calculate the likelihood that the total effective interference from all WLAN links in a coverage area,  $I_{total}$ , exceeds the maximum allowable received interference power,  $I_{max}$ . If the number of links in the coverage area,  $\eta A$ , is less than or equal to the maximum allowable links,  $m$ , then the probability of harmful interference is zero; otherwise, the interference will be harmful to an AWR and spectrum sharing is not advisable. The maximum allowable links,  $m$ , is calculated using (5.15) with all parameters represented in decibels summarized in Table 5-4. The OTR is included to model power transmitted outside of the radar receiver bandwidth of 2 MHz.

$$m = \left\lceil \frac{I_{max} (4\pi)^2 L_{misc} (R_{max} R_c)}{P_t G_t G_r \lambda^2} + OTR \right\rceil \text{ links} \quad (5.15)$$

Parameter		Value	Justification
$I_{max}$	= Maximum allowable received interference power	-142.6 dBW	Assumption [16]
$(4\pi)^2$		22.0 dB	Constant
$L_{misc}$	= losses due to building penetration and system losses	7.0 dB	Assumption [35]
$R_{max}R_c$	= Path loss distance is the product of the maximum and minimum possible separation between AWR and WLAN in a coverage area	108.8 dB meters for jetways	Derived from scenario
		104.9 dB meters for Victor airways	Derived from scenario
$P_t$	= WLAN transmitter power	-30.0 dBW	Derived from Link Budget
$G_t$	= WLAN transmitter antenna gain	0.0 dB	Assumption [52, 53]
$G_r$	= AWR receiver antenna gain	32.0 dB	Assumption see Table 3-1
$\lambda^2$	= wavelength at 9.35 GHz squared	-29.9 dB meters	Center frequency
		20.0 dB	200 MHz WLAN transmitter and a 2 MHz AWR receiver bandwidth
OTR	= on-tune rejection factor		
m	= maximum allowable WLAN links	20,127 links for jetway scenario	Derived from (5.10)
		8255 links for Victor airway scenario	

Table 5-4. Parameters for direct sequence spread spectrum WLAN to AWR interference calculations. The maximum allowable links is 20,127 links in a jetway and 8255 links in a Victor airway. The number of allowed links exceeds the number of expected links in a jetway and Victor airway coverage areas.

There are  $5.6 \times 10^6$  links in coverage areas below jetways and  $2.5 \times 10^6$  links for Victor airways, and the maximum allowable number of WLAN links is 20,127 for jetways and 8255 links for Victor airways. The total number of links far exceeds the maximum allowable in

coverage areas for jetways and Victor airways; therefore, DSSS WLANs cause harmful interference to AWR. Even assuming that links are not continuously operating, spectrum sharing is not feasible for all non-trivial probabilities that WLAN links do not interfere with a present AWR.

Favorable results can be achieved by holding the probability that a single WLAN link interferes with AWR constant at 1 and varying transmit power and link density. Reducing the number of links to 4 per square kilometer reduces the expected interference to allowable levels. But, reductions of transmit power as low as 0.1 mW still produces interference 5 dB higher than the allowable level. Intermittent transmissions do not allow spectrum sharing either; again, expected interference is 5 dB higher than the allowable level with each WLAN link only transmitting 1% of the time. A combination of lowered probability of transmission and transmit power, shown in Figure 5-8, does reduce interference to allowable levels. A direct sequence spread spectrum communications system does offer the opportunity to create a system that is capable of sharing spectrum with AWR. Spectrum sharing can be accomplished by reducing the number of links per squares kilometer, reducing the transmit power, and reducing the likelihood of transmission as allowed by the system parameters.

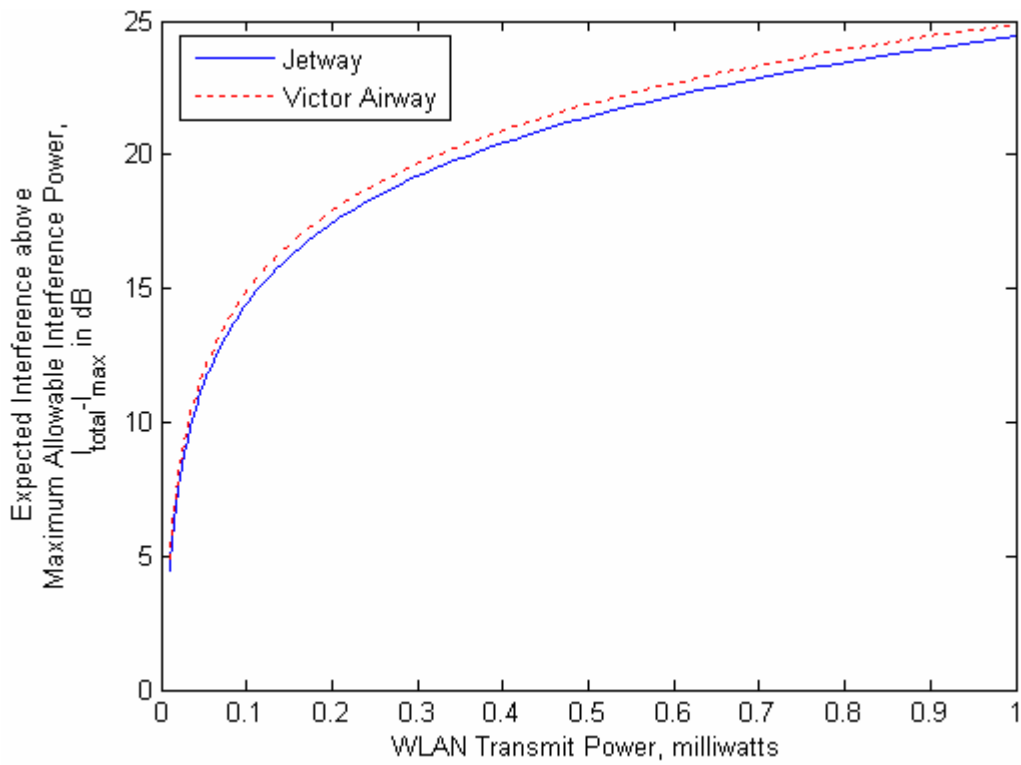


Figure 5-6. Expected interference above the maximum allowable interference versus WLAN transmit power. Interference into AWR receivers is expected to be at least 10 dB higher than the allowable level in both jetways and Victor airways with a minimum transmit power of 0.1 mW with the probability that a single WLAN link interferes with an AWR is 100%.

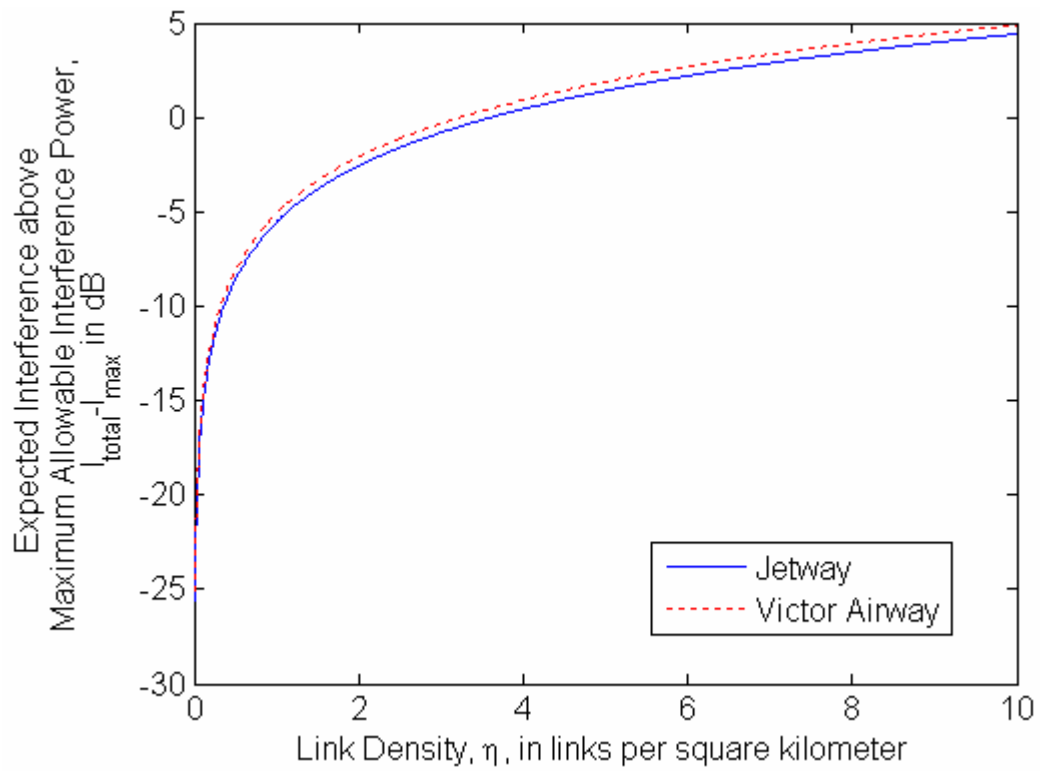


Figure 5-7. Expected interference above the maximum allowable interference versus link density. The expected interference approaches maximum allowable level as the link density is decreased to below 5 per kilometer.

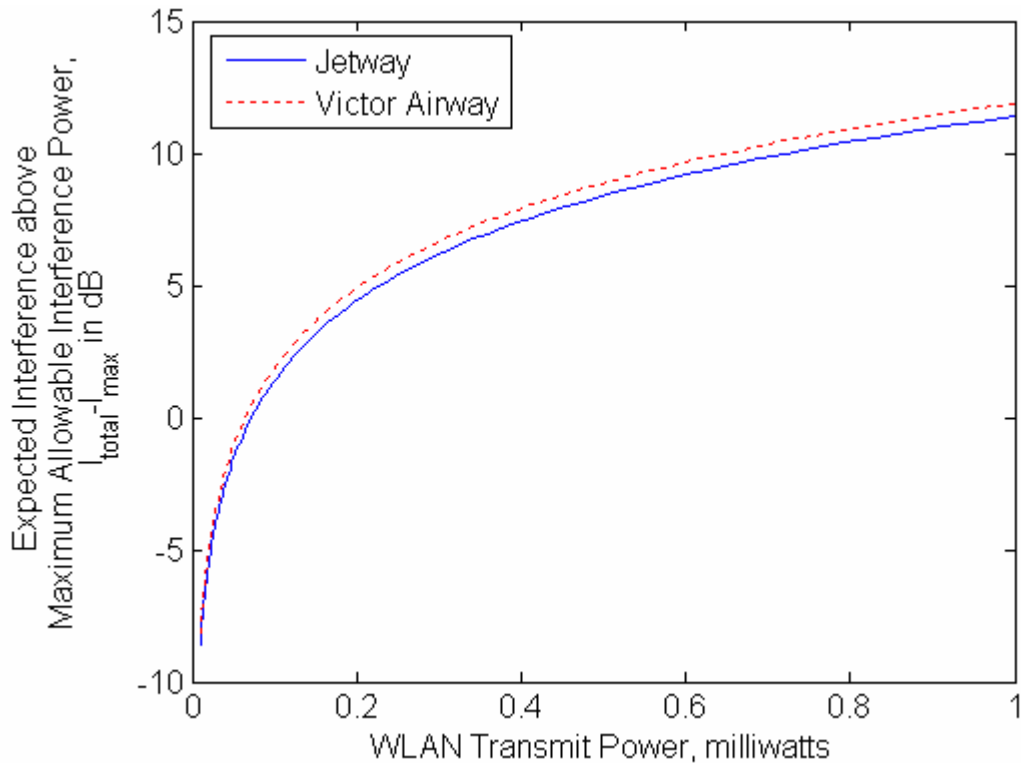


Figure 5-8. Expected interference above the maximum allowable interference versus WLAN transmit power. Interference into AWR receivers is below the maximum level in both jetways and Victor airways with a minimum transmit power of 0.1 mW and a probability that a single WLAN link interferes with an AWR of 5%.

### 5.3.2 Bit Error Rate of Direct Sequence Spread Spectrum Wireless Local Area Networks in Shared Spectrum with Airborne Weather Radar

Spectrum sharing between AWR and WLANs does cause harmful interference to an AWR, but the BER of WLAN links in shared spectrum are reasonably low. The assumptions used to develop (5.5) are valid for DSSS links and total BER calculations parallel the narrowband case. The use of 50% BER during interference is justified because the received interference from an AWRs is much larger than the received WLAN signal. Transmissions from AWR are modeled as pulsed interference over the entire band of operation of DSSS

links. This type of interference is treated as an additional noise source due to the despreading process in the DSSS WLAN receiver [37].

$$P_{b\_jammer} = Q\left(\sqrt{\frac{2GS\tau}{J}}\right) \quad (5.16)$$

Equation (5.16) shows the BER of a DSSS link in shared spectrum with an AWR, where the duty cycle of AWR is  $\tau$ , the signal power is  $S$ , the noise power is  $N$ , and the peak interference power is  $J$ . The received power from a desired WLAN signal is -122.8 dBW and the expected received power from an AWR is -89.6 dBW, resulting in a BER during interference of 50%.

The total BER, calculated with (5.5), in a jetway is  $6.5 \times 10^{-4}$ . The BER in a Victor airway is  $3.5 \times 10^{-4}$ . This total BER assumes the BER with no interference is  $10^{-4}$ , the BER with interference is 50%, the typical AWR duty cycle is 0.001, and the antenna is not pointing at the WLAN link 94% of the time due to horizontal scanning. WLANs in coverage areas defined by the jetway scenario have an average of 37 interfering AWR and 17 interferers are present in the Victor airway scenario.

As with the narrowband system, the BER of WLAN links in a coverage area with 37 AWRs is only slightly worse than with 17 AWR. In fact, bit errors are highly resistant to multiple aircraft carrying AWR. Even with the unlikely event that a WLAN link is within the coverage areas of 50 separate aircraft, the starred red curve shows the BER rate remains below  $5 \times 10^{-3}$  for the typical duty cycle of 0.001 (0.1%), and scan factor of 0.03. Although the BER is not sensitive to the number of AWR interferers, the duty cycle of the interferers greatly affects the BER. As with the narrowband case, BER increases to  $10^{-2}$  for both Victor airways and jetways for duty cycles above 0.1%.

### **5.3.3 Recommendation of Spectrum Sharing for Direct Sequence Spread Spectrum Wireless Local Area Networks**

Spectrum sharing between airborne weather radar and DSSS WLAN is not feasible because interference from the DSSS WLAN into AWRs is harmful under current assumptions. Harmful interference could be reduced to acceptable levels by a combination of lower link density, lower transmit power, and lower duty cycle. A system under these assumptions is capable of sharing spectrum with AWR, and the interference from AWR is sufficiently infrequent to not disrupt operation of the WLAN system.

### **5.4 Frequency Hopping Spread Spectrum Wireless Local Area Network**

A frequency hopping spread spectrum communications system distributes harmful interference from WLANs across a wide bandwidth, potentially reducing the impact of this interference to AWRs. The bandwidth is spread by hopping the center frequency of the transmit signal to  $N$  different frequencies. We assume the signal is hopped at a chipping rate,  $R_c$ , equal to the symbol rate,  $R_b$ . A symbol rate of 1 MHz is chosen to match the symbol rate of the narrowband WLAN. The bandpass bandwidth is 2 MHz non-coherent, non-phase continuous binary frequency shift keying (BFSK) per chip [36].

Binary modulation is used to reach the target BER of  $1 \times 10^{-4}$  with the required signal to noise ratio (SNR) of 12.3 dB. The required SNR for a BFSK signal in additive white Gaussian noise (AWGN) is calculated using (5.17) [30]. In (5.17), the probability of error,  $P_{eBFSK}$ , is related to the signal power,  $S$ , and the noise power,  $N$ . The BER calculation assumes an ideal non-coherent receiver with perfect synchronization and zero intersymbol interference.

$$P_{eBFSK} = \frac{1}{2} e^{-\frac{S}{2N}} \quad (5.17)$$

To meet the target SNR at the WLAN receiver, a link budget is used to determine the required transmit power. The transmit power is chosen to provide an SNR with sufficient link margin to account for idealization in the analysis and unexpected signal degradations. The power budget in Table 5-5 calculates the required transmit power of a WLAN device. The transmit power is selected for a specified transmitter gain and receiver gain to overcome the effects free space path loss and miscellaneous losses due to building penetration and system components. The noise power budget in Table 5-5 calculates the receiver noise power. For these calculations, a typical receiver with a noise figure of 10 dB is assumed. Notice that the noise bandwidth is 1 MHz because a non-coherent receiver uses an integrator which acts as a matched filter for an FSK signal. Additional noise introduced by non-coherent reception in the in-phase and quadrature channels is included in the BER equation.

A 2.5 mW transmitter operating at 9.35 GHz separated from the receiver by 50 meters results in a SNR of 15.6 dB. The SNR of 15.6 dB provides a margin of 3.3 dB over the minimum required SNR; consequently, a reliable link exists. This transmit power and distance is reasonable according to the assumptions and agrees with values of existing WLANs such as Bluetooth [53].

Parameter		Value	Justification
$P_t$	= WLAN transmitter power	-26.0 dBW	Derived from Link Budget
$G_t$	= WLAN transmitter antenna gain	0.0 dB	Assumption [52, 53]
$G_r$	= WLAN receiver antenna gain	0.0 dB	Assumption [52, 53]
$L_p$	= Free space path loss at 9.35 GHz over 50 meter	-85.9 dB	Path Loss Equation
$L_{misc}$	= losses due to building penetration and system losses	-7.0 dB	Assumption [35]
$P_r$	= Received power at RF filter	-118.9 dBW	Derived from Link Budget

Table 5-5. Power budget for frequency hopping spread spectrum WLAN link.

Parameter		Value	Justification
k	= Boltzmann's constant	-228.6 dBW/K/Hz	Physical Value
$T_s$	= $290(10^1 - 1)$	34.2 dBK	Assumption of inexpensive receiver
$B_N$	= 1 MHz	60 dBHz	Assumption [52, 53]
N	= Receiver noise power	-134.4 dBW	Derived from Link Budget

Table 5-6. Noise Power budget for frequency hopping spread spectrum WLAN receiver.

#### 5.4.1 Interference into Airborne Weather Radar from Frequency hopping spread spectrum Wireless Local Area Networks

The transmit power and BER derived from the link budgets and verified against known systems are now used to calculate (5.4): the likelihood,  $P_I$ , that the total effective interference from all WLAN links in a coverage area,  $I_{total}$ , exceeds the maximum allowable

received interference power,  $I_{max}$ . If the number of links in the coverage area,  $\eta A$ , is less than or equal to the maximum allowable links,  $m$ , then the probability of harmful interference is zero; otherwise, the interference will be harmful to AWR and spectrum sharing is not advisable. The maximum allowable links,  $m$ , is calculated using (5.10) with all parameters represented in decibels summarized in Table 5-7.

$$m = \left\lfloor \frac{I_{max} (4\pi)^2 L_{misc} (R_{max} R_c)}{P_i G_t G_r \lambda^2} \right\rfloor \text{ links} \quad (5.18)$$

Parameter		Value	Justification
$I_{\max}$	= Maximum allowable received interference power	-142.6 dBW	Assumption [16]
$(4\pi)^2$		22.0 dB	Constant
$L_{\text{misc}}$	= losses due to building penetration and system losses	7.0 dB	Assumption [35]
$R_{\max}R_c$	= Path loss distance is the product of the maximum and minimum possible separation between AWR and WLAN in a coverage area	108.8 dB meters squared for jetways 104.9 dB meters squared for Victor airways	Derived from scenario Derived from scenario
$P_t$	= WLAN transmitter power	-26.0 dBW	Derived from Link Budget
$G_t$	= WLAN transmitter antenna gain	0.0 dB	Assumption [52, 53]
$G_r$	= AWR receiver antenna gain	32.0 dB	Assumption see Table 3-1
$\lambda^2$	= wavelength at 9.35 GHz squared	-29.9 dB meters squared	Center frequency
$m$	= maximum allowable WLAN links	80 links for jetway scenario 32 link for Victor airway scenario	Derived from (5.10)

Table 5-7. Parameters for frequency hopping spread spectrum WLAN to AWR interference calculations. The maximum allowable links is 80 links in a jetway and 32 links in a Victor airway. There are more links expected than allowed in a coverage area for both jetways and Victor airways.

There are  $5.6 \times 10^6$  links in coverage areas below jetways and  $2.5 \times 10^6$  links for Victor airways, but the maximum allowable number of WLAN links is 80 for jetways and 32 for Victor airways. To model a FHSS WLAN it is assumed that each WLAN link is transmitting in frequencies uniformly distributed across the total 200 MHz spectrum of operation. The

receiver bandwidth of the AWR is similarly distributed across these 200 MHz. Any overlap in the transmission frequencies and receiver bandwidth is considered harmful interference.

The resulting probability that a single WLAN link interferes with AWR is

$$\rho = \frac{N_{AWR} (W_{WLAN} + W_{AWR})}{200}, \quad (5.19)$$

where  $N_{AWR}$  is number of AWRs,  $W_{WLAN}$  is the bandwidth of the WLAN transmitter, and  $W_{AWR}$  is the AWR receiver bandwidth. The bandwidths are normalized by the total bandwidth to create a valid probability from 0 to 1.

The parameter  $\rho$  is used in (5.3) to find  $P_I$ , the probability that the collective interference from all WLAN links in a coverage area causes harmful interference to a present AWR. This probability is plotted in Figure 5-9 over all possible values of  $\rho$ . For the frequency hopping spread spectrum case,  $W_{WLAN}$  equals 2 MHz and  $W_{AWR}$  2 MHz resulting in  $\rho$  equal to  $N_{AWR} \cdot 0.035$ . The AWR receiver bandwidth,  $W_{AWR}$ , of 2 MHz is based on data collected from typical AWR summarized in Table 3-1. Using these bandwidths,  $P_I$  is above 100% for both jetways and Victor airways. For all non-trivial probabilities that a single link interferes with a present AWR the probability of harmful interference does not allow spectrum sharing.

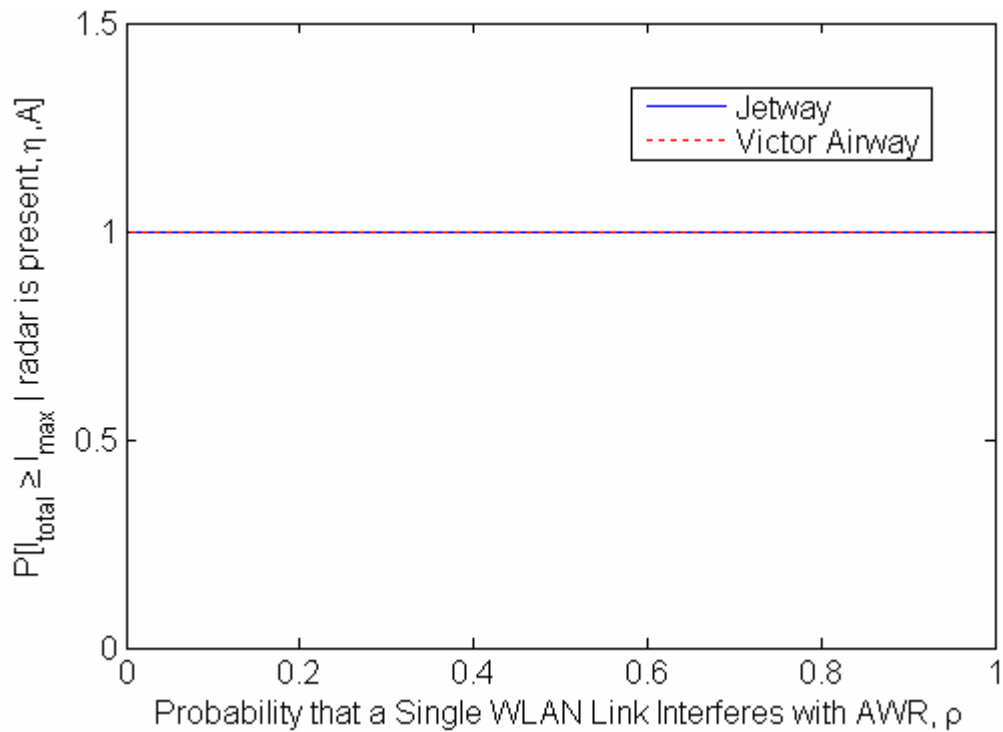


Figure 5-9. Probability that the total effective interference received by all WLAN links in a coverage area exceeds the maximum allowable received interference. Harmful interference is 100% likely in both jetways and Victor airways.

Results similar to the narrowband WLAN indicating spectrum sharing is not feasible are also found in the FHSS WLAN. These results are found by holding the probability that a single WLAN link interferes with an AWR constant at 0.035 (one AWR is present) and varying transmit power and link density. Even with transmit power at 0.1 mW, the interference is expected to be 20 dB higher than the allowable level. Reducing the number of links per square kilometer, on the other hand, does reduce the expected interference to allowable levels, but reductions below 1 link per square kilometer are required. A link density below 1 link per square kilometer is not acceptable for local area networks in urban areas, but other applications or scenarios for a communications system with extremely low link density may exist.

## 5.4.2 Bit Error Rate of Frequency hopping spread spectrum Wireless Local Area Networks in Shared Spectrum with Airborne Weather Radar

The feasibility of spectrum sharing also depends on the performance of the WLAN links. The BER of WLAN links in a coverage area combined with the probability of harmful interference to AWR is needed to fully evaluate spectrum sharing. The total BER, calculated with (5.20) for a FHSS link, in a jetway is  $6.5 \times 10^{-4}$ , and in a Victor airway is  $3.5 \times 10^{-4}$ . This BER assumes an average number of interferers,  $a$ , is 37 for the jetway scenario, and 17 for Victor airways. The BER with no interference is  $10^{-4}$  resulting from a SNR of 12.5 dB and 50% BER during interference. The duty cycle is 0.001 and the WLAN is only illuminated 94% of the time by the AWR antenna as it sweeps through its horizontal scan.

$$P_b = \left( e^{-a} + (1-\tau) \right) \frac{1}{2} e^{-\frac{s}{2N}} + \tau \left( a - e^{-a} \right) \frac{1}{2} \quad (5.20)$$

In the frequency hopping case, the BER of WLAN links in a coverage area with 37 AWRs is only slightly worse than with 17 AWRs. In fact, Figure 5-10 shows that bit errors are highly resistant to multiple aircraft carrying AWR. Even in the unlikely event that a WLAN link is within the coverage areas of 50 separate aircraft, the starred red curve shows the BER rate remains below  $5 \times 10^{-3}$  for the typical duty cycle of 0.1% and a scan factor of 6%.

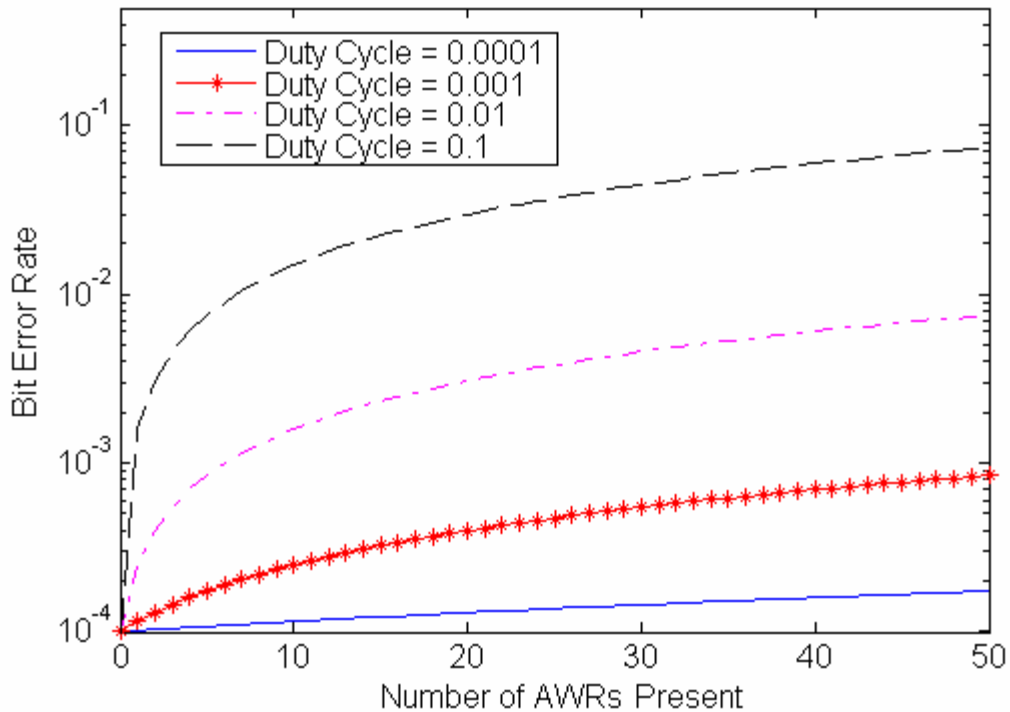


Figure 5-10. Bit error rate of a WLAN link in shared spectrum with AWRs versus the number of aircraft present carrying AWR. Duty cycles,  $\tau$ , are representative of duty cycles for AWRs shown in Appendix C.

The duty cycle of the interferers greatly affects the BER, and frequency hopping does not protect the system from interference because interference is expected over the entire 9.3 GHz – 9.5 GHz band. A similar result to the narrowband and DSSS case is found. Figure 5-11 shows a sharp rise in BER is seen as the duty cycle reaches 0.001 ( $\tau = 6 \times 10^{-5}$ ). Above an AWR’s typical duty cycle of 0.001, BERs continue to increase to  $10^{-2}$  for both Victor airways and jetways.

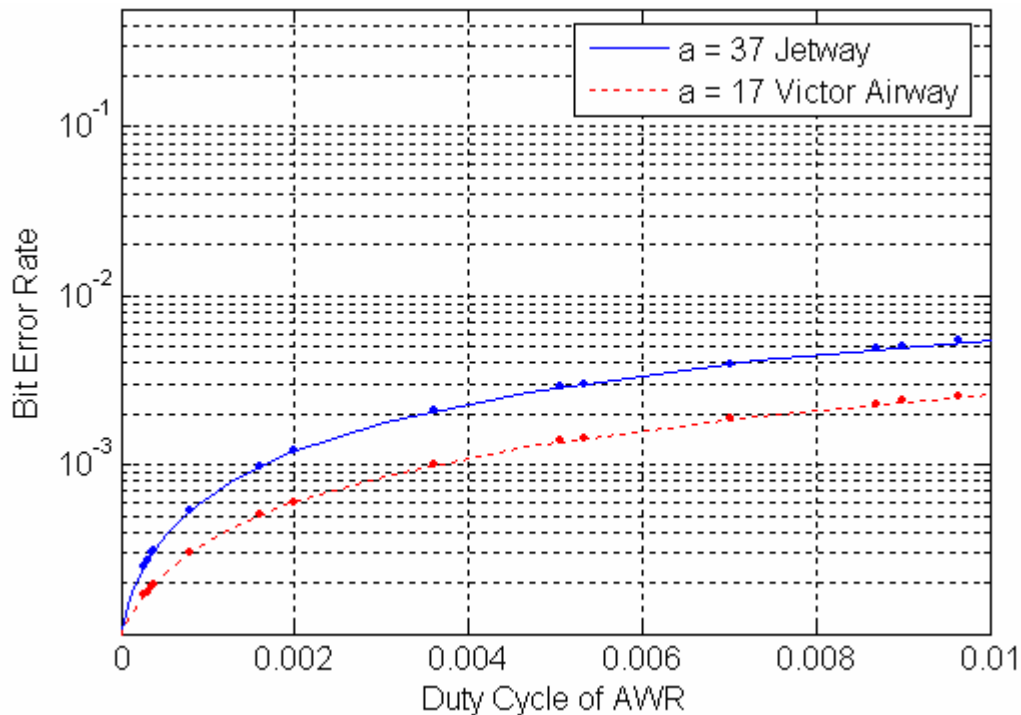


Figure 5-11. Bit error rate of a WLAN link in shared spectrum with AWR versus the duty cycle of the AWRs. Data points show duty cycles of real AWRs. Duty cycles of real AWRs reach 0.13, but duty cycles above 0.01 have unreasonably high BERs. An average of 37 and 17 AWRs interferers are plotted. WLANs operating under a jetway can expect an average of 37 interferers. In Victor airways the number of aircraft carrying AWR is 17.

#### 5.4.3 Recommendation of Spectrum Sharing for Frequency hopping spread spectrum Wireless Local Area Networks

Spectrum sharing between AWR and FHSS digital communications systems is not advisable. The high probability of the communications links causing harmful interference to airborne weather radar does not allow spectrum sharing. Though AWR cannot tolerate the interference, the bit error rates in the communications links are sufficiently low to operate in shared spectrum. If interference with AWR can be prevented by improvements to the basic FHSS system analyzed here, shared spectrum may be possible.

## 5.5 Recommendations

The feasibility of spectrum sharing between AWR and WLANs depends on the amount of interference received by an AWR. This is measured by the likelihood of harmful interference and the BER of the WLAN in shared spectrum. Metrics developed in this thesis to measure these two factors were applied to a narrowband, DSSS, and FHSS WLANs. Spectrum sharing between AWR and narrowband or FHSS digital communications systems is not advisable due to the high probability of the communications links causing harmful interference to airborne weather radar. DSSS WLANs can share spectrum with AWR with sufficiently low user density because a large amount of transmitted power is outside the AWR receiver bandwidth. In all cases, the BER in the communications links are sufficiently low to operate in shared spectrum.

## Chapter 6

### Conclusion

Spectrum sharing at 9.3 GHz – 9.5 GHz can provide a solution to the spectrum shortage problem. Opportunities for spectrum sharing are explored by avoiding sharing at congested frequencies near 2.4 GHz and 5.5 GHz and analyzing characteristics of flight paths of aircraft using airborne weather radar and the low duty cycle of radar transmissions. This thesis explores the feasibility of spectrum sharing between airborne weather radar (AWR) and wireless local area networks (WLANs) by developing the metric of likelihood of harmful interference. The likelihood of harmful interference measures the probability that interference emitted from a set of transmitters exceeds the allowable received interference power of a receiver. In typical worst case scenarios, results show that uniformly distributed WLAN links in metropolitan areas cause interference at least 10 dB above allowable levels. Bit error rate (BER) performance of the WLAN links were also quantified by metrics developed in this thesis. Calculations show that the BER due to AWR interference is  $3.5 \times 10^{-4}$  to  $6.5 \times 10^{-4}$ , infrequent enough to be handled by detection and error correction methods.

#### 6.1 Metrics for Analysis of Interference in Shared Spectrum

The likelihood of harmful interference measures the likelihood that the total interference,  $I_{total}$ , exceeds the maximum allowable received interference power,  $I_{max}$ . Equation (3.36) shows this likelihood for an AWR receiving interference from a coverage area that is uniformly occupied by WLAN transmitters. This likelihood depends on the

number of links in the coverage area,  $\eta A$ , and the expected interference of those links,

$$\frac{(4\pi)^2 L_{misc} (R_{max} R_c)}{P_t G_t G_r \lambda^2}, \text{ and the AWR's tolerability to interference, } I_{max}.$$

$$P_I = P\left[ I_{total} \geq I_{max} \mid \text{AWR is present, } \eta, A \right] = 1 - P\left[ S_{\eta A} \leq \left\lfloor I_{max} \frac{(4\pi)^2 L_{misc} (R_{max} R_c)}{P_t G_t G_r \lambda^2} \right\rfloor \mid \text{AWR is present, } \eta, A \right] \quad (3.36)$$

Parameters which can be varied to find compatible systems are the transmit power of the WLAN interferer,  $P_t$ , the WLAN antenna gain,  $G_t$ , the user density,  $\eta$ , and the likelihood that a single WLAN link interferes with an AWR. All other parameters are defined by the flight characteristics of aircraft carrying AWR or characteristics of the AWR. The maximum,  $R_{max}$ , and minimum,  $R_c$ , possible separation between the AWR receiver and WLAN transmitters is determined by the altitude of aircraft, the tilt angle of the AWR antenna, and the radiation pattern of the AWR antenna. The maximum allowable received interference power,  $I_{max}$ , is defined by the receiver's tolerability to interference. The interference received by the AWR receiver from WLAN links is modeled by the free space path loss equation with wavelength,  $\lambda$ , and miscellaneous losses,  $L_{misc}$ . The binomially distributed random variable,  $S_{\eta A}$ , is the number of interfering links arising from a sum of Bernoulli trials which model the likelihood that a single WLAN link in the coverage area is interfering with a present AWR.

Interference affecting AWR is caused by transmissions of WLAN links within a coverage area. The coverage area depends on the tilt angle of typical AWR, the beamwidth of the AWR, and the altitude of the aircraft carrying the AWR. These parameters were found by analyzing the flight characteristics of aircraft, the typical usage of AWR while aircraft are en route, and typical characteristics of AWR. A unique model of the beamwidth of AWRs was developed to include interference received from the entire antenna pattern. This model eliminates the sidelobes present in typical antenna patterns by consolidating all of the power received by these sidelobes into an equivalent power main lobe. Using the equivalent power

main lobe, the tilt angle, and altitude; the coverage area is defined for two scenarios that represent the typical worst case.

Two scenarios are chosen to represent the most likely and most severe cases of interference. A jetway is the heaviest traveled airspace by aircraft carrying AWR; therefore, a scenario considering WLANs operating under a jetway is an indicator of one possible worst case performance of WLANs and AWR in shared spectrum. A Victor airway is the lowest altitude route in which aircraft carry AWR; therefore, this scenario is also an indicator of worst case performance for AWR and WLANs operating in shared spectrum. [14, 15]

In addition for use in WLAN to AWR interference, the likelihood of harmful interference for WLAN to AWR interference can be applied to any situation where a uniformly distributed set of transmitters are interfering with a receiver and where the free space path loss can be assumed. When these assumptions are not valid, an applicable metric can be created with any distribution of interferers or any path loss to model any pair of systems. The expected interference above the allowable level, a variation of (3.36), measures the severity of the interference to show the expected interference above the allowable level. The extent of the interference and required reduction of interference necessary for spectrum sharing can be measured by adjusting parameters such as transmit power, link density, and likelihood of individual WLAN links interfering with AWR. By adjusting these parameters a system can be found that allows spectrum sharing.

The two scenarios used for WLAN to AWR interference analysis are also used to estimate the performance of WLAN links in spectrum shared with AWR. Performance of WLAN links in shared spectrum is modeled as a BER of a communications system in a pulsed jammer environment. The likelihood of bit errors during interference (jamming) depends on the number of AWRs with coverage areas over the link of interest and the likelihood that the AWRs are interfering with the link of interest. The coverage area for interference analysis for affected WLANs was found by using a distinct antenna pattern. This pattern considers the main lobe and first two sidelobes of the AWR antenna which

contribute the majority of interference. From the coverage area determined by the AWR antenna, the arrival and departure rate of AWR over the WLAN link is found. A model was developed from queuing theory to calculate the expected number of present AWR using the arrival and departure rate. The bit error rate of WLAN links in shared spectrum

$$P_b \leq (e^{-a} + (1-\tau)) P[\text{error|no interference}] + \tau (a - e^{-a}) \frac{1}{2} \quad (4.16)$$

depends on mean number of interferers,  $a$ , the likelihood that these interferers are interfering with WLANs,  $\tau$ , and the BER with no interference,  $P[\text{error|no interference}]$ . AWRs typically transmit with low duty cycles and rotate their beams in the horizontal direction to scan  $90^\circ$  of azimuth ahead of the aircraft. The low duty cycle and horizontal scanning limits the likelihood that AWRs are interfering with WLAN links. Typical coverage area are large, 200 – 500 km, resulting in low departure rates and consequently dozens of potentially interfering AWR, but the low duty cycle, 0.1%, and horizontal scanning minimizes the impact of AWR interference.

## 6.2 Results of Spectrum Sharing Analysis

The likelihood of harmful interference to AWR receivers, (3.36), depends on the radiation pattern of the AWR antenna and the transmit power of WLAN links. The radiation pattern covers an area on the surface of the Earth from which interference is received. Using an antenna pattern developed in this thesis, it was found that the coverage area is 2545 – 5568 square kilometers. In large metropolitan areas, such as Los Angeles or New York, links are uniformly distributed within the coverage area with a density of 1000 links per square kilometer. WLAN links within a coverage area transmit RF interference into the AWR receiver, and the many WLAN links (2 – 5 million) are the main contributors of interference. Because the large number of links is the main contributor of interference, reducing other parameters such as the transmit power of the WLAN links and the likelihood that an

individual link interference with AWRs does not significantly reduce the likelihood of harmful interference. To achieve significant reductions in harmful interference, the density of WLAN links must be reduced to 1 link per square kilometer for narrowband or frequency hopping spread spectrum links. The link density can be up to 4 links per square kilometer with direct sequence spread spectrum, because direct sequence spread spectrum distributes much of the WLAN transmit power beyond the AWR receiver bandwidth. Interference into AWR receivers is harmful in many cases, but interference from the AWRs do not cause significant degradations in performance of WLAN links. The expected BER of a WLAN link in shared spectrum is  $5 \times 10^{-4}$  to  $6.5 \times 10^{-4}$ , assuming the BER without interference is  $10^{-4}$ .

From these results we can conclude that spectrum sharing between communications systems and AWRs is feasible for a limited number of applications. Although widespread use of WLAN links is not appropriate for spectrum sharing, limited spectrum sharing can be achieved for applications where the number of active links is designed to be below acceptable levels. Systems with infrequent or scattered use for residential, commercial, industrial or agricultural applications warrant further study. Such systems include remote tagging of livestock or infrastructure diagnostics and data collection (e.g. wireless meter readers). Additionally due to their potential low link density, the downlink of regional wireless area networks with base stations sparsely distributed or satellite uplinks for home internet service warrant further study.

The results show that interference into AWR is problematic in spectrum sharing scenarios but interference into WLAN links does not prohibit spectrum sharing. Unique metrics developed in this thesis, the likelihood of harmful interference, (3.36), and BER of WLANs in shared spectrum, (4.16), are used to judge the feasibility of spectrum sharing between these two non-coordinating systems. Even though spectrum sharing is not feasible between airborne weather radar and wireless local area networks, the generalized approach used to develop these metrics can be applied to any system whose tolerability to interference can be measured as a BER or as a total received interference power.



# Appendix A

## Glossary of Terms and Acronyms

AGL	Above Ground Level – height of an object referenced from the ground.
AWR	Airborne Weather Radar – Radar used in commercial and general aviation to detect weather phenomena such as storms and wind-shear. ABR can also be used for ground mapping to aid in navigation [23].
BER	Bit Error Rate – Probability of bit error in a communications system.
BPSK	Binary Phase Shift Keying – A modulation technique where data is encoded as phase changes in the transmit waveform using only two possible symbols.
CFAR	Constant False Alarm Rate – A radar receiver processor that automatically adjusts the decision threshold for detection to maintain a constant probability of false alarm.
Chipping Sequence	A pseudo-random sequence whose pulse period is much smaller than the data symbol period. The chipping sequence is multiplied to the data sequence to generate a spread spectrum signal with bandwidth much wider than necessary to carry the data.
Coverage Area	Area on the ground within the 3 dB beamwidth of a radar antenna pattern. Used to calculate the received interference by airborne weather radar.
Coverage Path	The diameter of the coverage area as defined by a cone representing the radar beam intersecting with a plane representing the Earth. In two dimensions the beam is represented as a triangle and the Earth plane as a line.
DSSS	Direct Sequence Spread Spectrum – A spread spectrum technique where the original data signal is multiplied by a high rate chipping sequence.
EM	Electromagnetic Spectrum – Range of electromagnetic waves

with frequencies from 1Hz-10<sup>24</sup>Hz. Electromagnetic waves are called waves, emissions or signals depending on context.

ESD	Energy Spectral Density – The squared magnitude of the Fourier transform of a pulse shape in time.
E[I]	Expected Level of Interference – The expected value of interference from a coverage area filled with uniformly distributed interferers.
FAA	Federal Aviation Administration - the body which regulates all airspace in the United States
FCC	Federal Communications Commission – The FCC is responsible for “processing applications for licenses and other filings; analyzing complaints; conducting investigations; developing and implementing regulatory programs; and taking part in hearings.”[40]
FHSS	Frequency Hopping Spread Spectrum – A spread spectrum technique where the original data waveform is spread by moving the center frequency to different nonoverlapping frequency channels.
FSK	Frequency Shift Keying – A modulation technique where data is sent on two or more discrete frequencies where each frequency represents a different symbol. We assume non-coherent and non-phase synchronous frequency shift keying that can be decoded with a simple energy detector.
$I_{\max}$	Maximum allowable received interference power. See $P_I$ .
$I_{\text{total}}$	Total effective interference from all WLAN links in a coverage area. See $P_I$ .
IF	Intermediate Frequency – A frequency between the incoming radio frequency and baseband where signal processing or other receiver operations are performed.
I/N	Interference to Noise Ratio – The level of received interference to the noise of a receiver measured at the intermediate frequency stage of a receiver after the radio frequency bandwidth filter but before any processing or digitization.

ISI	Intersymbol Interference – interference between symbols within the same pulse stream. See Nyquist zero intersymbol interference criterion
ITS	Institute for Telecommunications Sciences – A line office of the NTIA which provides engineering support by conduction and reporting on research and experiments.
ITU	International Telecommunications Union – International standards and regulatory body for communications.
Jetway	Class A airway as defined by the FAA in 14-1-2(a) of [15].
M/M/∞ Queuing System	A queuing system defined with Poissonly distributed arrivals, Exponentially distributed departures and infinite queues. This type of queuing system is used to determine the number of airborne weather radar that interfere with a wireless local area network link.
MSL	Mean Sea Level – height of an object referenced from sea level.
NTIA	National Telecommunications and Information Administration - “manages the Federal use of spectrum; performs cutting-edge telecommunications research and engineering, including resolving technical telecommunications issues for the Federal government and private sector; and administers infrastructure and public telecommunications facilities grants.”[39]
OTR	On-Tuned Rejection Factor – Impact of lessened interference due to interference bandwidths greater than radar receiver bandwidths.
$P_b$	Probability of Bit Error – The likelihood incorrectly decoding a bit.
$P_I$	The likelihood that the total effective interference from all WLAN links in a coverage area, $I_{total}$ , exceeds maximum allowable received interference power, $I_{max}$ .
PSD	Power Spectral Density – A measurement of the frequency content of a time limited signal.
PSK	Phase Shift Keying – A modulation technique where data is encoded as phase changes in the transmit waveform.

Primary Service	A service as defined by Part 2.105 of [41] which has been allocated spectrum according to Part 2.101 of [41].
Primary User	A device providing a primary service as defined in Part 2.105 of [41].
Pulsed Jammer	An jammer that transmits intermittently in order to generate higher levels of interference over shorter periods of time when compared to a constantly active jammer.
Radionavigation	“Radiodetermination used for the purposes of navigation, including obstruction warning.”[41]
Radiodetermination	“The determination of the position, velocity and/or other characteristics of an object, or the obtaining of information relating to these parameters, by means of the propagation properties of radio waves.”[41]
Roll-Off Factor	A variable that controls the pulse width of a raised cosine pulse. The roll-off factor ranges from 0 to 1. Zero corresponds to the smallest possible bandwidth and one corresponds to the widest possible bandwidth.
RF	Radio Frequency - A subset of electromagnetic spectrum ranging from 3kHz-300GHz [28]. Also transmit frequency of radar or communications devices.
Secondary Service	A service as defined by Part 2.105 of [41]. Secondary services are prohibited from causing harmful interference to primary users and cannot claim protection from primary users. See Part 2.015(i)(ii)(iii) of [41].
Secondary User	A device providing a secondary service as defined in Part 2.105 of [41].
SNR	Signal to Noise Ratio – The ratio between signal power and noise power either in decibels or as a linear ratio.
SIR	Signal to Interference Ratio – The ratio between signal power and noise power either in decibels or as a linear ratio.
SINR	Signal to Noise Plus Interference Ratio – The ratio between signal power and noise plus interference power in decibels or as a linear ratio.

Total Effective Interference

The total interference received by an AWR directly related to AWR characteristics (tilt angle, beamwidth, and receiver bandwidth), aircraft characteristic (altitude of aircraft), and WLAN characteristics (transmit power, user density, and transmit frequency).

Victor Airway

Class E airway as defined by the FAA in 14-1-2(e) of [15].

WLAN

Wireless Local Area Network – A data network consisting of wireless communications devices.



## Appendix B

### Link Budgets for Wireless Local Area Networks

Parameter		Value	Justification
$P_t$	= WLAN transmitter power	-30.0 dBW	Derived from Link Budget
$G_t$	= WLAN transmitter antenna gain	0.0 dB	Assumption [52, 53]
$G_r$	= WLAN receiver antenna gain	0.0 dB	Assumption [52, 53]
$L_p$	= Free space path loss at 9.35 GHz over 50 meter	-85.9 dB	Path Loss Equation
$L_{misc}$	= losses due to building penetration and system losses	-7.0 dB	Assumption [35]
$P_r$	= Received power at RF filter	-122.9 dBW	Derived from Link Budget

Table B-1. Power budget for narrowband WLAN link.

Parameter		Value	Justification
$k$	= Boltzmann's constant	-228.6 dBW/K/Hz	Physical Value
$T_s$	= $290(10^1 - 1)$	34.2 dBK	Assumption of inexpensive receiver
$R_b$	= 1 MHz	60 dBHz	Assumption [52, 53]
$N$	= Receiver noise power	-134.4 dBW	Derived from Link Budget

Table B-2. Noise Power budget for narrowband WLAN receiver.

<b>Parameter</b>	<b>Value</b>	<b>Justification</b>
$P_t$ = WLAN transmitter power	-30.0 dBW	Derived from Link Budget
$G_t$ = WLAN transmitter antenna gain	0.0 dB	Assumption [52, 53]
$G_r$ = WLAN receiver antenna gain	0.0 dB	Assumption [52, 53]
$L_p$ = Free space path loss at 9.35 GHz over 50 meter	-85.9 dB	Path Loss Equation
$L_{misc}$ = losses due to building penetration and system losses	-7.0 dB	Assumption [35]
$P_r$ = Received power at RF filter	-122.9 dBW	Derived from Link Budget

Table B-3. Power budget for direct sequence spread spectrum WLAN link.

<b>Parameter</b>	<b>Value</b>	<b>Justification</b>
$k$ = Boltzmann's constant	-228.6 dBW/K/Hz	Physical Value
$T_s$ = $290(10^1 - 1)$	34.2 dBK	Assumption of inexpensive receiver
$B_n$ = 1 MHz	60 dBHz	Assumption [52, 53]
$N$ = Receiver noise power	-134.4 dBW	Derived from Link Budget

Table B-4. Noise Power budget for direct sequence spread spectrum WLAN receiver.

Parameter		Value	Justification
$P_t$	= WLAN transmitter power	-26.0 dBW	Derived from Link Budget
$G_t$	= WLAN transmitter antenna gain	0.0 dB	Assumption [52, 53]
$G_r$	= WLAN receiver antenna gain	0.0 dB	Assumption [52, 53]
$L_p$	= Free space path loss at 9.35 GHz over 50 meter	-85.9 dB	Path Loss Equation
$L_{misc}$	= losses due to building penetration and system losses	-7.0 dB	Assumption [35]
$P_r$	= Received power at RF filter	-118.9 dBW	Derived from Link Budget

Table B-5. Power budget for frequency hopping spread spectrum WLAN link.

Parameter		Value	Justification
$k$	= Boltzmann's constant	-228.6 dBW/K/Hz	Physical Value
$T_s$	= $290(10^1 - 1)$	34.2 dBK	Assumption of inexpensive receiver
$R_b$	= 1 MHz	60 dBHz	Assumption [52, 53]
$N$	= Receiver noise power	-134.4 dBW	Derived from Link Budget

Table B-6. Noise Power budget for frequency hopping spread spectrum WLAN receiver.



## Appendix C

### Typical Airborne Weather Radars Characteristics

Model	Peak Power (W)	PRF (pps)	Pulse Width (us)	Antenna Gain (dBi)	Vertical Beamwidth (degrees)	Source
Honeywell RDR4000	Unknown	Unknown	Unknown	28.5, 31, 33, 34.8	8, 5.6, 4.2, 3	[43]
Collins WXR-2100	150	9000-180	1-20	34	3.5	[42]
Collins WRX-700x	Unknown	Unknown	Unknown	Unknown	3.5	[55]
Airborne Weather Radar	10,000	2000-230	0.19-234	32	4	[16]
Unknown Magnetron	10,000	1600, 800, 200	0.5, 2, 10	27, 31, 33	7.3, 4.8, 3.6	[21]
Unknown Solid State	125	6000, 1600, 380	0.06, 0.17, 0.8	33, 35	2.9, 3.6	[21]



## Appendix D

### United States Frequency Allocations at 9.3GHz-9.5GHz[12]

Frequency	Services	Footnote #	Footnote
9300-9500		5.427	In the bands 2 900-3 100 MHz and 9 300-9 500 MHz, the response from radar transponders shall not be capable of being confused with the response from radar beacons (racons) and shall not cause interference to ship or aeronautical radars in the radionavigation service, having regard, however, to No. 4.9.
		5.474	See Above
		5.475	The use of the band 9 300-9 500 MHz by the aeronautical radionavigation service is limited to airborne weather radars and ground-based radars. In addition, ground-based radar beacons in the aeronautical radionavigation service are permitted in the band 9 300-9 320 MHz on condition that harmful interference is not caused to the maritime radionavigation service. In the band 9 300- 9 500 MHz, ground-based radars used for meteorological purposes have priority over other radiolocation devices.
9300-9500	RADIONAVIGATION	5.476	In the band 9 300-9 320 MHz in the radionavigation service, the use of shipborne radars, other than those existing on 1 January 1976, is not permitted until 1 January 2001.
9300-9500	Radiolocation		
9300-9500		5.427	See Above
		5.474	See Above
		US67	The use of the band 9300-9500 MHz by the meteorological aids service is limited to groundbased radars. Radiolocation installations will be coordinated with the meteorological aids service and, insofar as practicable, will be adjusted

			to meet the requirements of the meteorological aids service.
		US71	In the band 9300-9320 MHz, low-powered maritime radionavigation stations shall be protected from harmful interference caused by the operation of land-based equipment.
9300-9500	RADIONAVIGATION	5.476	See Above
		US66	The use of the band 9300-9500 MHz by the aeronautical radionavigation service is limited to airborne radars and associated airborne beacons. In addition, ground-based radar beacons in the aeronautical radionavigation service are permitted in the band 9300-9320 MHz on the condition that harmful interference is not caused to the maritime radionavigation service.
9300-9500	Radiolocation	US51	In the band 9300-9500 MHz, the radiolocation service may be authorized for non-Federal use on the condition that harmful interference is not caused to the Federal radiolocation service.
		G56	Federal radiolocation in the bands 1215-1300, 2900-3100, 5350-5650 and 9300-9500 MHz is primarily for the military services; however, limited secondary use is permitted by other Federal agencies in support of experimentation and research programs. In addition, limited secondary use is permitted for survey operations in the band 2900-3100 MHz.
9300-9500	Meteorological Aids		

## References

- [1] "Statistical Abstract of the United States - Section 24. Information and Communications," United States Census Bureau 2007.
- [2] W. Krenik and C. Panasik, "The Potential for Unlicensed Wide Area Networks," 2004.
- [3] J. Mitola, "Cognitive Radio for Flexible Mobile Multimedia Communications," *Proc. IEEE Intl. Workshop on Mobile Multimedia Commun.*, pp. 3-10, 1999.
- [4] A. Batra, W. Krenik, and C. Panasik, "Cognitive Radios for Unlicensed WANs," *BWRC Cognitive Radio Workshop*, 2004.
- [5] W. Krenik and A. Batra, "Cognitive Radio Techniques for Wide Area Networks," *Proc. Conference on Design Automation*, pp. 409-412, 2005.
- [6] C. Cordeiro, K. Challapali, D. Birru, and S. Shankar, "IEEE 802.22: The first worldwide wireless standard based on cognitive radios," *Proc. IEEE Dynamic Spectrum Access Nets.*, pp. 328-337, 2005.
- [7] S. Shankar, C. Cordeiro, and K. Challapali, "Spectrum Agile Radios: Utilization and Sensing Architectures," *Proc. IEEE Dynamic Spectrum Access Nets.*, pp. 160-169, 2005.
- [8] R. W. Brodersen, A. Wolisz, D. Cabric, S. M. Mishra, and D. Willkomm, "CORVUS: A Cognitive Radio Approach for Usage of Virtual Unlicensed Spectrum," 2004.
- [9] S. Haykin, "Cognitive Radio: Brain-Empowered Wireless Communications," *IEEE Communications*, vol. 23, pp. 201-220, February 2005.
- [10] J. O. Neel, "Analysis and design of cognitive radio networks and distributed radio resource management algorithms," Ph.D dissertation, Dept. of Electrical and Computer Eng., Virginia Polytechnic Institute and State University, Blacksburg, Virginia, 2006
- [11] (2004) FCC Wireless Telecommunications Bureau Rules & Regulations: Code of Federal Regulations Title 47. [Online]. Available: <http://wireless.fcc.gov/rules.html>
- [12] (2003) Manual of Regulations & Procedures for Federal Radio Frequency Management. [Online]. Available: <http://www.ntia.doc.gov/osmhome/redbook/redbook.html>
- [13] (2007) FlightAware - Free Flight Tracker -IFR Flight Status, Tracking, History, Maps. [Online]. Available: <http://flightaware.com/>
- [14] (2007) FAA - Instrument Procedures Handbook (IPH). [Online]. Available: [http://www.faa.gov/library/manuals/aviation/instrument\\_procedures\\_handbook/](http://www.faa.gov/library/manuals/aviation/instrument_procedures_handbook/)

[15] (2007) FAA Order 7400.2F: Procedures for Handling Airspace Matters. [Online]. Available:

[http://www.faa.gov/airports\\_airtraffic/air\\_traffic/publications/atpubs/AIR/index.htm](http://www.faa.gov/airports_airtraffic/air_traffic/publications/atpubs/AIR/index.htm)

[16] F. H. Sanders, R. L. Sole, B. L. Bedford, D. Franc, and T. Pawlowitz, "Effects of RF interference on Radar Receivers," National Telecommunications and Information Administration TR-06-444, September 2006.

[17] P. Joe, J. Scott, J. Sydor, A. Brandao, and A. Yongacoglu, "Radio Local Area Network (RLAN) and C-Band Weather Radar Interference Studies," in *32nd Conference on Radar Meteorology*, 2005.

[18] A. Brandao, J. Sydor, W. Brett, J. Scott, P. Joe, and D. Hung, "5GHz RLAN Interference on Active Meteorological Radars," in *61st IEEE Vehicular Technology Conference*, 2005, pp. 1328-1332.

[19] F. H. Sanders, R. L. Hinkle, and B. J. Ramsey, "Analysis of Electromagnetic Compatibility Between Radar Stations and 4 GHz Fixed-Satellite Earth Stations," National Telecommunications and Information Administration 94-313, July 1994.

[20] Radio Technology & Compatibility Group, "Airborne Radar Interference into 32 GHz Fixed Links," Radiocommunications Agency 563, 12 September 2000.

[21] Alenia Marconi Systems Limited, "The Report of an Investigation into the Characteristics, Operation and Protection Requirements of Civil Aeronautical and Civil Maritime Radar Systems," Radiocommunications Agency, London, UK 45002656, October 2002.

[22] M. I. Skolnik, *Introduction to Radar Systems*, 3 ed. New York: McGraw-Hill, 2001.

[23] S. Parry, "Airborne Radar Systems," International Telecommunications Union JRG-41, May 23, 2005.

[24] C. Wolff. (2007) Radar Principles. [Online]. Available: <http://www.radartutorial.eu/index.en.html>

[25] F. H. Sanders, R. L. Hinkle, and B. J. Ramsy, "Measurement Procedures for the Radar Spectrum Engineering Criteria (RSEC)," National Telecommunications and Information Administration TR-05-420, March 2005.

[26] "Mathematical Model for Radiation Patterns for Radar Antennas For Use in Interference Assessment," National Telecommunications and Information Administration RCG-44, 2006.

[27] "Revision of Parts 2 and 15 of the Commission's Rules to Permit Unlicensed National Information Infrastructure (U-NII) devices in the 5 GHz band," FCC 06-96, 2006.

[28] J. P. Camacho, "Federal Radar Spectrum Requirements," National Telecommunications and Information Administration NITA Special Publication 00-40, 2000.

[29] R. Sole, "Radar Sepctrum Engineering Criteria (RSEC): Advanced Software Tool," 3.31.o-0.4.15.2005 ed Washington, D.C.: National Telecommunications and Information Administration, 2005.

[30] J. G. Proakis, *Digital Communications*, 4 ed. Boston: McGraw Hill, 2001.

[31] S. Haykin and M. Moher, *Introduction to Analog and Digital Communications*, 2nd ed.: Wiley, 2007.

[32] T. Pratt, C. Bostian, and J. Allnutt, *Satellite Communications*, 2nd ed.: Wiley & Sons, 2002.

[33] L. W. Couch, II, *Digital and Analog Communication Systems*, 7th ed. Upper Saddle River: Prentice Hall, 2007.

[34] M. Willis. (2006) Gas Loss Estimator. [Online]. Available: <http://www.mike-willis.com/software.html>

[35] T. S. Rappaport, *Wireless Communications: Principles and Practice*, 2 ed. Upper Saddle River: Prentice Hall PTR, 2002.

[36] R. M. Buehrer, *Code Division Multiple Access*: Morgan & Claypool Publishers, 2006.

[37] R. M. Buehrer, "Spread Spectrum," Virginia Polytechnic Institute and State University, 2006.

[38] (2007) Weather Radar. [Online]. Available: [http://en.wikipedia.org/wiki/Weather\\_radar](http://en.wikipedia.org/wiki/Weather_radar)

[39] (2007) National Telecommunications & Information Administration About Page. [Online]. Available: <http://www.ntia.doc.gov/ntiahome/aboutntia/aboutntia.htm>

[40] (2007) About the FCC. [Online]. Available: <http://www.fcc.gov/aboutus.html>

[41] "Title 47 of the Code of Federal Regulations," FCC 1998.

[42] (2000) Collins WXR-2100. [Online]. Available: <http://www.rockwellcollins.com/ecat/at/Datasheets/WXR2100.pdf>

[43] (2007) RDR-4000 3-D Volumetric Weather Radar. [Online]. Available: <http://www.honeywell.com/sites/servlet/com.merx.npoint.servlets.DocumentServlet?docid=DBE671D92-9F7A-19D7-2F4C-DA84D07F559F>

[44] (2007) RDR-4B - Radar - Honeywell Aerospace. [Online]. Available: [http://www.honeywell.com/sites/aero/Radar3\\_C867EC130-221E-7DEE-00E1-9B9088CBF060\\_H5CBA7513-E2B2-3320-D5A0-AF32226E4F40.htm](http://www.honeywell.com/sites/aero/Radar3_C867EC130-221E-7DEE-00E1-9B9088CBF060_H5CBA7513-E2B2-3320-D5A0-AF32226E4F40.htm)

[45] AA 757/767 Radar Manual. [Online]. Available: <http://www.artietheairplane.com/radar.htm>

[46] J. C. Barr, *Airborne Weather Radar: A User's Guide*. Iowa: Iowa State University Press, 1993.

[47] (2006) Density Using Land Area. [Online]. Available: <http://www.census.gov/population/www/censusdata/density.html>

[48] (2007) Google Maps. [Online]. Available: <http://maps.google.com>

[49] Google Maps. [Online]. Available: <http://maps.google.com/>

[50] "Mathematical Model for Radiation Patterns for Radar Antennas for Use in Interference Assessment," National Telecommunications and Information Administration - ITS, Mainz, Germany 2006.

[51] A. Leon-Garcia, *Probability and Random Processes for Electrical Engineering*, 2 ed. Reading: Addison Wesley Ongman, 1994.

[52] "Wireless LAN Medium Access Control (MAC) and Physical Layer (PHY) Specifications," IEEE Std. 2003.

[53] "Specification of the Bluetooth System," November 4 2004 2004.

[54] B. S. Peterson. (2007) Airport Flight Delay Tracker - FAA Next Gen Air Traffic Control Plan - GPS - Popular Mechanics. [Online]. Available: [http://www.popularmechanics.com/science/air\\_space/4219569.html?page=1](http://www.popularmechanics.com/science/air_space/4219569.html?page=1)

[55] FMR-200x. [Online]. Available: <http://www.rockwellcollins.com/ecat/gs/FMR-200X.html>